NTNU
Norwegian University of
Science and Technology

Estimation of Fuel Savings from Rapidly Reconfigurable Bulbous Bows

Exemplifying the Value of Agility in Marine
Systems Design

Jon Hovem Leonhardsen

MASTER'S THESIS IN MARINE TECHNOLOGY

SPRING 2017

For stud. techn. Jon Hovem Leonhardsen

Estimation of Fuel Savings from Rapidly Reconfigurable Bulbous Bows
Exemplifying the Value of Agility in Marine Systems Design

Background

This project is intended to analyze the value of having a flexible bulbous bows (bulbs), that is, being able to dynamically change the geometry of the bulb during operations. The purpose of the bulb is to reduce the ships wave resistance, by generating a wave that cancels out the wave generated from the hull. Bulbs have traditionally been designed and optimized for a specific service speed and loading condition. However, ships face a broad spectrum of operating conditions, as they have to take on a broad variety of trades, and one aspect of this is variations in sailing speed, which is the focus in this thesis. Hydrodynamic speed variations may occur on a transit-to-transit basis, or on longer time scales. An example of the latter is containerships that recently have seen large reductions in operating speeds - slow steaming.

As ship owners have noticed this trend and how sailing speed varies dependent on a wide range of operational and market-oriented variables, recent developments have been towards designing the bulb for a broader range of operating conditions. This design strategy is known as *robust* design, and is essentially suboptimal for each speed scenario. However, based on the variety of operating conditions ships are facing, the strategy is superior to optimizing the bulb for a fixed service speed. Lately there have also been several examples of bulb retrofits, where bulbs designed for a fixed speed are replaced by robust bulb designs. Bearing this in mind, the hypothesis is that there exists an untapped potential with respect to resistance minimization, by introducing a *flexible* bulb design. A flexible bulb design implies the option of changing the geometry of the bulb according to the desired speed for one specific trade – or ultimately during the voyage.

Objective

The overall objective of this thesis is to estimate fuel savings from being able to reconfigure the bulb geometry with different frequencies, with the intention of analyzing the value of being agile. Embedded in this objective are the sub-objectives of analyzing sailing speed variations by investigation of historical speed records, in addition to developing a Monte Carlo Method for simulating a bulb that can change geometry according to the aforementioned variations.

Tasks

The candidate shall/is recommended to cover the following tasks in the master's thesis:
a. Describe the problem of suboptimal bulb designs, and the principles behind the different approaches for handling context uncertainty.
b. Review state-of-the-art within the topic, with focus on applications of Automatic Identification Systems (AIS) data for sailing speed analytics and bulb design for varying operating conditions.
c. Identify, filter and extract relevant ship segments from AIS data by use of heuristics.
d. Exemplify the underlying dynamics behind sailing speed variations by use of extracted data.

e. Propose a suitable stochastic process for simulation of sailing speed. Fit historical speed records from AIS data to the selected process, generate stochastic parameter probability density functions.
f. Develop a Monte Carlo Method (MCM) for valuation of bulbous bow agility, with speed probability density functions and resistance data for different bulb design as key input.
g. Evaluate results and compare to benchmark fuel savings from robust bulb designs. Evaluate and discuss methodology, with emphasis on key assumptions.

Cooperation with other projects
Resistance data utilized in this thesis are to be received from stud. techn. Andreas Watle, who works on his master's thesis "Flexible Bulbous Bow Design - A Hydrodynamic Study" in parallel with this study.

General
In the thesis the candidate shall present his personal contribution to the resolution of a problem within the scope of the thesis work.

Theories and conclusions should be based on a relevant methodological foundation that through mathematical derivations and/or logical reasoning identify the various steps in the deduction.

The candidate should utilize the existing possibilities for obtaining relevant literature.

The thesis should be organized in a rational manner to give a clear statement of assumptions, data, results, assessments, and conclusions. The text should be brief and to the point, with a clear language. Telegraphic language should be avoided.

The thesis shall contain the following elements: A text defining the scope, preface, list of contents, summary, main body of thesis, conclusions with recommendations for further work, list of symbols and acronyms, reference and (optional) appendices. All figures, tables and equations shall be numerated.

The supervisor may require that the candidate, in an early stage of the work, present a written plan for the completion of the work. The original contribution of the candidate and material taken from other sources shall be clearly defined. Work from other sources shall be properly referenced using an acknowledged referencing system.

The work shall follow the guidelines given by NTNU for the MSc Thesis work. The work load shall be in accordance with 30 ECTS, corresponding to 100% of one semester.

The thesis shall be submitted electronically on DAIM:
-   Signed by the candidate.
-   The text defining the scope included.
-   Computer code, input files, videos and other electronic appendages can be uploaded in a zip-file in DAIM. Any electronic appendages shall be listed in the thesis.

Supervision
Main supervisor: Professor Bjørn Egil Asbjørnslett
Co-supervisor: PhD cand. Carl Fredrik Rehn
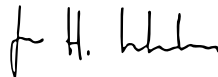**Deadline: 11.06.2017**

Preface

This thesis marks the final part of my Master of Science degree with specialization in Marine Systems Design at the Department of Marine Technology (IMT). The work has been carried out at the Norwegian University of Science and Technology (NTNU) during the spring term of 2017, and corresponds to 30 ECTs.

The thesis is a continuance of my project thesis, which under the name "Flexible Bulbous Bows - Approaching the Value of Agile Bulbs in Uncertain Operating Conditions" was carried out during the fall of 2016. Although the master's thesis builds on theory and data addressed in the project thesis, it can and should be read as an independent piece of work.

For those interested, I strongly recommend to read the thesis in its entirety, as it presents somewhat unconventional concepts and methodologies. The thesis encompasses a wide range of disciplines, which resulted in several decisions and assumptions regarding both input data and methodology along the way. The assumptions are addressed and discussed as they arise, some of them essential to acknowledge in order to follow the reasoning.

Although the thesis is carried out as an individual project, the project is conducted in partly collaboration with stud. techn. Andreas Watle, who specializes in Marine Hydrodynamics. His thesis is named "Flexible Bulbous Bow Design - A Hydrodynamic Study", and provided resistance data for different bulbous bow geometries, which he obtained through Computational Fluid Dynamics analyses. In addition, two different groups of Bachelor students at the Department of Mechanical Engineering at NTNU campus Kalvskinnet have worked on concept development and structural calculations of a flexible bulbous bow.

Trondheim, June 8, 2017

Jon Hovem Leonhardsen

Acknowledgment

Summary

This thesis analyzes the value of having geometrical bulbous bow flexibility in the context of sailing speed variability. The purpose of the bulbous bow, fitted on the foremost part of the hull, is to reduce wave-making resistance (an important fuel consumption-determinant) by the principles of destructive interference. Suboptimal containership bulbs have in the recent years received increased attention. The industry-wide adoption of slow steaming after the global recession in 2008 has entailed bulbs that operate off their intended design condition, yielding poor performance. Decreasing operating speeds have triggered a new design paradigm, where bulb design is conditioned on an average performance over a projected operating profile rather than to a specific design point. This approach is essentially a robust design strategy, accounting for context uncertainty without external interference during the life-cycle of the design object. However, the principles of average performance imply potential for further improvement, by incorporation of a dynamic bulb geometry that can adapt to the operating conditions.

The value of bulb flexibility is driven by the context uncertainty, which in this thesis is focused on sailing speed variability. Large amounts of historical speed records from Automatic Identification System (AIS) data were analyzed, and it became evident that significant variations can occur both during transits, and from transit to transit. As sailing speed during transit is bounded by technical and operational factors, the mean-reverting Ornstein-Uhlenbeck (OU) process was proposed as a stochastic representation of sailing speed. The underlying key assumption was that transit speed can be represented by three parameters; mean value, volatility and mean reversion rate. Parameters were estimated by running a regression on filtered transit time series for the entire Panamax containership segment, resulting in probability density functions (PDFs) representing possible transit speed dynamics. Sailing speed was simulated according to the OU process with transit-specific parameters sampled from the PDFs.

Resistance data for seven bulb configurations with constant cross-section, but different lengths, represented the flexible bulb. The option of switching between the associated fuel curves was the model representation of bulb reconfigurations. By combining sailing speed and resistance input, the aggregated fuel consumption was estimated with Monte Carlo simulations. The value of flexibility is derived from the option of minimizing fuel consumption by switching fuel curves, and the analysis was conducted with different time periods allowed between reconfigurations. The objective being to evaluate the value of *agility*, that is, the value of being able to rapidly reconfigure the bulb.

The value of agility was investigated through a case study calibrated to a reference ship similar to the KRISO Container Ship (KCS), for which resistance data was available. Bulb reconfiguration periods in the range between two hours and two weeks were analyzed, yielding average fuel savings in the range between 2.86% and 2.76%, respectively. The fuel consumption with bulb flexibility was compared to the original bulb of the KCS, and the fuel savings from agility had an upper bound of 3.7%, which was the maximum resistance reduction in the set of bulb configurations and speeds. The relatively modest difference between high and low agility is explained by the fact that two out of the seven bulb configurations covered the speed regime between 13 and 18.8 knots, speeds the reference ship holds 93% of the time.

It is concluded that the results leave few incentives for incorporating bulb flexibility, as fuel savings from robust bulb retrofits are reported in the range between 5% and 10%. However, as flexibility in theory should outperform robustness, recommendations for further work include identification of valuable bulb flexibility, as this study only analyzed the value of adjusting the length parameter of the bulb. It is emphasized that the numerous assumptions, potentially uncertain input parameters and marginalization of certain fuel consumption-determinants make the analysis incomplete, underscoring that the results should be treated accordingly.

Sammendrag

Denne oppgaven analyserer verdien av å ha geometrisk fleksibilitet i bulben i forbindelse med hastighetsvariasjoner. Hensikten til bulben, montert fremst på skroget, er å redusere bølge-motstanden (en viktig determinant av drivstofforbruk) ved destruktiv interferens. Suboptimale containerskipbulber har i de senere år fått økt oppmerksomhet. Den bransjeomfattende utbre-delsen av slow steaming etter den globale resesjonen i 2008 har medført at bulber opererer uten-for tilsiktet designkondisjon, noe som gir lav ytelse. Fallende operasjonshastigheter har trigget et nytt designparadigme, hvor bulbdesign blir tilpasset for en gjennomsnittlig ytelse over en anslått operasjonsprofil, i stedet for et spesifikt designpunkt. Denne tilnærmingen er i praksis en robust designstrategi, hvor kontektsusikkerhet blir tatt høyde for uten ekstern innblanding gjennom designobjektets livssyklus. Prinsippene bak gjennomsnittlig ytelse impliserer likevel et potensiale for ytterligere forbedring, ved å innkorporere en dynamisk bulbgeometri som kan endres avhengig av operasjonskondisjonen.

Verdien av bulbfleksibilitet er drevet av kontekstusikkerheten, som i denne oppgaven er fokusert på hastighetsvariasjoner. Store mengder Automatic Identification Systems (AIS) data ble analy-sert, og det kom frem at signifikante variasjoner kan oppstå både under transitt, og fra transitt til transitt. Ettersom hastighet under transitt er avgrenset av tekniske og operasjonelle faktorer, ble den middel-reverterende Ornstein-Uhlenbeck-prosessen (OU) foreslått som en stokastisk representasjon av hastighet. Den underliggende antagelsen var at transitthastighet kan repre-senteres av tre parametere; gjennomsnittsverdi, volatilitet og middel-reversjonsrate. Parame-terene ble estimert ved regresjon på filtrerte transitttidsserier for hele Panamax containerskip-segmentet, som resulterte i sannsynlighetsdensitetsfunksjoner (SDFer) som representerte mulige transitthastighetsdynamikker. Seilehastighet ble simulert i henhold til OU-prosessen med transitt-spesifikke parametere samplet fra SDFene.

Motstandsdata for syv ulike bulbkonfigurasjoner med konstant tverrsnitt, men forskjellig lengde, representerte den fleksible bulben. Muligheten til å bytte mellom de tilhørende drivstoffkurvene var modellrepresentasjonen av bulbrekonfigurasjon. Ved å kombinere seilehastighets- og mot-standsinput kunne det aggregerte drivstofforbruket estimeres med Monte Carlo-simuleringer. Verdien av fleksibilitet er avledet fra muligheten til å minimere drivstofforbruket ved å bytte drivstoffkurve, og analysen ble gjennomført med forskjellig tidsperiode tillatt mellom rekon-figurasjoner. Hensikten med dette var å evaluere verdien av *agilitet*, som er evnen til å kunne rekonfigurere bulben hurtig.

Verdien av agilitet ble undersøkt gjennom en case-studie kalibrert til et referanseskip liknende KRISO Container Ship (KCS), for hvilket motstandsdata var tilgjengelig. Bulbrekonfigurasjonsperioder mellom to timer og to uker ble analysert, som ga drivstoffbesparelser i området mellom 2.86% og 2.76%, respektivt. Drivstofforbruket med bulbfleksibilitet ble sammenliknet med drivstofforbruk med originalbulben til KCS, og drivstoffbesparelsene fra agilitet hadde en øvre grense på 3.7%, ettersom dette var den maksimale motstandsreduksjonen i settet av bulbkonfigurasjoner og hastigheter. Den relativt moderate forskjellen mellom høy og lav agilitet ble tilskrevet at to av de syv bulbkonfigurasjonene dekket hastighetsområdet mellom 13 og 18.8 knop, som er området referanseskipet seiler i 93% av tiden.

Det er konkludert med at resultatene indikerer få incentiver for å innkorporere bulbfleksibilitet, ettersom drivstoffbesparelser fra robuste bulber er rapportert i området mellom 5% og 10%. Likevel, ettersom fleksibilitet i teorien burde utkonkurrere robusthet, inkluderer anbefalinger for videre arbeid identifikasjon av verdifull bulbfleksibilitet, ettersom denne studien kun analyserte verdien av å kunne justere lengdeparameteren til bulben. Det er understreket at de mange antagelsene, potensielt usikre inputparametrene og marginaliseringen av noen drivstofforbrukdeterminanter gjør analysen ufullstendig, og at resultatene burde tolkes i henhold til dette.

Contents

List of Figures

List of Tables

Chapter 1

Introduction

1.1 Background

In 2008, Maersk defined a new industry standard as the first liner to implement slow steaming as a strategic tool. The motivation being skyrocketing bunker prices, which imposed the Danish giant an enormous fuel bill. Slow steaming is simply the term for ships steaming at lower engine speeds, and because fuel consumption is roughly proportional to sailing speed to the power of three, reduced speed resulted in a significant reduction in fuel expenses. While high bunker prices triggered slow steaming, the global recession in 2008 and 2009 dramatically shifted supply and demand balances, resulting in excess fleet capacity. Consequently, the incentives for slow steaming raised as increased transit times absorbed up to 4.1% of the global fleet[1].

While slow steaming proved to be a simple and effective solution to the shifted market dynamics, naval architects saw potential for further savings through bulbous bow optimization. The primary purpose of the bulbous bow is to minimize wave resistance by generating counteracting waves by the principles of destructive interference, which made bulbous bows designed for significantly higher service speeds perform poor at operations off the design condition. Consequently, a new paradigm for bulbous bow design was entered. While bulbous bows traditionally had been designed to one specific design point, often fully loaded and high speed, the new practice became to design bulbous bows according to projected operating profiles. This practice has resulted in numerous bulbous bow retrofits over the recent years, where point optimized bulbs are cut off and replaced by bulbs designed to exhibit an average performance over a wide range of operating conditions.

The new bulb design practice can be interpreted as a *robust* design strategy, that is, a *passive* way of handling context uncertainty without external interference. However, while robust bulbs have proven to outperform the point optimized alternative, the design strategy essentially entails suboptimality at each specific speed scenario. Following this logic, there is a potential for

---

[1] http://www.maersk.com/en/the-maersk-group/press-room/press-release-archive/2010/9/slow-steaming-here-to-stay

further fuel savings by incorporating system *flexibility*, that is, an *active* way of handling un-certainty. With bulbous bow flexibility, the option of dynamically adapting the bulbous bow according to the experienced operating condition is introduced. In theory, the bulb can be continuously optimized to the desired sailing speed, and the value of the flexibility is conse-quently driven by how fast and how well the bulb can adapt to speed variability. In this light, the motivation for the thesis is to analyze the potential fuel savings from being able to dynami-cally change the geometry of the bulbous bow, and investigate the importance of being able to change *fast*.

On a higher level, the motivation for the study is rooted in energy efficiency and reduced emis-sions. Fuel consumption is linearly correlated to CO_2 emissions, and according to MARPOL Annex VI, Chapter 4 (IMO, 2011), which entered into force in January 2013, new ships must im-prove efficiency with 10% by 2020, 20% by 2025, and 30% by 2030. In addition, it was established industry goals of reducing CO_2 emissions with 20% by 2020, and 50% by 2050. These ambitious environmental goals call for technological innovations, and sets the scene for this thesis.

Problem Formulation

This study can roughly be divided into two problems;

The first problem is related to the *context analysis*; How much and how fast does sailing speed vary during and between transits? The primary goal of the context analysis is to model sailing speeds as a stochastic process, by analyzing large amounts of historical speed records.

The second problem is related to the *system response valuation*; What is the resulting value of being able to adapt to the uncertain context? The primary goal of the system response valua-tion is to develop a methodology for modelling changes in bulb configuration, and derive the associated value of being able to change with different frequencies.

1.2   Literature Review

The thesis encompasses a wide range of disciplines, including AIS based speed analytics, stochas-tic modelling of sailing speed, bulbous bow theory, design under uncertainty and Monte Carlo valuation of flexible designs. This section will summarize some previous studies within these fields.

Smestad (2015) investigated the quality and utility of Automatic Identification System (AIS) data, and used heuristics to identify specific ship types, which enables segment analyses without access to commercial databases. While this study seeks to predict future sailing speeds based on AIS data, several studies has utilized AIS data to investigate speed dynamics. Adland and Jia (2016b) used AIS data to show that operational variables (weather, commercial factors) are important determinants for short term speed variations. They also noted that AIS speed data is incomplete due to varying signal coverage. Adland and Jia (2016a) analyzed dynamic speed choice in bulk shipping by investigation of AIS data, and found that ship owners do not tend to optimize sailing speeds according to economic theory, in line with the findings of Aßmann (2012) and Aßmann et al. (2015). Jonkeren et al. (2012) found that speed variations do depend on non-fuel variables, and suggested more research on the topic. AIS data is also used to assess ship efficiency, for example by estimation of fuel consumption based on AIS speed records (Smith et al., 2013).

While the applications of AIS based speed analytics for prediction and forecasting of sailing speed are limited, some studies have utilized historical speed records from other sources. Coraddu et al. (2014) generated probability density functions for speed and draught by use of noon-to-noon reports, with the purpose of predicting the energy efficiency operational indicator by Monte Carlo simulations. Other studies have combined speed records with other information for speed predicting purposes. Mao et al. (2016) presented a statistical approach for prediction of sailing speed by use of engine revolutions per minute (RPM), met-ocean data and speed records.

Several studies have addressed bulbous bow design in the context of varying speed. Lu et al. (2016) proposed a hydrodynamic optimization design methodology accounting for an entire operating profile, and demonstrated a decrease in resistance of 2.845%. Filip et al. (2014) evaluated the benefits from retrofitting the bulbous bow to a slow steaming operating profile by CFD, yielding a power reduction of approximately 7%, while Wagner et al. (2014) obtained an effective power reduction of 2.7% by scenario based optimization. In addition to numeric fuel reductions, Chrismianto and Kim (2014) found that higher sailing speeds yield a longer optimal bulb design. Chirica and Giuglea (2015) investigated the resistance reduction from having a flexible bulbous bow on a small passenger ship (25 meters long) operating inland. Although they did not obtain significant reductions from varying the length of the bulb, they point out the potential for fuel savings.

While state-of-the-art bulbs currently are designed to exhibit an average performance over a

wider range of sailing speeds, this thesis seeks to explore the value of flexible and agile designs. De Neufville and Scholtes (2011) emphasizes that flexibility in design limits possible losses and increases possible gains. Fricke and Schulz (2005) defines flexibility as a system capability to adapt to external changes easily, while agility represents the systems capability to adapt rapidly. Rehn (2015) demonstrated that Monte Carlo simulations is an efficient way of valuing complex design flexibility in marine systems.

What Remains to be Done?

From the literature review it became clear that although there has been a growing number of AIS related studies over the recent years, applications to sailing speed modelling for forecasting is non-existent. Consequently, the author is left with the complex and intriguing task of exploring this new academic branch, in addition to make and discuss necessary assumptions.

Moreover, there exists no studies on the topic of valuation of structural bulbous bow flexibility in any sense. While there has been conducted valuation studies on flexibility in marine design, the bulb case differs in the sense that the underlying uncertainty is observed in operational rather than market-oriented variables.

1.3 Objectives

The objectives of this thesis are:

1. Filter and extract relevant ship segments from AIS data by use of heuristics.

2. Exemplify the underlying dynamics behind sailing speed variations by use of extracted data.

3. Propose a suitable stochastic process for simulation of sailing speed.

4. Fit historical speed records from AIS data to the selected process, generate stochastic parameter probability density functions.

5. Develop a Monte Carlo Method (MCM) for valuation of bulbous bow agility, with speed probability density functions and resistance data for different bulb design as key input.

6. Calibrate the speed input to a reference ship, and conduct a case study that estimates the value of having an agile bulb.

1.4   Limitations and Delimitations

The main limitations of this study is related to the available data. The work rely on two key input sources, whereby one is AIS data representing the operational variations, and the other is resistance data for different bulb designs. Although resistance is mostly dependent on speed, draught and trim are also influencing factors. However, the only reliable dynamic data included in AIS messages is speed and position (Ljungberg, 2017), entailing that the context analysis is solely focused on speed variations. In addition, the available resistance data includes Computational Fluid Dynamics analyses of seven different bulb lengths (in addition to the hull model original) at constant draught and five different speed intervals.

The study is consequently delimited to analysis and modelling of sailing speed, and valuation of flexibility within the solution space bounded by the resistance data.

Fundamental and statistical analyses of the underlying reasons for speed variability is also considered outside the scope of this thesis. The scope is to quantify *how* speed variability occurs, not *why*. However, the topic is addressed, and causalities discussed and exemplified.

Finally, the scope is delimited to encompass analysis of speed variability for *containerships*. This argued with the fact that most bulbous bows retrofits over the recent years have been within this segment, and that their bulb shapes are distinct and potentially suitable for flexibility. In addition, the CFD results utilized in this study stem from analyses of a containership hull model.

1.5   Structure of the Report

The rest of the thesis is structured as follows:

Chapter 2 intends to establish a high level motivation for the work, rooted in naval architecture, marine systems design and design under uncertainty. Basic resistance and bulbous bow theory is coupled with performance under uncertain operating conditions, in a bid to underscore the purpose of the thesis.

The data foundation utilized to evaluate uncertain operating conditions is described in Chapter 3. Fundamentals of AIS data is addressed, before the methods for obtaining segment specific data by heuristics is elaborated.

Chapter 4 breaks sailing speed variability into long-, mid-, and short-term variations. The underlying causalities behind the different variations are discussed and exemplified. In addition, the chapter addresses the assumption of using speed over ground as an estimator for speed through water.

In Chapter 5, the procedure for fitting historical speed records to a stochastic model is explained. A mean reverting stochastic process is proposed, and the estimation of model parameters is addressed in detail.

The general methodology for simulating fuel savings is layed out in Chapter 6. Here, the different model input is addressed, and key assumptions and procedures are elaborated.

A case study is conducted in Chapter 7, in order to quantify the expected fuel savings from having bulbous bow flexibility. The selection of case is explained, and a number of assumptions related to power and fuel calculations are discussed. Aggregated fuel consumption is simulated and compared to empirical data for verification, before the different levels of agility subject for simulation is addressed.

Chapter 8 summarizes the results from the case study, and chapter 9 discusses the results and the methodology used to obtain them. Chapter 10 presents the conclusion of the thesis, and states recommendations for further work.

Figure 1.1 presents a flow chart of the key parts of the study. Starting from raw AIS data, the main flow follows the thicker arrows, resulting in fuel savings as a function of reconfiguration period.
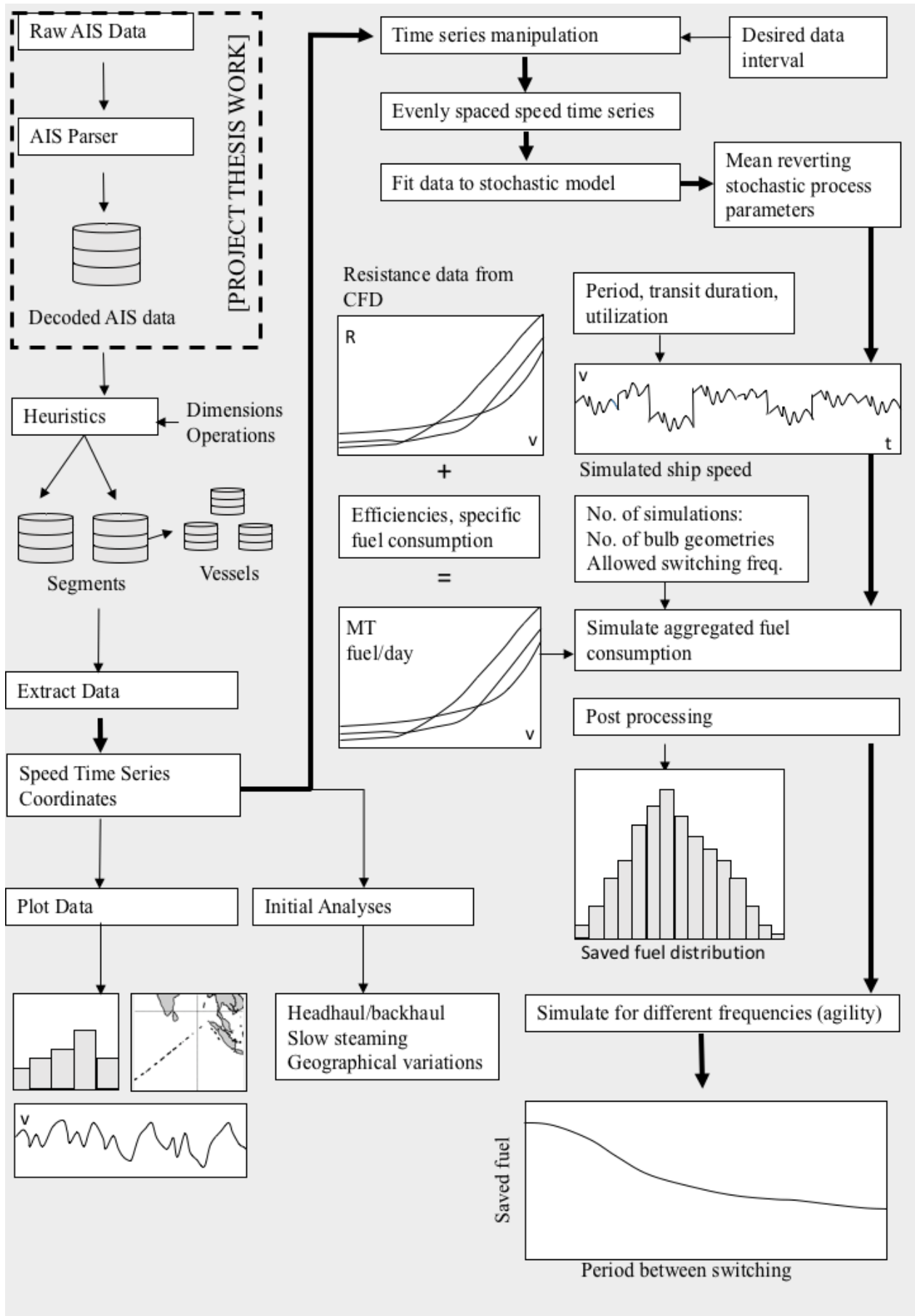
Figure 1.1: General flow of work

Chapter 2

Background and Motivation

2.1 Naval Architecture and Performance Metrics

Tupper (2013) defines naval architecture as the science of making a ship fit for purpose. The somewhat ambiguous term *fit for purpose* can be summarized as the ship's ability to operate safely, reliably and economically. The economical metric includes, in addition to the financial performance, the environmental footprint of the ship, which in recent years has gained increased attention. Although all three metrics have operational determinants, for example how the master alters speed according to weather or schedule, they are heavily influenced during the design process. Ferreiro and Hocker (2007) defines naval architecture the following way:

The branch of engineering concerned with the application of ship theory within the design and construction process, with the purpose of predicting the characteristics and performance of the ship before it is built.

Further, they concretise the term *ship theory* as the science of explaining the physical behaviour of a ship, through the use of fundamental mathematics or empirically derived data. The performance of the ship can be divided into the three previously addressed metrics. Safety and reliability refer to the ship's ability to float upright, have adequate stability, withstand external loads and maintain the desired sailing speeds in the expected sea conditions. While the financial part of the economical metric is the driver and motivation for designing and building a ship in most cases, safety and reliability are vital metrics for designers for obvious reasons. However, as a result of continuously improved competence and computer-aided tools, safety and reliability are considered relatively straight forward to get right in the design process, compared to the economical performance metric.

The financial performance is the hardest to predict at the design stage. As for any business, the ship's economy can be divided into a revenue domain and a cost domain. Revenue is determined by the state of the market, which essentially is driven by the global economy, and via supply and demand balances observed in freight rates. Although the ship design process in

broader terms is considered to encompass market analyses in order to determine the main dimensions needed to absorb the expected demand, the cost domain is a more complex design issue from a technical point of view.

The cost domain consists of capital expenditures (capex), operational expenditures (opex), and voyage related expenditures (voyex). Capex can be interpreted as the investment cost of the vessel. Opex is the day-to-day cost of sailing, including crew and insurance costs, while voyex in essence is the fuel cost. Capex is obviously directly affected by the design process, in terms of steel, machinery and labour costs. However, fuel costs account for 50% to 75% of opex and voyex (Notteboom and Cariou, 2009), making this expenditure an important subject for minimization. Fuel consumption is essentially driven by the ship's total resistance, which in terms are dependent on the hull shape and friction. Thus, the economical performance of a ship, both in terms of profit and emissions, is heavily dependent on hull design.

Recalling Ferreiro and Hocker (2007) definition of naval architecture, they emphasize the prediction of characteristics and performance of a ship before it is built. While prediction of performance related to revenue is an isolated economical and strategic issue, prediction of cost related performance is more of a techno-economical challenge. Different operating conditions yield different optimal hull designs, leaving the designers with the complex task of predicting draught and service speed *before* they decide on hull geometry and different resistance minimizing means. Here, we touch the core problem of this study, which on a high level deals with resistance minimization under uncertain operating conditions. More specifically, we will evaluate the influence of the bulbous bow in this context, and eventually estimate the potential fuel savings from having dynamical bulb flexibility. The next sections will address resistance and bulbous bow theory, and connect bulb design to *design under uncertainty* in the light of marine systems design.

2.2 The Bulbous Bow and Resistance

In order to understand the bulbous bow and when it is beneficial, it is important to understand the breakdown of ship resistance. This chapter will address the ship resistance components, the bulb's purpose in this context, and describe how different operating conditions call for different bulb designs. Section 2.2.1 and 2.2.2 are based on material from the project thesis, and written in cooperation with stud. techn. Andreas Watle.

2.2.1 Resistance

The resistance forces acting on a ship moving through water can be divided into two main components; pressure force and shear force. The pressure force is acting in a direction normal to the surface of the body, and is mainly caused by the wave making of the hull. The shear force, often referred to as viscous resistance, is acting tangentially to the surface, that is, in the direction of the local relative fluid motion. This force is caused by the friction between the fluid and the body. In ship resistance theory, a common simplification is to divide the total resistance into wave making resistance and viscous resistance, under the assumption that these components are independent of each other (Steen, 2007).

The wave resistance is a significant component to the total resistance of the ship. The wave generation of the hull moving through the water is a result of the pressure difference induced by the free surface effects. It is common to assume that the pressure resistance and the wave resistance of the ship are equal, although viscous effects such as flow separation will create pressure resistance, called viscous pressure resistance. For ships, the viscous pressure resistance is usually small compared to the wave resistance, and is therefore studied separately. The wave resistance can be described with a hull moving through water. As the hull moves through water, the volume displacement alters the velocity along the hull. At the forward part of the hull, the water is forced outwards, and at the aft, it flows back towards the centre line of the ship. Bernoulli's equation describes the wave making

$$\frac{\rho}{2}v^2 + \rho g z + p = constant \tag{2.1}$$

Here, ρ is the water density, v is the flow velocity along the hull, g is the gravitational acceleration, z is the surface elevation and p is the atmospheric pressure. The velocity of the flow around the ship hull will be retarded and accelerated in the bow and after body respectively. This will lead to a change in the free surface elevation, as the pressure at the surface has to be equal to the atmospheric pressure. The velocity around the ship will increase towards the middle of the ship, and the same physical phenomena results in a change in wave elevation along the hull.

A typical distribution of the resistance components as a function of Froudes number F_N is shown in figure 2.1[1]. Froudes number is a dimensionless ratio of the flow velocity, i.e. the ship speed, to the ship length, given by $F_N = \frac{V}{\sqrt{gL}}$. The figure is only illustrative, and aims to provide an understanding of how the main resistance components vary as a function of speed.

---

[1]Simplified sketch based on resistance breakdown presented by Steen (2007)
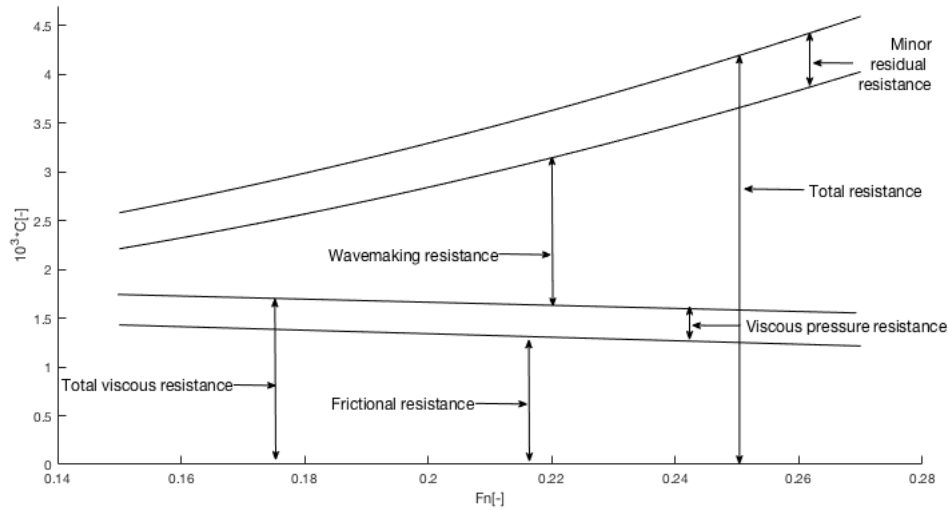
Figure 2.1: Resistance components as a function of F_N [-]

2.2.2 Reducing Resistance with the Bulbous Bow

In order to improve the hull's resistance characteristics, a bulbous bow can be fitted to the forward part of the hull. The primary aim of the bulb is to generate a wave forward of the vessel, with the purpose of minimizing the waves propagating down the length of the hull. This would occur by the principle of destructive interference when the waves interact. The interaction affects the wave making resistant component, which becomes more dominating as the ship's velocity increases, as shown in figure 2.1.

In addition to influencing the hull's wave system, bulbous bows also affect the frictional resistance. The additional wetted surface added by the bulb will always increase the frictional resistance, which is the biggest contributor to the viscous resistance. The introduction of the bulb will in some cases improve the fairing around the forebody, and thus change the hull's viscous pressure field, which can reduce the viscous resistance. For full, slow ships, the reduction of viscous resistance due to the smoothing of the fore body can take presence over the wave canceling effects of the bulb (Kracht, 1978).

As figure 2.1 suggests, the two biggest contributors to the total resistance are frictional and wave-making resistance. In literature, the two dominating components are often defined as residual and frictional resistance, whereby wave-making resistance is the majority of the residual component.

2.2.3   The Relationship Between Ship Type and Bulb Design

The geometry and general shape of bulbous bows vary significantly across ship segments, and is determined by the operating profile of the ship in question. As figure 2.1 shows, wave resistance takes dominating presence in the higher Froude regime. Consequently, the bulb design for a ship operating at high sailing speeds differ significantly from a slower ship's bulb. Bulb design for faster ships is characterized by an additive and distinct shape, and are often longer than bulbs designed for slower sailing speeds. This is explained by the fact that the length of the bulb is roughly proportional to its internal volume, meaning that small increments in length will increase the potential of the wave generated. This is the desired effect when the waves generated by the hull are large, which is the case for ships at high sailing speeds. For ships operating in the lower Froude regime, the bulb's primary purpose is to improve the viscous characteristics, by extending the waterline.

Containerships, as opposed to tankers and most bulk ships, often carry perishable and other time-sensitive cargo. There may be up to hundreds of different owners of the containers on board a ship, who want the cargo delivered as soon as possible. This makes the time pressure greater than for other segments, who often carry cargo for one owner at a time. As a result, container vessels tend to be faster than general cargo ships, with maximum speeds reaching 30 knots (Tupper, 2013). Consequently, containerships often operate in a high Froude regime, which in terms results in a relatively high fraction of wave resistance. The ship design is obviously affected by this, and materialize in more slender bodies and distinct bulb shapes.

2.3   Marine Systems Design

While the design of bulbous bows can be considered a typical design task within the technical domain of naval architecture, the previously mentioned context uncertainties calls for a broader term. Expanding the design problem to encompass the context the design object is supposed to thrive in, the flexible bulbous bow problem is a typical problem within the academic field known as *marine systems design*. Marine systems design encompasses several academic fields, spanning from market analysis and idea generation to engineering design. The field is broad in the sense that projects often demands complete end-to-end solutions, leaving a lot of responsibility and decision making to the design team. While a design objective may be formulated like: *Design a bulk carrier where: D = x; B = y; L = z; d = t; V = h.*, Erichsen (1989) provides an intu-

itive example on how design objectives rather are formulated in the context of marine *systems* design: *Design the transport of x tons of iron ore per year from point A to point B..*

Although both formulations eventually result in the design of bulk carriers, the difference in scope is clear. The latter expands the solution space, increasing the chances of designing a suitable system. The dimensions specified in the first objective might not match the demand for iron ore transportation, or maybe two smaller bulk vessels is a better solution given the expected operating conditions. The key takeaway is that marine systems design should involve comprehensive analysis of the context surrounding the subject for design, that being variations in operating conditions or the global economy.

In this thesis, the marine system includes the operating context and the bulbous bow. Following the logic of Erichsen (1989), the design objective may be formulated like this: *Design a bulbous bow that under the operating conditions in region A continuously minimizes fuel consumption.*

2.4   Design Under Uncertainty

Marine systems intended to operate within shipping and offshore markets are subject to substantial amounts of uncertainty with respect to their future operating context. The projects are often capital-intensive and of high complexity, designed to provide a service for several decades. Thus, marine systems design is closely related to *design under uncertainty*, a sub-field of systems design aiming to enhance the performance of engineering systems in the context of uncertain operating environments. Sources of uncertainty may be related to supply and demand of a service, commodity prices, environmental regulations or, in the case of hull and bulbous bow design, operating conditions.

Design under uncertainty requires that designers recognize and acknowledge the presence of uncertainty, and proactively approaches the design process according to distributions of future possibilities (De Neufville and Scholtes, 2011). The probabilistic representation of the future can be embedded in designs in different ways, and some approaches and terms are presented and clarified in the following sections.

2.4.1   Robust Design

Robustness in engineering design is best understood as the *passive* way of dealing with uncertainty. Given distributions representing the future operating context, a robust optimized design is the design that exhibits the best *averaged* performance over the entire life-cycle of the design object, without external interference. Fricke and Schulz (2005) define robustness as the systems ability to be insensitive towards changing environments.

In the context of bulb design, robustness has gained increased attention over the recent years as a result of slow steaming. Rather than optimizing the bulbous bow for an intended service speed, designers take the entire operating profile into consideration, ensuring that the selected bulb design minimizes the total fuel consumption instead of minimizing the fuel consumption at a specific service speed. While robust design is a relatively simple way of proactively incorporating future uncertainties, the principle of *average performance* implies that there exists a potential for further increase in performance, by introducing *flexibility in engineering design.*

2.4.2   Flexible and Agile Design

While robustness is passive, flexibility is an *active* way of handling uncertainty. Fricke and Schulz (2005) define flexibility as a systems ability to be changed easily, meaning that the systems can be changed from external to cope with changing environments. In his thesis on Identification and Valuation of Flexibility in Marine Systems Design, Rehn (2015) suggests fuel switching and capacity expansion as potential design flexibilities, among other. Here, the flexibility takes presence in the fact that the ship is built with the possibility of *easily* switch fuel or expand capacity, should the operating context speak in favour of it. In the real options valuation space, the term *trigger level* is often used to describe the level where the operating context reaches the threshold where changing the system becomes beneficial. In the case of fuel switch, the trigger level may be the price premium between two alternative fuels. Similarly, the trigger level for a capacity expansion may be quantified in market rates (driven by demand) for a transport service.

Flexible bulbous bow design refers to the option of easily change the geometry of the bulbous bow according to the operating context. Here, operating context refers to the operating conditions (sailing speed) of the vessel. In contrast to price premiums and market rates, the operating condition will fluctuate frequently within the technical boundaries of the ship design. The trig-

ger level will in this thesis be speed levels. Should the speed exceed or fall below the trigger level, a change in geometry might be beneficial. However, the speed could return to the initial value in a matter of hours, calling for a reverse change. Consequently, the value proposition of flexible bulbous bows is not only driven by how easy it is to change, but also by how *fast* it is possible to change the system.

Fricke and Schulz (2005) define *agility* as a systems ability to change rapidly. Similarly to flexibility, the changes on the system come from external. In this thesis, the term *flexibility* will refer to the number of possible bulb configurations easily adapted to, while *agility* refers to how fast a ship can change to a new configuration. The value and need for these abilities are driven by the uncertainty in the operating context. Consequently, it is vital to model and quantify the resulting variations properly. The next chapter will address the data foundation used for evaluating variations in sailing speed.

2.4.3   Visualizing the Flexible Bulb

Before we dive deep into the context analysis and resulting value of being able to adapt, an example of how bulb flexibility materialize is presented. Figure 2.2 displays a concept model of a bulbous bow with flexibility in the length direction. The model is developed by Bang et al. (2017), who have worked on concept development of flexible bulbous bow in parallel with this study. Later in this thesis, the value of being able to extend and shorten the bulb will be discussed and analyzed, and it is recommended to keep the presented concept in mind.
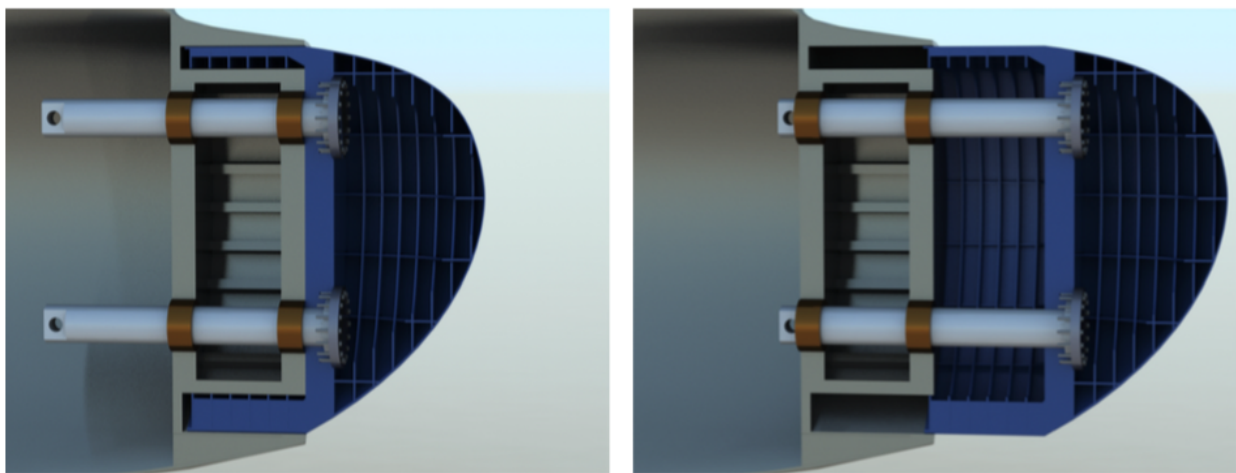
Figure 2.2: Concept model, flexible bulbous bow (Bang et al., 2017)

Chapter 3

Data Foundation

One of the cornerstones of this study is that sailing speeds can be modelled based on historical speed records. As opposed to Mao et al. (2016), who *predicted* sailing speed by combining historical speed records, engine revolutions per minute and met-ocean data, this thesis focus on *replicating the characteristics* of speed variations, solely based on historical speed records. Coraddu et al. (2014) generated distributions of sailing speeds from noon-to-noon reports, and used the distributions to sample daily sailing speeds in a bid to simulate the Energy Efficiency Operational Index. While their procedure essentially is similar, their assumption of using averaged sailing speeds to simulate sailing fundamentally contradicts with this thesis' sub-objective of capturing the frequency of sailing speed variations. Consequently, we need extensive amounts of data with high resolution, that is, speed records with small intervals.

Automatic Identification System (AIS) data will serve as the basis for speed modelling in this thesis. The following sections will address the fundamentals of AIS data, how the available data is decoded and extracted, and finally how relevant data is filtered by use of heuristics. Section 3.1, 3.2 and 3.3 are adopted from the project thesis.

3.1   AIS Data

Automatic Identification System is an automatic tracking system used on ships, that communicates through the maritime Very High Frequency (VHF) system. AIS data can be exchanged with other ships located nearby, AIS base stations or with satellites. The latter exchange type is known as S-AIS. The information exchanged from the vessels include static data such as navigational data, dynamic data from the ship sensors such as speed, in addition to voyage related data such draught and estimated time of arrival. The different message types are presented in table 3.1. Message type 1 and 2 contain the exact same information, and will for simplicity be merged into the same category when handling the data, and be referred to as message type 1. Message type 3 contains essentially the same information as message type 1, with minor differences. Message type 4 does not contain any information related to operating conditions, and will in this project

Table 3.1: AIS message types

ID	Name	Description
1	Position report	Scheduled position report
2	Position report	Assigned scheduled position report
3	Position report	Special position report, response to interrogation
4	Base station report	Position, UTC, date and current slot number of base station
5	Static and voyage related data	Scheduled static and voyage related vessel data report

Table 3.2: Key information, message type 1

Information	Description
Unixtime	Time stamp, number of seconds elapsed since 1 January 1970
Position	Latitude and longitude coordinates
Speed	Speed over ground (SOG) in knots
MMSI	Maritime Mobile Service Identity, vessel ID

be omitted for storage and efficiency reasons. Table 3.2 contains the information of key interest for message type 1, which according to Smestad (2015) constitutes 72.5% of the messages. Here, it is noteworthy that the speed is given as speed over ground, and not speed through water. The difference between speed over ground and speed through water can be significant if the ship is exposed to currents, and in the context of resistance and bulb design, speed through water is the metric of interest. This issue will be addressed in detail in section 4.4.

Message type 1 does not contain vessel descriptive information, and must be analyzed in combination with message type 5, which contains information on ship type and dimensions. Content of message type 5 is presented in table 3.3. As table 3.2 and table 3.3 show, neither of the message types contains both MMSI and speed information. MMSI is included in both message types, and will be used to connect vessel specific information to the operating conditions.

3.2 Available Data

The available data is the same data set that was utilized during the project thesis, and was provided by the Norwegian Coastal Administration, by courtesy of Harald Åsheim. The Norwegian Coastal Administration is in possession of AIS data retrieved from both base stations and satellites. AIS base stations' detection capabilities are limited to a maximum reach 40-50 nautical

Table 3.3: Key information, message type 5

Information	Description
Unixtime	Time stamp, number of seconds elapsed since 1 January 1970
Vessel specifications	Length and breadth in meters
Draught	Real time draught in meters
IMO number	International Maritime Organization identification system
Origin	Origin of voyage
Destination	Destination of voyage
ETA	Estimated time of arrival, measured in unixtime
MMSI	Maritime Mobile Service Identity, vessel ID
Ship Type	Ship type category

Table 3.4: Raw structure of AIS data

Arbitrary S-AIS message
/s:ASM//Port=638//MMSI=,c:1280622239*78/!BSVDM,1,1„A,14cTbj0vAV16ctLelSOB>Aih0D01,0*54

miles off-shore (Skauen et al., 2013), while S-AIS data can be detected from around the globe. As this study aims to investigate variations in operational conditions for vessels operating deep sea, S-AIS data is utilized. The Norwegian Coastal Administration is in possession of S-AIS data from July 2010 to the end of 2015, and the data accumulates to a total of 170 gigabytes. The data is structured as one file per day, where one file contains all messages received from all active vessels. The data is coded, and table 3.4 shows the raw structure of one single message. 170 GB data of S-AIS data is roughly equal to 2.5 billions AIS messages.

3.3   Decoding Data

The raw data is decoded by utilizing an open source aisparser provided by Lane (2006). The parser was installed as an external Python module, and extracted to an SQLite database by use of a Python script developed by Smestad (2015). All data handling, analyses and visualization in this project are conducted in Python. An initial verification of the data was conducted by finding the number of unique MMSI's in the database. According to Equasis (2016), there was a total of 87,223 vessels in the world fleet in 2015. In comparison, the number of unique MMSI's obtained from the database was 88,024. The deviation may be a result of vessels changing owner in the period.

3.4 Data Filtering

The database obtained from the decoding process contains all S-AIS messages exchanged in the period between August 2010 and December 31 2015. Obviously, a lot of this data is less interesting for this study, as it contains operational data for vessels ranging from fishing vessels and offshore vessels to tankers and bulk vessels. Hence, the data must be filtered. The static AIS messages, message type 5, contains a two-digit number specifying the ship type. The first digit represents the general category of the vessel. For example is category 6 denoting passenger ships, category 7 cargo ships, and category 8 tankers. The second digit provides additional information regarding the vessels' cargo, specifying how hazardous the cargo is. Containerships fall under category 7, meaning that the ship type field in the static messages will have a value in the range between 70 and 79. Thus, we want to extract the messages exchanged from ships with ship type between 70 and 79, and insert them into new tables in the database. In SQLite, this procedure is translated into the following query:

```
INSERT INTO CargoMT1 SELECT * FROM GlobalMT1
    WHERE userid IN(SELECT userid FROM GlobalMT5
        WHERE GlobalMT5.ship_type >= 70 AND GlobalMT5.ship_type < 80)
```

Here, userid is the MMSI number, which is the only link between dynamic and static messages. A similar, but simpler, query is applied for message type 5. At this point, the dynamic and static AIS messages for all cargo vessels are extracted and inserted into separate tables. However, the cargo category is extensive, and includes ship segments such as ore carriers, bulk carriers, cargo barges and general cargo ships. Counting the number of unique MMSI numbers in the cargo ship data reveals that approximately 36,000 vessels are included in the cargo category, and considering that the total number of containerships adds up to approximately 5,200 (Equasis, 2016), additional data filtering is obviously needed.

3.4.1 AIS Heuristics

In order to extract containerships from the more general cargo category, some heuristics from Smestad (2015) are adopted. He found that 92% of container vessels have a maximum speed above 15.9 knots, while 92% of bulk carriers have a maximum speed of 15 knots or less. He also discovered that RoRo vessels and Panamax container vessels are very hard to distinguish by maximum speed, implying that the heuristic will include RoRo vessels. This heuristic was
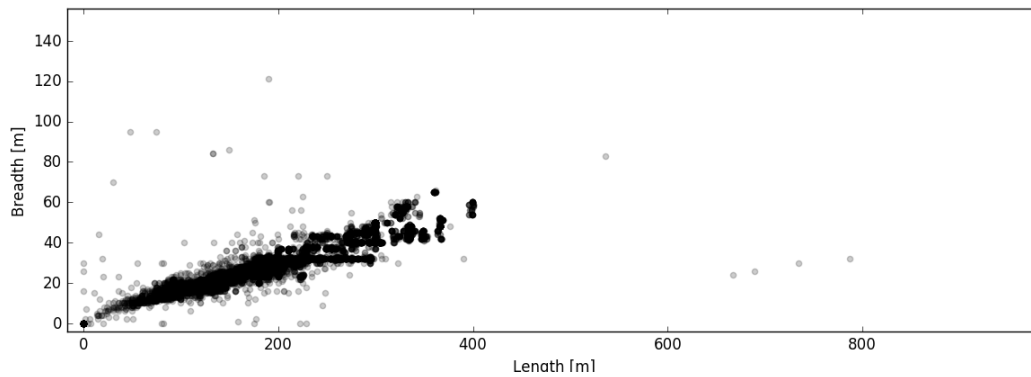
Figure 3.1: Length vs beam, sample of ships with maximum speed above 15.9 knots

applied by first creating a table of unique MMSI numbers and the corresponding maximum recorded speed, which is formulated as the following query:

```
INSERT INTO MaxRecordedSpeed
    SELECT CargoMT1.userid, max(CargoMT1.sog)
        FROM CargoMT1 GROUP by userid
```

The table MaxRecordedSpeed contains the MMSI number and maximum speed for all ships classified as cargo ships. Further, new dynamic and static tables for the vessels with maximum speed above 15.9 knots were created, and filled with the following query:

```
INSERT INTO FastShipsMT1 SELECT * FROM CargoMT1
    WHERE userid IN(SELECT userid FROM MaxRecordedSpeed
        WHERE MaxRecordedSpeed.sog >= 15.9 knots)
```

This heuristic included approximately 20,000 ships. Figure 3.1 displays the length and beam pairs of these vessels, revealing that there are several erroneous ship dimensions in the data set.

In combination with removal of the erroneous data points, operational data for vessels below 200 meters of length are filtered out, because ships below 200 meters are assumed to be harder to distinguish and few vessels below this length operate deep sea. Approximately 4,600 vessels remained in the sample after this criteria was applied. According to Equasis (2016), the world fleet included approximately 2,900 containerships with a gross tonnage (GT) of 25,000 or more as of 2015, which in the case of containerships is roughly analogue to a length of 200 meters or more. Allegedly, the sample of 4,600 ships does not only contain containerships. Smestad (2015) utilized the fact that the difference between maximum and minimum draught is signif-
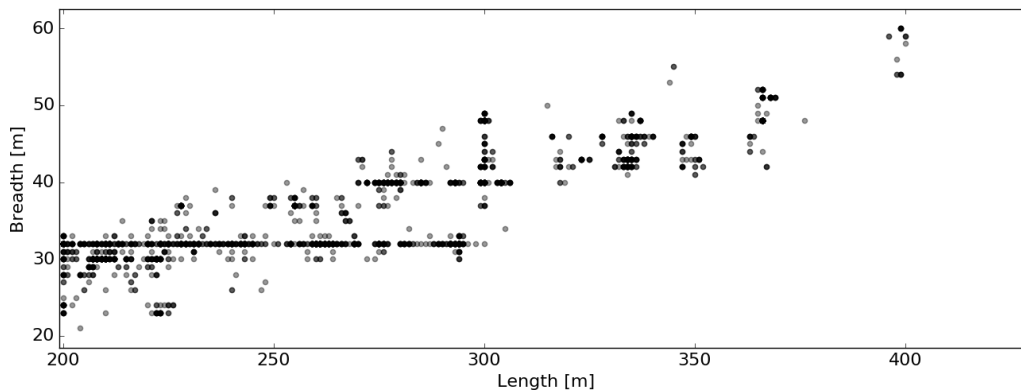
Figure 3.2: Length vs beam, containerships longer than 200 meters

icantly lower for containerships than for other cargo ships such that bulk vessels and tankers, and discovered that a heuristic filtering out vessels with difference in maximum and minimum draught above 5.5 meters worked well for identification of containerships.

The delta-draught heuristic was implemented in SQLite similarly to the maximum speed heuristic, and left approximately 3,000 vessels in the sample. Figure 3.2 shows length versus breadth for the sample of what should consist of mostly containerships. While the number of ships in the sample matches the number suggested by Equasis (2016) pretty good, the sample is likely to contain RoRo ships, and possibly other misidentified ship types. In order to filter out samples of similar ships, which is preferable for statistical analyses of AIS data, the filter criteria with respect to ship dimensions can be delimited. Later in this study the Panamax container fleet will be utilized to analyze speed characteristics. Hence, the Panamax containerships are filtered out by limiting the beam to the range between 31 and 33 meters (due to the canal width), and length between 250 and 295 meters. According to the ship register of Sea-web[1], only five RoRo and Car Carriers as of 2016 has a Panamax beam and a length above 250 meters. These vessels were removed individually.

In addition to the Panamax containership fleet, a group of containerships above 350 meters of length were filtered out. This sample group consists of New-Panamax, Post Panamax III and Triple-E vessels, and will be used to investigate some trade patterns and speed variations. Fleet information on the two groups are presented in table 3.5.

In the group of large container vessels, three different clusters are identified. There are 21 vessels between 350 and 354 meters of length, 176 vessels between 363 and 370 meters of length, and 49

---

[1]`http://www.sea-web.com/`

Table 3.5: Fleet specifications

Segment	Number of Vessels	Average Length [m]	Average Breadth [m]
Large Vessels	246	371	50
Panamax	710	276	32

vessels between 396 and 400 meters, among them Maersk's Triple-E fleet. The beam of the ships ranges from 41 to 60 meters. Obviously, all of the vessels in the Panamax group have a beam of 32 meters. The lengths range between 251 and 295 meters, and are more or less uniformly distributed, with two exceptions. 172 ships have a length between 260 and 261 meters, and 208 ships have a length between 294 and 295 meters. The fact that close to 30% of the identified Panamax vessels have the extreme length within their segment indicates that ship owners strive to maximize the payload capacity within the breadth constraint of the Panama canal.

Chapter 4

Breakdown of Sailing Speed Variability

Having extracted and filtered out historical speed records, a natural step before technical stochastic analyses of speed variability is to investigate and exemplify the dynamics and causalities behind speed variations. This chapter introduces the time frames *long-term*, *mid-term* and *short-term*, in a bid to document how and when different speed variations occur.

4.1   Long-Term Variations

Long-term speed variations, or trends, are essentially driven by two key factors; the bunker price, or implicit the oil price, and the state of the market, which is reflected in the freight rates and number of idled ships. The effect of the bunker price is obviously related to the non-linear relationship between speed and fuel consumption, with an exponent roughly equal to three. Following this logic, a speed reduction of 20% will result in fuel savings in the order of 50%. With fuel expenses accounting for 50% to 75% of total operating expenses, the strong impact of the oil price is obvious. Ronen (2011) concluded that an increase in bunker price will call for lower sailing speeds, and consequently more ships in order to meet the service demand.

The other long-term trend driver is the state of the market, i.e. the freight rates, which applies for vessels operating in both the spot -, time- and bareboat charter market (Gkonis and Psaraftis, 2012). In the spot market, the ship owner covers fuel expenses and receives the freight rate. High freight rates will increase the revenue per unit distance sailed, which will increase the ship owner's incentives for speeding up. The same goes for ships operating in the time- and bareboat charter markets. In these markets, the charterer covers both fuel expenses and charter costs. High freight rates increase the charter costs per unit time, and increase the incentives for minimizing the charter time.

Slow steaming, which simply implies steaming at lower engine speeds, exemplifies how the market and bunker price influence the sailing speeds. As a result of peak bunker prices in 2007, and the global recession in 2008, ship owners found an effective measure in slower sailing. Not only

did slow steaming reduce fuel expenditures significantly, it also absorbed excess fleet capacity by increasing transit times. Since then, slow steaming has become the industry standard. According to data obtained from DNV GL (found in appendix C.2), a typical 8,500 TEU containership has reduced the weighted mean speed from 23 knots in 2007, to 16.5 knots in 2013. This speed reduction resulted in a reduction in weighted mean fuel consumption from 196 to 98 metric tons per day. Following the logic behind long-term speed variations, slow steaming will not sustain if the market rates rises while the bunker price remains low (approximately 300$/MT at the time of writing).

However, while predicting rates and fuel prices is an impossible exercise with context uncertainty, there is no certainty in predicting steaming speeds even if prices and rates were deterministic. Maloni et al. (2013) concluded that slow steaming is optimal for a wide range of freight volumes and fuel prices, and there is no immediate signs of ships speeding up to pre-slow steaming levels. In addition to the economical aspect, slow steaming entails significant environmental benefits due to the reduced fuel consumption. The increased focus on reduced CO_2 emissions (IMO, 2011) is strongly indicating that sailing speeds are beyond peak levels.

4.2 Mid-Term Variations

Speed variations on mid-term are often a result of tactical planning problems and decisions, which include service selection, scheduling, speed optimization, cargo routing and fleet deployment (Brouer et al., 2017), and refers to speed variations from transit to transit. While these tactical factors in theory determines the sailing speed, Adland and Jia (2016b) points out that weather conditions, contractual limitations and supply chain considerations may govern the speed choice in practice. Adland and Jia (2016a), Aßmann (2012) and Aßmann et al. (2015) investigated the impact of the macro variables addressed under the long-term variations, and found that these variables have small impact on mid-term speed choice. Lindstad et al. (2013) investigated the optimal speed as a function of freight rates and sea conditions with respect to profit, cost and emissions. They concluded that varying speed according to the variables could reduce both cost and emissions significantly, a finding that in practice would entail mid-term speed variations.

An example of mid-term speed variations are presented in figure 4.1, which shows how the average speed can vary from transit to transit in a relatively short period of time. The example vessel is a 240 meters long Panamax vessel, operating on service between Australia, New Zealand and
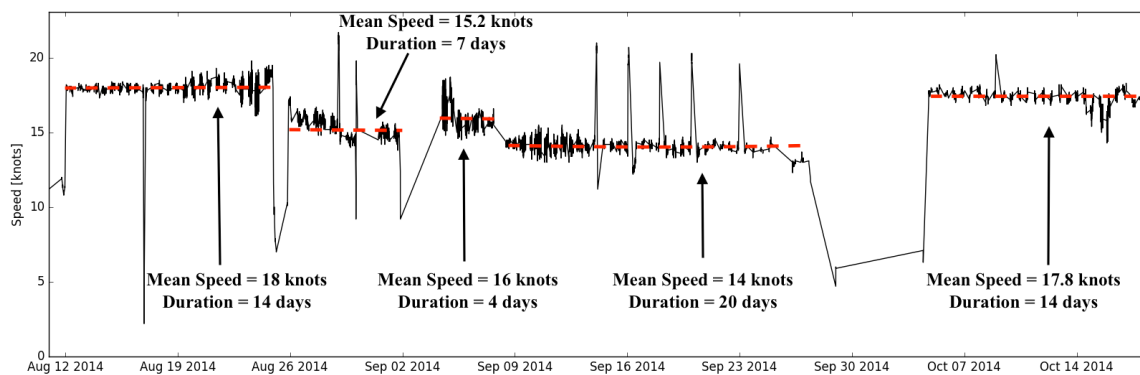
Figure 4.1: Mid-term speed variations, example Panamax vessel

Panama. As the figure shows, the mean transit speeds vary from 14 knots to 18 knots in the period between August 11 to October 18 in 2014. In addition, the plot reveals additional fluctuations around the transit means. The casualty behind the observed mid-term variations can be numerous, among them headhaul versus backhaul speed differences. Headhaul refers to the direction on which the vessel is loaded, while backhaul refers to the return trip. The industry standard entails faster sailing on the headhaul transits, as customers are waiting for cargo.

The world trade is asymmetrical, and according to WorldShippingCouncil (2014), the trans-Pacific container trade volume from Asia to North-America is twice as large as the opposite direction. Likewise, the trade volume from Asia to Europe through the Suez canal is twice as large as from Europe to Asia. This observation indicates that the average speed should be higher for west bound transits through Suez, and for east bound transit across the Pacific Ocean. The headhaul-backhaul dynamics are investigated for the two samples of containerships filtered out in subsection 3.4.1.

Table 4.1 and table 4.2 contain speed statistics for the two segments on the Europe-Asia and trans-Pacific trade, respectively. The total amount of exchanged AIS messages from vessels in the large segment is approximately 3.3 million, while the Panamax vessels exchanged approximately 31.4 million messages.

From table 4.1 it becomes evident that the large container vessels sail at significant higher speeds on the west bound transit through Suez, on average. The messages exchanged along this trade route account for approximately 48% of the total amount of messages in this segment, suggesting that vessels above 350 meters are regularly assigned to service on the Europe-Asia trade. There is no significant difference in the Panamax segment. However, it can be observed that

Table 4.1: Head- and backhaul average speed: Europe - Asia

Segment	Headhaul (Asia - Europe)			Backhaul (Europe - Asia)		
	Speed [knots]	St. dev.	Observations	Speed [knots]	St. dev.	Observations
Large Vessels	18.4	14.5%	664,311	16.7	17.5%	925,504
Panamax	16.3	26%	545,476	16.2	27%	397,132

Table 4.2: Head- and backhaul average speed: Trans-Pacific

Segment	Headhaul (Asia - North-America)			Backhaul (North-America - Asia)		
	Speed [knots]	St. dev.	Observations	Speed [knots]	St. dev.	Observations
Triple-E	18.8	14.7%	517,647	16.4	17.7%	690,914
Panamax	18.34	11.3%	4,215,056	16.4	16%	5,302,668

the standard deviation is relatively high. The reason for this may be rooted in the relatively low number of exchanged messages along the route. Of approximately 31.4 million messages, only three percent are exchanged from vessels travelling from Asia to Europe and back. This observation indicates that Panamax vessels are not commonly assigned to service along this route, which is reflected in more diffuse trade patterns.

Table 4.2 reveals significant higher sailing speeds in the headhaul direction for both segments. Exchanged messages for the large container segment account for approximately 37% of the total amount, and approximately 30% for Panamax vessels. Evidently, both segments are well represented on trans-Pacific services, and it is fair to conclude that the headhaul-backhaul dynamics are present for both segments, as well as for the large container vessel segment on the Europe-Asia trade. This is in line with the findings of Adland and Jia (2016b), who analyzed AIS speed records for Very Large Crude oil Carriers.

Another insight derivable from table 4.1 and table 4.2 is the standard deviations. For all three segment-trade combinations with sufficient data foundation, the standard deviations are higher on the backhaul transit. This reflects another tactical scheduling factor in liner shipping, namely that vessels may utilize the buffer time on the backhaul transit and speed up, should they fall behind on schedule. Consequently, one can observe more variations in sailing speed on the backhaul transits, as displayed in figure 4.2.

Figure 4.3 shows a visualization of vessel movements for the group of container vessels above 350 meters of length. Obviously, there is no sailing through the Panamax canal. Almost 90% of the AIS messages are exchange from either the trans-Pacific trade or the main Asia-Europe trade through the Suez canal, implying that the largest container vessels are mainly deployed
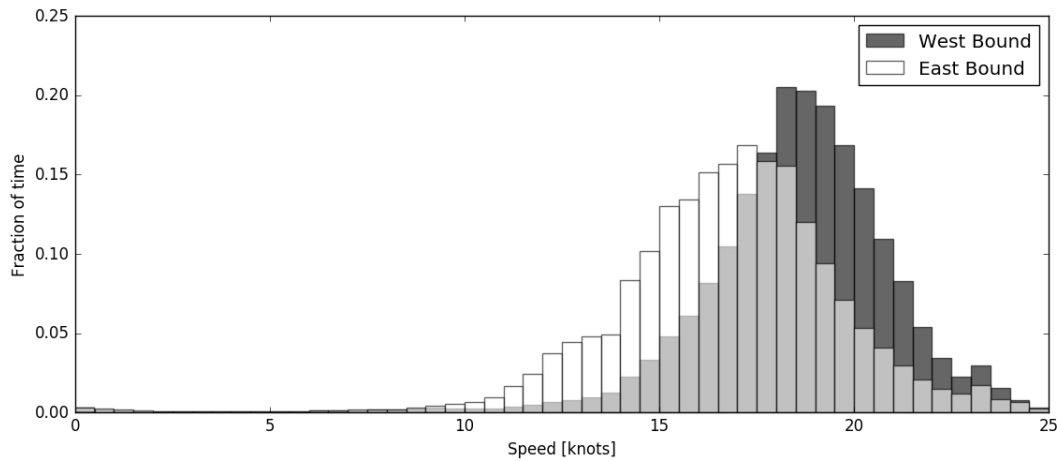
Figure 4.2: Speed distribution: Headhaul and backhaul Europe-Asia, large containerships
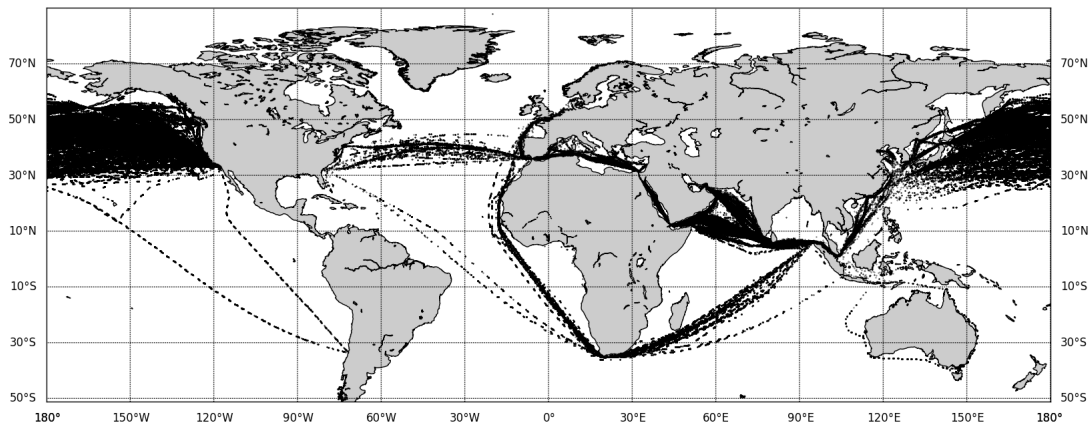
Figure 4.3: New-Panamax, Post-Panamax III and Triple-E movements

on these services. Figure 4.4 shows vessel movements for a subgroup of Panamax vessels with length between 280 and 290 meters. In this case, the traffic through the Panama canal is as evident as expected. Compared to the larger containerships, the Panamax vessels have a more diverse span of trades. This is most likely a result of the limited amount of ports capable of handling the larger vessels.

4.3   Short-Term Variations

Short-term variations refers to intra-transit speed variations, that is, variations experienced during a transit. As opposed to long- and mid-term speed variations, which are results of market
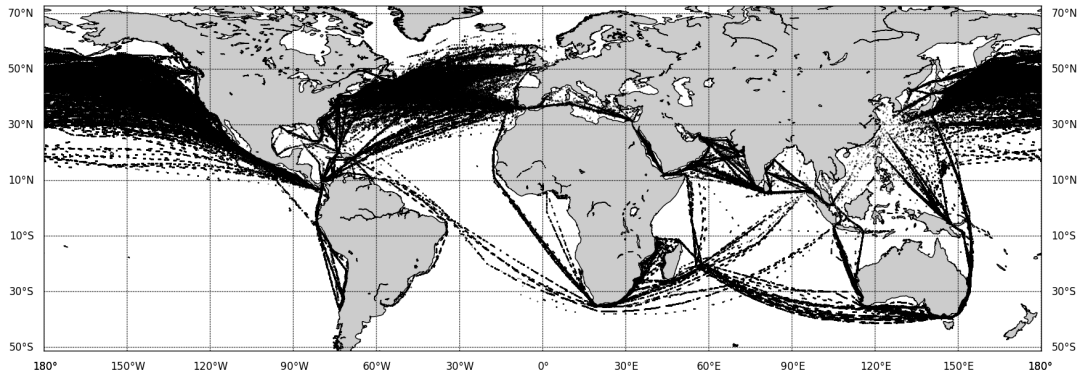
Figure 4.4: Panamax containership movements

dynamics, route planning and speed optimization, short-term variations is a result of more unpredictable day-specific circumstances. Because of the exponential relationship between speed and fuel consumption, variability around the transit mean speed should be avoided, and it can be concluded that the majority of short-term variability in speed is undesirable. According to a client case study conducted by DNV GL (DNVGL, 2015a), an 8,500 TEU container vessels can obtain fuel savings in the range of USD 100,000 per trans-Pacific transit from sailing at constant speed. The company points out that these variations stem from weather and crew behaviour. In addition, it seems like vessels starts transits at higher speeds in order to reduce the probability for being late, eventually slowing down when the port of arrival is closer.

Weather Impact

Met-ocean conditions are often, and naturally, mentioned in the literature as the single most important reason for voluntary and involuntary speed loss, and consequently speed variations (Prpić-Oršić and Faltinsen, 2012). This section will present a simple investigation of the relationship between waves and speed variations, and discuss the impact of ocean currents. The wave data analyzed in this section is downloaded from the website of Hycom[1].

Figure 4.5 shows a box plot[2] of combined significant wave height and swell in the Pacific Ocean

---

[1]The HYCOM consortium is a multi-institutional effort sponsored by the National Ocean Partnership Program (NOPP), as part of the U. S. Global Ocean Data Assimilation Experiment (GODAE), to develop and evaluate a data-assimilative hybrid isopycnal-sigma-pressure (generalized) coordinate ocean model (called HYbrid Coordinate Ocean Model or HYCOM).

[2]Box and whisker plots are uniform in their use of the box: the bottom and top of the box are always the first and third quartiles, and the band inside the box is always the second quartile (the median). The height of the whiskers describes the variations in the rest of the data set.
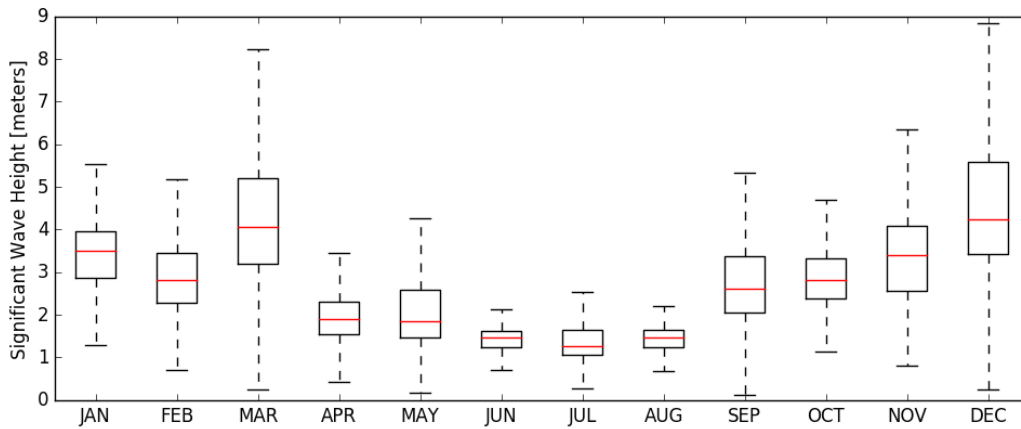
Figure 4.5: Significant wave height Pacific Ocean
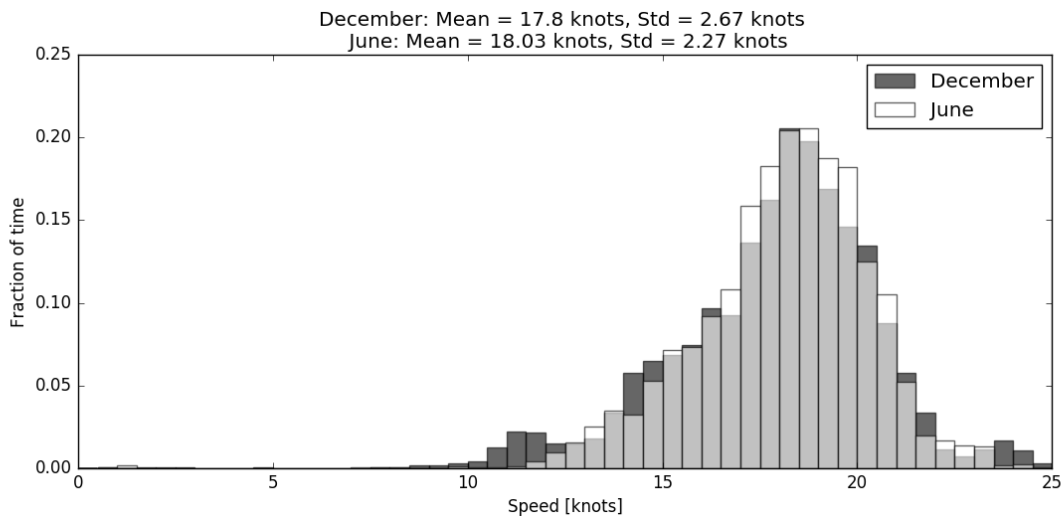
Figure 4.6: Speed distribution Pacific Ocean, December and June

in 2012 between 30°N and 50°N, the latitude range in which the majority of ships cross the Pacific. The seasonal variations are evident, which makes it trivial to investigate the correlation between ship speed and waves. Hypothetically, the seasonality should lead to higher speed variations and potentially lower average speeds in December than in June, for example.

Figure 4.6 shows the speed distribution for the Panamax fleet operating in the area in question. The figure reveals a lower standard deviation and a marginal higher average speed in June, which is in line with the hypothesis. As the dark bars representing December shows, rougher sea will sometimes force the crew to slow down for safety or comfort reasons. This is quantitatively exemplified in this case by looking at speed records below 12 knots; in June, less than 0.2% of the records where below 12 knots, while the same fraction for December is above 5%. Although it

seems like higher waves result in higher speed variability, finding the actual correlation between speed loss and wave characteristics is an extensive task alone, and will not be analyzed in detail in this study.

4.4   Speed Over Ground versus Speed Through Water

The speed records included in the AIS messages is measured as speed over ground (SOG). With AIS data as basis for the analyses, this study implicit assumes that sailing speed variations can be evaluated from the vessels' speed relative to the ground, and not through water. The fact that the speed through water (STW) is the determinant of resistance and fuel consumption makes this assumption one of the most critical of this study. Although Smith et al. (2013) claimed that the effects of currents should be negligible for trans-oceanic voyages (deep-sea transits), the potential source of uncertainty should be evaluated.

Ideally, speed variations should be analyzed with STW records, but no such data sets were available. However, SOG and STW records were obtained for an Open Hatch Carrier, in order to document and investigate how the records may differ, and comment on the resulting consequences for this study. An Open Hatch Carrier can be classified as a general cargo ship, and has a body similar to bulk vessels. Thus, the vessel analyzed in this section is designed for steaming at significant slower speeds than containerships. The purpose of this analysis is solely to point out the difference between the records. The data set includes approximately 53,000 data points with 15 minutes intervals, and spans from October 2014 to March 2017. Figure 4.7 shows and excerpt of the speed time series. Here, the green line represents the speed through water, and the red line represents the speed over ground.

As the figure reveals, both STW and SOG varies significantly over the displayed time period. However, it can be observed that speed over ground shows more short-term variability, suggesting that some of these variations should be ascribed to ocean currents. For example will a ship sailing at a speed of 17 knots over ground with currents acting in the opposite direction at one knot experience a speed through water of 18 knots.

Table 4.3: Speed statistics, speed over ground vs speed through water

Measure	Mean [knots]	Standard Deviation [knots]
Speed Over Ground	12.76	1.93
Speed Through Water	12.78	1.86
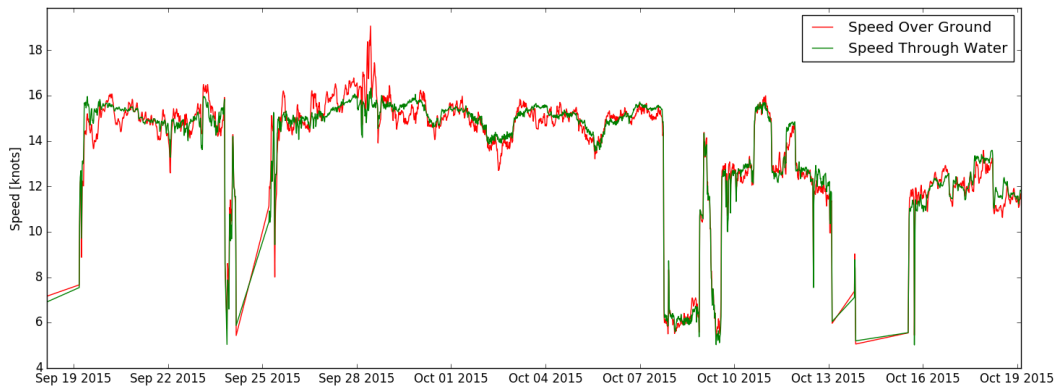
Figure 4.7: Speed over ground vs speed through water
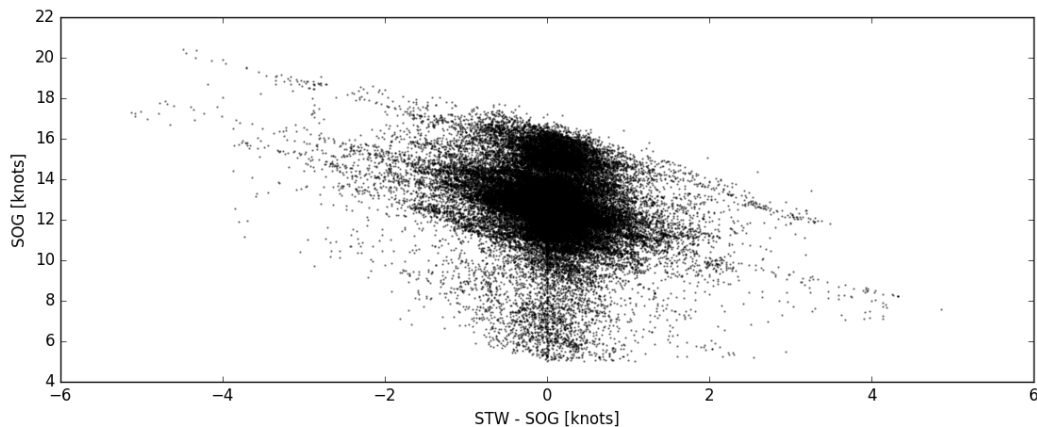
Figure 4.8: Record differences: Speed over ground and speed through water

Figure 4.8 shows a scatter plot of the relationship between (STW - SOG) and SOG. The plot is informative in the sense that it reveals where the absolute difference between speed through water and speed over ground is high. A weak downward trend line can be observed in the plot, indicating that some of the extreme SOG values should be corrected for ocean currents. From the trend it becomes evident that the higher SOG records are records where the difference between STW and SOG is high, and consequently that the highest STW records are in the range of 18 knots. Similarly, the trend indicates that some of the low SOG records should be corrected upwards. However, it can be observed that the majority of the records have a relatively uniform distributed difference, which calls for more detailed analyses.

Related to the agile space of this study, the interesting variations are the sequential variations, i.e. how much the speed changes from one time increment to the next. Figure 4.9 shows a scatter of the sequential changes between SOG records and the associated sequential changes
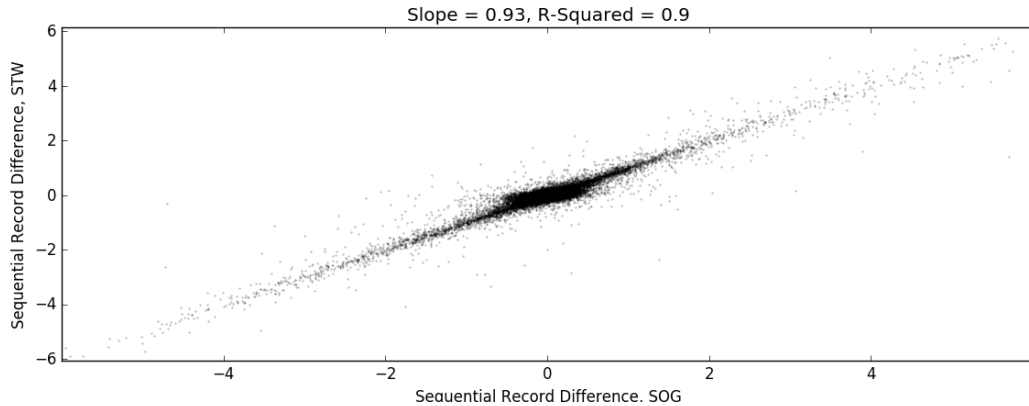
Figure 4.9: Sequential record differences: Speed over ground and speed through water

Table 4.4: Correlation, speed through water and speed over ground

Time Frame	Slope	R-Squared
15 Minutes	0.93	0.90
1 Hour	0.89	0.86
2 Hours	0.84	0.81
6 Hours	0.80	0.80
12 Hours	0.84	0.83
1 Day	0.87	0.86
3 Days	0.93	0.93
1 Week	0.99	0.96
2 Weeks	0.98	0.98

between STW records. A slope and r-squared value both equal to 1 would indicate that the two measurements corresponds perfectly.

As the plot title of figure 4.9 shows, the slope is equal to 0.93, and the r-squared equal to 0.9. Essentially, the slope indicates that for each knot SOG moves up or down, the STW moves 0.93 knots in the same direction. This means that the speed through water has a less volatile behaviour than the speed over ground. The r-squared of 0.9 implies that the model explains 90% of the variability around the mean, essentially confirming the linearity observable from the plot. This analysis explains the relationship between STW and SOG measurements with 15 minutes sample intervals. In order to evaluate how well SOG predicts STW in general, the same analysis is conducted for different time intervals.

The results are summarized in table 4.4. Higher r-squared values indicates better suitability for SOG as an estimator for STW, while the slope serves as an indicator on the relative volatility of the STW. It appears that the slope and the r-squared are somewhat correlated. From the

results it seems like SOG has lowest suitability as an estimator for STW on six hours intervals. Moreover, it seems like six hours is the interval where the STW variations are lowest relative to the corresponding SOG variations. This may be rooted the nature of ocean currents, and the time periods of which the ship experience currents acting a particular way at a time.

This section aimed to investigate the goodness of SOG as an estimator for STW. It should be noted that the analyses were carried out for one specific vessel, meaning that the results should be handled as indicators and points for discussion more than anything else. However, the results showed some clear trends, as it became evident that the STW varies less than SOG for all time intervals analyzed. At one and two weeks time intervals, it seems like SOG captures the actual STW variations with high accuracy. Connecting this insight to the mid-term speed variations displayed in figure 4.1, an initial conclusion may be that SOG tends to slightly exaggerate short-term variations, while it serves as a good estimator for mid-term variations.

Chapter 5

Statistical Representation of Speed

While chapter 4 addressed and exemplified underlying reasons for speed variability, this chapter will introduce a more technical framework for describing the variations statistically. Specifically, a stochastic process for replicating characteristics of speed variations is proposed, and the methodology for estimating the process parameters from historical speed records is explained.

5.1   Sailing Speed as Exogenous Random Variable

Stochastic modelling of historical operating speeds for forecasting purposes is not a straight forward procedure, and requires a substantial amount of assumptions. First and foremost, one can argue that sailing speed is not a random variable, as the speed at any time is determined by the captain or commanding officer. The commanding officer will alter the speed according to variations in met-ocean conditions and other daily circumstances (Ljungberg, 2017)[1], resulting in intra-transit variations and consequently affecting the short-term volatility of the operating speed. However, even the captain has limited room for maneuvering, as the average speed is contractually agreed upon when the trade is closed. As addressed in section 4.1, this speed is mainly dependent on two factors; the oil price and the freight rate (Ljungberg, 2017). Based on that assumption it should be possible to model the speed as a function of two independent stochastic processes. However, these contracts are of high complexity, affected by the bargaining power of the stakeholders, and includes a high number of embedded reservations regarding met-ocean conditions. In combination with the previously mentioned short-term variations, the human factored nature of the trade contracts makes it hard to predict operating speeds.

While optimization studies often calculates the optimal speed based on bunker price and freight rates, which are commonly modelled as stochastic processes (McNichols and Rizzo, 2012; Sødal

---

[1] Knut Ljungberg at DNV GL was interviewed on the topic, and provided a general understanding of the dynamics behind speed variations.
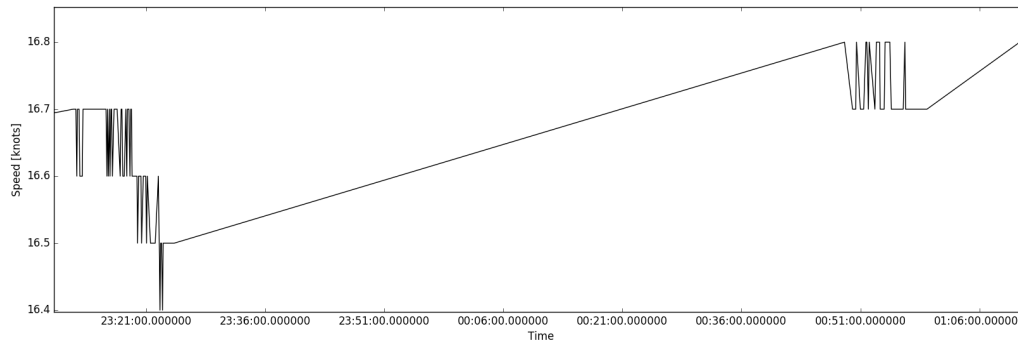
Figure 5.1: Infrequently exchanged AIS messages

et al., 2009), this study will treat the speed itself as an *exogenous* random variable. An exogenous variable is a variable that affects the model, but the model can not affect the variable. The assumption of exogenous speed variations is discussed in detail in section 9.2.1. The hypothesis is that this approach will yield a lower bound value estimation for the flexible bulb case, as the operating decision maker will have a lower threshold for altering the speed if the bulb can be adjusted. However, retrieving statistical characteristics for historical operating speeds is complicated due to the nature of S-AIS data. The intervals between the messages exchanged with satellites are highly infrequent, dependent on the satellites' relative position to the ship. Figure 5.1 displays the infrequent AIS messages exchanged from a container ship operating in the Pacific Ocean.

5.2 Identification of Stochastic Process

Sailing speed is in principle continuous data, but the speed records included in AIS messages are *quantized* to discrete intervals of 0.1 knots. Likewise, the messages are exchanged in continuous time, but the data is *sampled* at discrete intervals down to one second. Although speed records are discrete both in speed and time, the sailing speed process is essentially continuous. Hence, the AIS data provides discrete *time series* representing continuous processes. The objective is to fit these time series to a *continuous-time stochastic process*, in order to simulate future sailing speeds. A continuous-time stochastic process can be defined as a collection of random variables, and is observed in continuous time.

Stochastic processes are separated into different categories, and there exists a vast amount of different processes within each category. This study will not drill deep into the extensive field

of stochastic theory, so Tufto (2017)[2], professor at the Department of Mathematical Sciences at NTNU, was consulted on the topic. The key takeaway from this interview was that the selected process must account for the fact that sailing speed is bounded by technical and operational limitations. Technical in the sense that the process should not be able to generate sample paths that drifts above the maximum sailing speed, and operational in the sense that a sample path that drifts towards zero is unlikely during sea passage. Thus, the stochastic process representing sailing speeds should be *stationary*, meaning that process parameters does not change over time.

It is also assumed that sailing speed satisfies the *Markov property*, entailing that the current sailing speed only depends on the immediate preceding speed, and not the sailing speeds before. We will also assume that sailing speed follows a *Gaussian process*, which means that the randomness is normally distributed. Finally, as the average sailing speed for a transit often is pre-defined, the variations during a transit will likely fluctuate around (revert to) a mean value. These characteristics of sailing speed call for a *mean-reverting* stochastic process. The *Ornstein-Uhlenbeck* process is the only nontrivial stochastic process that satisfies the stationary, Markov and Gaussian conditions, and was consequently suggested as an appropriate representation of sailing speed. The process is by definition mean-reverting.

Mao et al. (2016) addressed the high auto correlation of speed records, which means that the correlation from one speed record to the next is high. This is logical in the sense that ships does not alter the speed significantly over short time periods. The assumption of high auto correlation supports the Ornstein-Uhlenbeck process as a stochastic representation of speed, as the process can be considered the continuous-time analogue of the discrete-time first order autoregressive process AR(1). For the AR(1) process, the current value is based on the immediate preceding value. An Ornstein-Uhlenbeck process has to satisfy the following stochastic differential equation (SDE):

$$dx_t = \theta(\mu - x_t) + \sigma dW_t \tag{5.1}$$

Here, x_t and dx_t represent the sailing speed at time t and the change in absolute terms, respectively. θ is the mean reversion rate. The mean reversion rate is a parameter representing how fast the process reverts towards the mean value. μ represents the mean value, σ the standard deviation and dW_t follows a Wiener process. The SDE has the following analytical solution:

$$x_t = x_0 e^{-\theta t} + \mu(1 - e^{-\theta t}) + \sigma e^{-\theta t} \int_0^t e^{\theta s} dW_s \tag{5.2}$$

---

[2]Jarle Tufto, professor at the Department of Mathematical Sciences at NTNU provided input at February 2
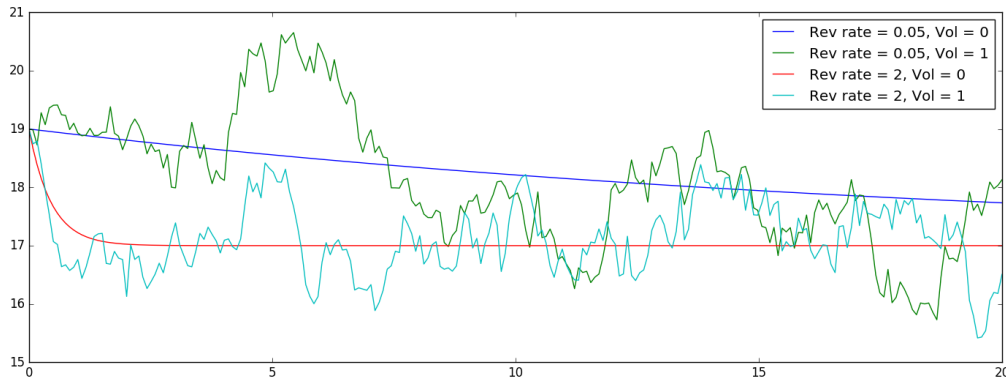
Figure 5.2: Ornstein-Uhlenbeck sample paths, mean = 17, $X_0 = 19$

In order to simulate this process, it can be discretized and approximated via:

$$X_{n+1} = X_n + \theta(\mu - X_n)\Delta t + \sigma \Delta W_n \tag{5.3}$$

Here, X_n represents the speed at time index n. ΔW_n are independently identically distributed (iid) Wiener increments, that is, normal variates with mean equal to zero and variance equal to Δt. Thus, $W_{t+\Delta t} - W_t \sim N(0, \Delta t) = \sqrt{\Delta t} N(0, 1)$. Figure 5.2 shows sample paths of the Ornstein-Uhlenbeck process with different σ and θ values. The blue and red lines show how the process behaves with absence of volatility. With high reversion rate, the process quickly drifts towards the mean, while a lower reversion rate results in a slower drift. With presence of volatility, it can be observed that a high reversion rate makes the process fluctuate frequently around the mean, while a lower reversion rate results in more diffuse variations. A reversion rate of zero implies no drift towards the mean, while a reversion rate below zero means that the process will drift away from the mean. Thus, θ must be strictly larger than zero in order for the process to make sense.

The model can be calibrated to historical data by linear regression, where θ and μ are the coefficients of a linear fit between the speeds and their difference scaled by the time interval parameter. The following linear regression is ran in order to estimate the parameters (Sundar, 2016):

$$\frac{\Delta X_n}{\Delta t} = -\theta X_n + \theta \mu + \frac{\sigma}{\Delta t}\Delta W_n \tag{5.4}$$

Calibrating data to the Ornstein-Uhlenbeck from this regression is done by using built-in Python functions. As displayed in figure 5.1, AIS messages are exchanged with highly inconsistent frequency. While the process parameters can be estimated by regression of these *unevenly spaced*

time series, time series with equal spacing reduce the number of computations necessary to estimate the parameters, as several messages sometimes are exchange within the matter of seconds. Obviously, the sailing speed does not change over such small time periods, resulting in excess data. This is solved by *resampling*[3] the data, and the next section will address the procedure and how relevant data is filtered out.

5.2.1   Parameter Estimation

While AIS messages are exchanged at all modes of operation (port, anchor, sailing, etc.), the interesting data for this study is the speed records exchanged during *sea passage*. A sea passage can be defined as the part of the transit (port to port) where the vessel has reached the intended sailing speed, and does not include the initial and final navigation from and to port. However, for simplicity, sea passages will be referred to as transits in this thesis. Transit speed records are interesting because wave resistance takes significant presence in the higher Froude regimes, and the primary purpose of the bulbous bow is to reduce this resistance component. Consequently, the goal is to estimate the process parameters of time series identified as transits. Transits are identified by filtering out time series spanning a minimum time period with consecutive speed records above an assumed minimum steaming speed, and the speed records will only be resampled (to evenly spaced records) for transit time series.

Frequency of messages exchanged with satellites varies from a few seconds to several hours, and in some cases days and weeks. In order to run the parameter estimation regression efficiently, it is preferable with equally spaced data points. The introduction of section 5.2 addressed how continuous data is sampled to discrete time intervals, and what we essentially want to do is to resample the space values (speed records), to pre-defined time intervals. First, the time interval must be determined. In this study, the frequency of speed variations is of high interest, arguing for a small time interval. On the other hand, a small time interval results in more data points, which is an important aspect bearing in mind that several millions of speed records are analyzed. Some experiments were carried out for different time intervals, and it became evident that sampling at two hour intervals captured variations of the actual speed records with relatively high accuracy, while keeping an acceptable computational run time. Essentially, this means that sailing speed variations within two hour periods are negligible, or at least neglected in this study.

---

[3]Note that the term resampling in this thesis refers to allocating data to pre-defined time intervals, and not the correct definition of the statistical term

The resampling procedure is two-fold; speed records within time periods of two hours are averaged to a single sample, while interpolated samples are allocated to the time intervals where speed records are absent. While the assumption of average resamples is rather straightforward and explained by the low variability within two hours, the interpolation requires a somewhat elaborated argumentation. The core issue is to define a maximum interpolation time span such that the true characteristics of transit speed variations are retained, while still filtering out as many transit time series as possible.

Allowing interpolation over long time periods will result in a higher number time series identified as transit time series, but the characteristics are manipulated to a greater extent due to the high amount of interpolated samples. On the other hand, allowing interpolation only over short time periods will yield higher quality of the time series, as the manipulation is limited. However, few sequences of speed records have consecutive data points with small intervals over longer time periods, meaning that strict interpolation rules will result in few transit time series. Essentially, it is a quality or quantity kind of problem. Similar to the determination of time interval, the maximum interpolation span was determined by experiments with different values. Interpolation over 12 hours was the lowest time period that retained an acceptable number of transit time series.

Table 5.1 presents a pseudo-code explaining the resampling algorithm, which is executed in the code found in appendix D.3. Figure 5.3 displays the complete set of transit time series in the period between 2012 and 2015 for a Panamax container vessel after running the algorithm. Here, T_{min} set to ten days, N_{min} to 1000, Δt_{max} equal to 12 hours, and minimum steaming speed equal to 12 knots. This implies that each time series represents a transit of ten days or more, with no interpolation between speed records with intervals above 12 hours. In other words, if the interval between two records is above 12 hours, the speed records will not be treated as records in the same transit. In this specific case, approximately 35 time transits satisfied the transit identification criteria, which resulted in 35 estimations of Ornstein-Uhlenbeck parameters.

Figure 5.4 shows one of the transit time series, where the solid line represents the resampled AIS speed records and the dashed line represents a OU sample path based on parameters estimated from that specific time series. From a visual point of view, the behaviour of the simulated process seems to replicate the dynamics of the actual sailing speed, which indicates that the Ornstein-Uhlenbeck process can be a good representation of speed variations.

While plots of actual speed and simulated speed are valuable for comparison and verification, the desired output from the resampling algorithm and parameter estimation regression is prob-

Table 5.1: Resampling algorithm, pseudo code

Step	Procedure	Action
1	Loop through raw data, index = i. Check if t_{i+1}-t_i <= Δt_{max}	If yes, append data to TS, and i = i + 1. Else, store TS and proceed to step 2.
2	Check if length of TS >= N_{min}.	If yes, proceed to step 3. Else, clear TS. Return to step 1, i = i + 1.
3	Check if $TS_{t,end}$ - $TS_{t,start}$ >= T_{min}.	If yes, TS is qualified for data manipulation, proceed to step 4. Else, clear TS. Return to step 1, i = i + 1.
4	Create time vector, TM_t, from $TS_{t,start}$ to $TS_{t,end}$ with increments equal to Δt. Pre-allocate speed vector, TM_s, with equal length.	-
5	Loop through TS, index = m, and TM, index n.	For each increment n in TM, store either an averaged or interpolated speed value at $TM_{s,n}$ depending on the time spacing in TS. Proceed to step 6 for parameter estimation based on TM.
6	From the equally spaced time series TM, estimate the Ornstein-Uhlenbeck parameters according to equation 5.4, and store them.	Clear TM and TS. Return to step 1, i = i + 1.
Δt_{max}	Maximum allowed interpolation span	
T_{min}	Minimum duration of a transit	
N_{min}	Minimum allowed number of speed records within a transit	
Δt	Pre-defined time interval for the resampled time series	
TS	Time series representing transits before resampling	
TM	The resampled transit time series, from which the process parameters are estimated.	
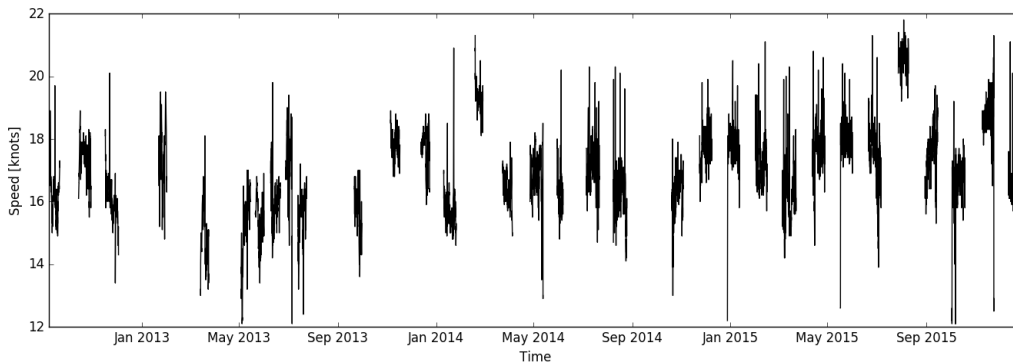
Figure 5.3: Transit time series obtained from resampling algorithm
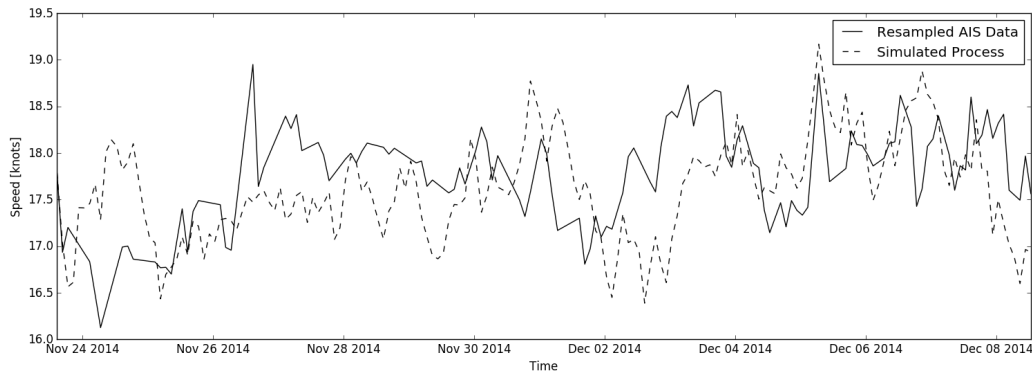
Figure 5.4: Simulated sample path vs AIS speed records, example vessel

ability density functions (PDF) of the Ornstein-Uhlenbeck parameters, from which random values can be sampled to simulate a transit. As figure 5.3 showed, roughly 35 sets of parameters were obtained from analyzing a single vessel. From a statistical point of view this number is relatively low, as it is impossible to evaluate how often the different parameters occurs. By feeding entire segments into the algorithm, a more descriptive output can be obtained. The next sections will address the fitting of PDFs to the Ornstein-Uhlenbeck parameters.

5.3 Probability Density Functions

As Monte Carlo simulations is the key methodology for evaluating the fuel savings from bulb flexibility, it is important to have probability density functions to describe the value-driving sailing speed variations. The distributions will be used to sample a mean speed, standard deviation and mean reversion rate for each simulated transit, and this section explains how Ornstein-Uhlenbeck parameters obtained from the procedure described in table 5.1 are fitted to probability density functions.

5.3.1 Mean Transit Speed

Resampling and parameter estimation of the Panamax containership fleet described in section 5.2.1 resulted in 4,363 sets of parameters, each set representing the speed dynamics of one single transit. This data can be used to obtain PDFs for each parameter, which in terms can be
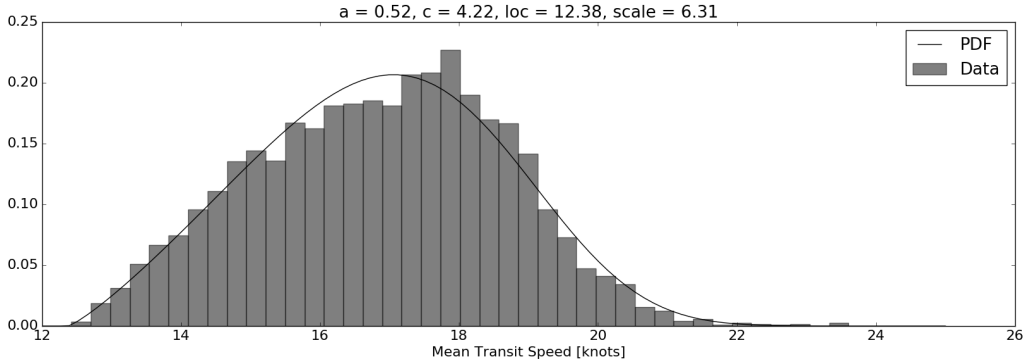
Figure 5.5: Mean transit speed distribution, Panamax containerships

sampled to simulate speed variations for transits. An open-source Python script[4] was utilized in order to obtain the best fitted statistical distributions. The script tests 82 different distribution functions in the SciPy[5] library, and returns the distribution with the least residual sum of squares (RSS) between the distribution's histogram and the data's histogram. Running the script on the mean transit speed data for the Panamax fleet returned the generalized gamma distribution, which has two shape parameters, *a* and *c* (Johnson et al., 1970). In addition, a *scale* and *loc* parameter shifts the distribution to fit the data. Figure 5.5 shows a histogram of the data, and the corresponding PDF, which is given by the following equation:

$$f(x; a, c) = \frac{|c| x^{(ca-1)}}{\Gamma(a)} e^{-x^c} \tag{5.5}$$

Here, x, a, and |c| > 0, and Γ is the gamma function. Accounted for the *scale* and *loc* parameters, the PDF becomes $f(y; a, c)/scale$ where $y = (x - loc)/scale$. The SciPy has built-in functions for distribution sampling.

5.3.2 Intra-Transit Volatility

Running the same distribution fitting script on the intra-transit volatility returned the inverse gamma distribution. The PDF of the inverse gamma distribution has two shape parameters α and β, and is given by:

$$f(x; \alpha, \beta) = \frac{\beta^\alpha}{\Gamma(\alpha)} x^{-(\alpha+1)} e^{-\frac{\beta}{x}} \tag{5.6}$$

---

[4]Adopted from following forum: https://stackoverflow.com/questions/6620471/fitting-empirical-distribution-to-theoretical-ones-with-scipy-python

[5]SciPy is a Python-based ecosystem of open-source software. https://www.scipy.org
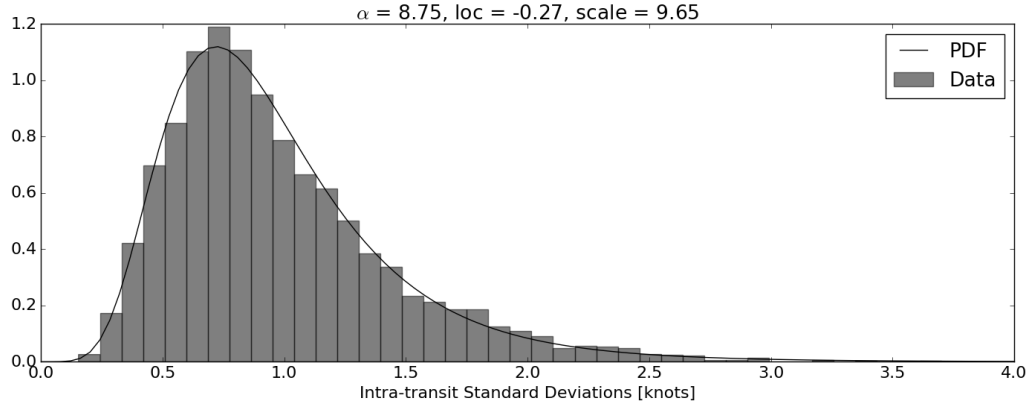
Figure 5.6: Intra-transit speed volatility distribution, Panamax containerships

In Python, β is set to 1 by default, and the distribution is fitted with α as the only shape factor, in addition to the *scale* and *loc* parameters. The distribution function is shifted with *scale* and *loc* equivalently to the Generalized Gamma Distribution. Figure 5.6 shows a histogram of the standard deviations, and the corresponding PDF.

5.3.3 Mean Reversion Rate

The reversion rates are fitted to an Exponentially modified Gaussian distribution, which in Python is described with shape parameter $K > 0$, *scale* and *loc*. The distribution can be interpreted as the sum of a normally distributed random number with an exponentially distributed random value. Here, the mean of the normal distribution is equal to *loc* and the standard deviation equal to *scale*. The probability density function is given by:

$$f(x;K) = \frac{1}{2K}e^{1/(2K^2)}e^{-x/K}\text{erfc}(\frac{-(x-1/K)}{\sqrt{2}})$$ (5.7)

where,

$$\text{ercf}(x) = 1 - \text{erf}(x) = \frac{2}{\pi}\int_x^\infty e^{-t^2}dt$$ (5.8)

Figure 5.7 displays the histogram of the data, and the fitted probability density function.
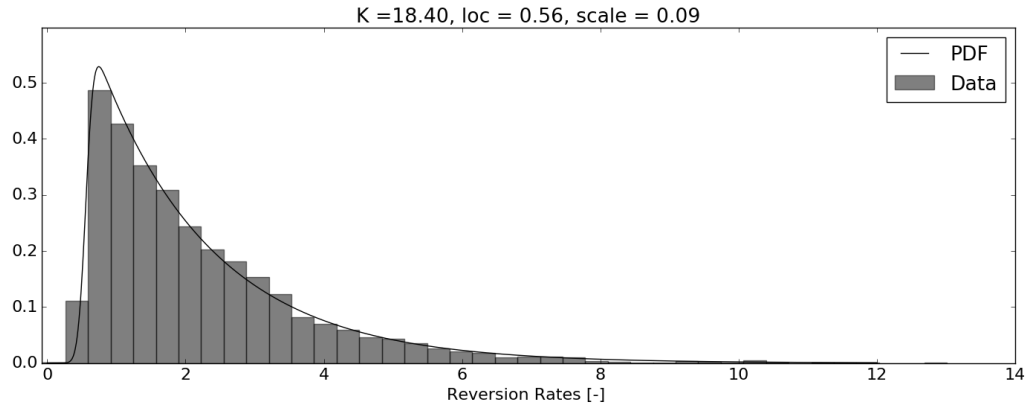
Figure 5.7: Mean reversion rate distribution, Panamax containerships

Table 5.2: Correlation table, Ornstein-Uhlenbeck parameters

Parameter		μ	σ	θ
Mean speed level	μ	-		
Standard deviation	σ	0.011	-	
Mean reversion rate	θ	0.069	0.033	-

5.3.4 Parameter Correlation

In order to determine whether the parameters are correlated or not, a simple r-squared test is ran on the data sets, with results displayed in table 5.2. As the results shows, there is no significant correlation between the parameters. Essentially, this means that parameters can be sampled independently in a simulation.

Chapter 6

General Methodology and Simulation Procedure

This chapter will introduce the generic framework used to analyze the value of being able to reconfigure the bulbous bow geometry. The framework has two key input sources; resistance data and stochastic representation of speed. Calculations and assumptions for converting the resistance data to fuel consumption are elaborated, before the methodology for simulating sailing speed according to the probability density functions and the Ornstein-Uhlenbeck process is explained. Finally, the Monte Carlo Method (MCM) used for valuation is presented.

6.1   Input to Simulation Model

6.1.1   Resistance Data - CFD Results

Resistance data is obtained from the masters thesis on the hydrodynamic effects of bulbous bow geometry. In that study, computational fluid dynamic analyses are conducted for different bulbous bow geometries in different speed regimes, and the resistance data are received on the format presented in table 6.1. Here, dx, dy and dz represent the bulb's geometrical change in the respective direction, compared to the original bulbous bow. R_W, R_F and R_T represent wave resistance, frictional resistance and total resistance. The purpose of this data is to obtain fuel

Table 6.1: Format of CFD input data

Speed [knots]	dx [m]	dy [m]	dz [m]	R_W [N]	R_F[N]	R_T [N]	ID
12	1.0	0.0	0.0	15431.5	421136.5	436567.9	1
⋮	⋮	⋮	⋮	⋮	⋮	⋮	⋮
24	1.0	0.0	0.0	119957.2	941034.1	1060991.3	1
⋮	⋮	⋮	⋮	⋮	⋮	⋮	⋮
12	0.0	0.5	0.5	16705.5	420767.0	437472.5	36

curves for different bulb configurations fitted on the same hull. This data is essential for the study, because bulb reconfigurations are represented by switching between fuel curves.

6.1.2   Calculation of Fuel Consumption

Due to the nonlinear relationships between resistance, power, and consequently fuel consumption, it is not possible to use aggregated resistance in order to evaluate fuel savings from flexible bulbous bows. Hence, the resistance data must be converted into power and fuel consumption. The equations and relationships in this section are obtained from MAN (2011). For each resistance and speed pair, the effective power P_E needed to move the ship through the water is obtained by the following relationship:

$$P_E = R_T V \tag{6.1}$$

Here, R_T represents the total resistance, and V represents the speed through water. Further, the thrust power delivered by the propeller to the water P_T is obtained by:

$$P_T = \frac{P_E}{\eta_H} \tag{6.2}$$

The hull efficiency, η_H, is equal to $(1 - t)/(1 - w)$, where t is the thrust deduction coefficient and w is the wave fraction coefficient. The thrust deduction coefficient is a dimensionless expression of the thrust deduction factor F. This factor represents the extra resistance the hull experiences due to the suction effect of the propeller. If T represents the thrust the propeller must deliver to move the ship through the water, T has to be equal to $R_T + F$. Hence, t is equal to $(T - R_T)/T$. The wave fraction coefficient w is a dimensionless expression of the effective wake velocity at the propeller. As a result of the boundary layer caused by the friction of the hull, the water velocity arriving at the propeller V_A will be lower than the ship's speed through water V. The effective wake velocity V_W represents the difference between V and V_A, and $w = V_W/V$. This value is heavily dependent on the shape of the hull, but also on the location and size of the propeller.

Increased block coefficient results in increased hull efficiency η_H, which is usually in the range between 1.1 and 1.4 for ships with one propeller, and between 0.95 and 1.05 for ships with two

propellers. Further, the power delivered to the propeller is obtained by:

$$P_D = \frac{P_T}{\eta_B} \tag{6.3}$$

The propeller efficiency behind hull, η_B, is the product of the relative rotative efficiency η_R and the open water propeller efficiency η_0. The latter is the efficiency of the propeller when it operates in a homogeneous wake field without a hull. η_0 can vary between 0.35 and 0.75, with high values occurring when the wake fraction coefficient is low. The relative rotative efficiency is accounting for the rotational nature of the water flowing to the propeller behind the hull. For ships with one propeller the rotational flow is beneficial, and the efficiency is in the range between 1.00 and 1.07, while it for ships with two propellers is approximately 0.98.

In order to obtain the brake power P_B of the main engine, which determines the fuel consumption, we use the following relationship:

$$P_B = \frac{P_D}{\eta_S} \tag{6.4}$$

Here, η_S is the shaft efficiency, and represents the power loss between the engine and the propeller. Multiplying the hull efficiency η_H and the propeller efficiency behind the hull η_B with the shaft efficiency η_S, we get the total efficiency η_T. Thus, we have the following relationship between the brake power of the main engine, the effective power and the resistance obtained from CFD analyses:

$$P_B = \frac{P_E}{\eta_H \eta_B \eta_S} = \frac{P_E}{\eta_T} = \frac{R_T V}{\eta_T} \tag{6.5}$$

With P_B calculated, we need information on specific fuel consumption *sfc*, in order to aggregate the fuel consumption.

6.1.3 Specific Fuel Consumption

Specific fuel consumption is by definition the fuel consumption of the engine related to brake power (Stapersma et al., 2002).

$$sfc = \frac{\dot{m}_f}{P_B} \tag{6.6}$$

Here, $\dot{m}_f$ represents the amount of fuel consumed per unit time, and is essentially the fuel consumption as a function of engine speed. Specific fuel consumption is often specified in the specifications of the engine, and is measured in amount of consumed fuel per kilowatt-hour (kWh). Having the relationship between brake power and sailing speed and engine specifications obtained, the fuel consumption as a function of sailing speed can be obtained by rear-

ranging equation 6.6.

6.1.4 Sailing Speed and Transit Characteristics

The other key input to the model is the probability density functions (PDF) representing the Ornstein-Uhlenbeck parameters addressed in section 5.3. The purpose of this input is essentially to make the model replicate speed variations according to historical records. Consequently, it is of great importance to calibrate the PDFs for the specific vessel subject for simulation to ensure that the simulated variations are realistic.

In addition, the model need transit characteristics. In this study, transits are simplified by assuming an average duration. Combining this average duration with an utilization factor, that is, the fraction of time the vessel spends at sea, results in a number of transits over a period. Thus, the length of the period we want to simulate defines the number of simulated transits.

6.2 Simulation of Sailing Speed and Fuel Consumption

This section will lay out the general methodology for simulating sailing, aggregating the corresponding fuel consumption and estimating the resulting value of having geometrical bulbous bow flexibility. The calculations are executed in the code found in appendix D.4. For each transit, i.e. sailing from one port to another, within the specified time period, the model samples OU parameters according to the probability density functions obtained in section 5.3, representing the speed characteristics. Having selected the transit specific set of OU parameters, the model alters the speed every second hour according to the OU process described in section 5.2. The Monte Carlo Method is in essence the generation of random objects or processes (Kroese et al., 2014), which makes the generation of sailing speeds a Monte Carlo method by definition. Figure 6.1 shows a plot of sailing speed sample paths over the course of a year. In this case, the transit duration was set to 20 days, and the different transits are visually separated on the plot by the vertical lines.

Next, the *agility* of the simulated system, i.e. how fast the bulb geometry can be reconfigured, is specified. This is a static variable (valid through the entire simulation), and can only be changed manually between simulations. Further, the associated fuel consumption at each generated speed point is calculated for each bulb design based on the resistance input described in section 6.1.1. According to the allowed reconfiguration frequency and number of available bulb
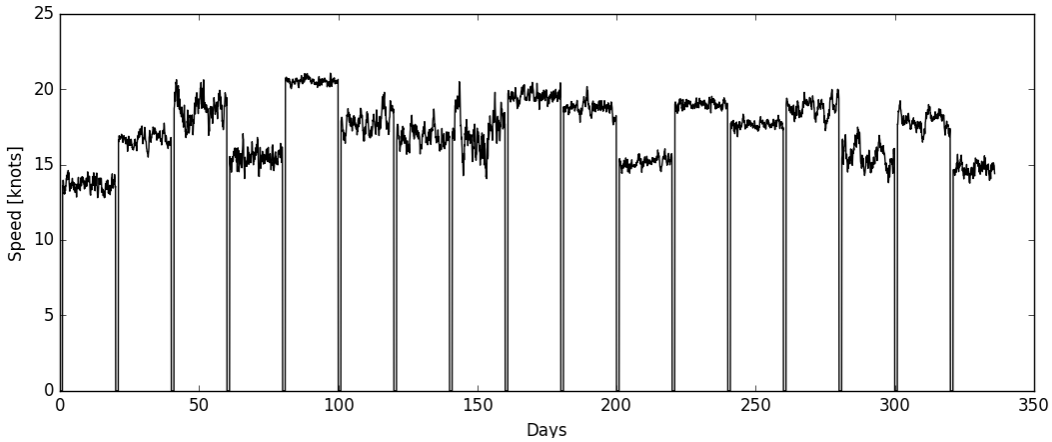
Figure 6.1: Sailing speed sample path, one year

configurations, the simulated ship can change bulb geometry if the experienced speed yields a lower fuel consumption for another bulb design. Essentially, in line with the constraints, the model switches fuel curve in the set of bulb designs and associated fuel curves to minimize the fuel consumption. Switching fuel curve in the model represents a real world change of bulb geometry, and the possibility to minimize fuel consumption at certain time steps drives the value of flexibility. The aggregated fuel consumption for a vessel with flexible bulbous bow FC_{flex} is obtained by:

$$FC_{flex} = \sum_{t=1}^{T} \sum_{i=1}^{N} \frac{R}{24} f_{bi}(v_i) \tag{6.7}$$

where,

$$b_i \in (B_i) \tag{6.8}$$

Here, T is the number of transits in one simulated period. N is the number of increments in each transits, as the simulation is discrete in time (discretized continuous-time stochastic process). R represents the time delta between time indices in unit hours, and is divided by 24 as the fuel consumption is given as metric tonnes per day. The fuel consumption f is a function of speed v, which takes a new value at each time index i according to the OU process. The fuel consumption curves are indexed by b_i, which consequently represents the bulb geometry at time index i. b_i must be in the dynamic set of allowed bulb configurations B_i. Assume a ship with three different bulb configurations are simulated, with the option of changing every fourth hour. The ship starts out with bulb ID 1. At time index $i = 0$, zero time has passed and the set of allowed bulb configurations is complete; $B_0 = \{1, 2, 3\}$. At this point, the commanding officer decides to switch configuration to bulb ID 2, based on the expected sailing speed for the hours ahead. Thus, b

takes the value 2. At time index $i = 1$, two hours have passed since the last change in geometry, and it not possible to take on a new configuration. Consequently, B_i only contains b_{i-1}, and $B_1 = \{2\}$. In general, the selection of b can be mathematically formulated by minimizing the fuel consumption at speed v_i:

$$Z = \min f_{bi}(v_i) \tag{6.9}$$

s.t.

$$b_i = \begin{cases} \{1, ..., N_b\}, & \text{if } R(i - i_c) \geq t_{min} \\ b_{i-1}, & \text{otherwise} \end{cases}$$

N_b represents the number of bulb configurations, i_c the most recent time increment with bulb reconfiguration, and t_{min} the minimum allowed period between reconfigurations.

Aggregated fuel consumption for a ship without bulb flexibility is calculated similarly to equation 6.7, without the option of minimizing fuel consumption by switching fuel curve. If we denote the fuel consumption for a static bulbous bow FC_{stat}, the percentage fuel saved from having flexibility F_{saved} is given by:

$$F_{saved} = \frac{FC_{stat} - FC_{flex}}{F_{stat}} \tag{6.10}$$

The absolute value of saved fuel can be interpreted as the shaded areas on figure 6.2. The lower plot illustrates speed variations similar to the simulated process presented in figure 6.1, while the resulting variations in fuel consumption for two different bulb designs are displayed in the upper. In this illustrative case, one bulb is obviously better suited for higher speeds, while the other one is better suited for lower speeds. Assuming for this example that the original bulb is the one optimized for high speeds, i.e. the line with lower amplitude, the added value from flexibility between the two configurations will be the sum of the shaded areas. The hypothesis is that for every bulb configuration option that is added, the shaded area expands and the value of flexibility increases.

6.2.1 The Value of Agility

The value of agility can be derived from figure 6.3. The figure shows an excerpt of a sailing speed sample path (red line), and the corresponding fuel consumption for two different bulb designs. Chapter 7 elaborates how the fuel consumption data is calculated. In this case, the vessel can choose between the original bulb (designed for high speeds), and a bulb optimized to
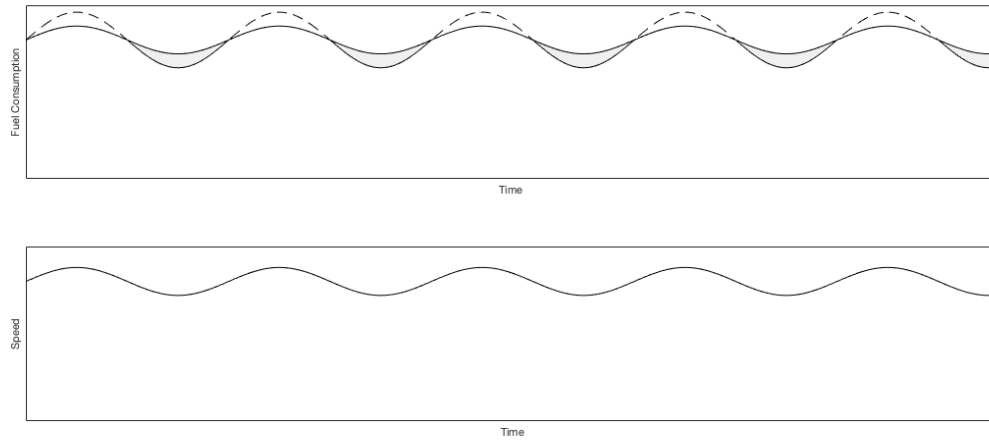
Figure 6.2: Speed variations and associated fuel consumption, illustration
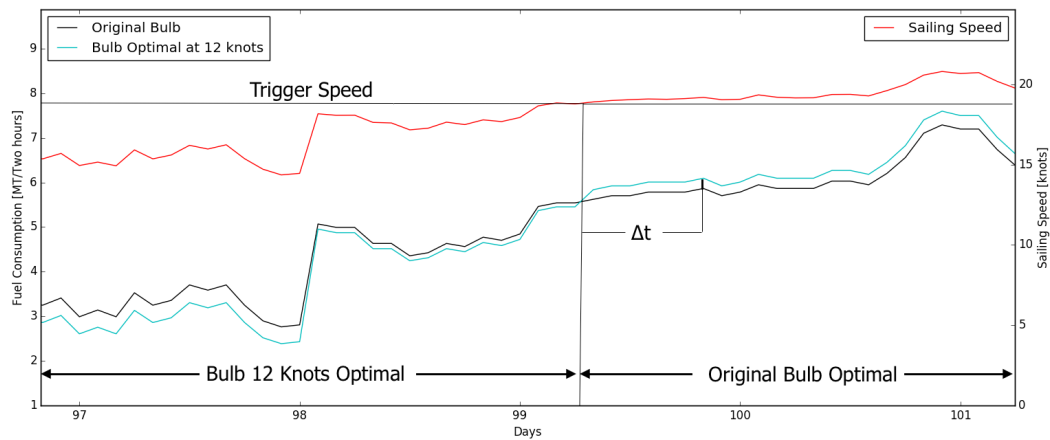
Figure 6.3: Speed sample path with associated fuel consumption for two bulb configurations

a design point at 12 knots. At sailing speeds below approximately 19 knots, the bulb optimized for 12 knots yields a lower fuel consumption. Thus, 19 knots represents the trigger speed, and when the vessel speeds up above this level, it becomes beneficial to reconfigure the bulbous bow. Now the agility part becomes interesting; if we let t^* denote the trigger time, and Δt the time period from when the trigger speed is reached until the bulb reconfiguration is executed, the *lost opportunity cost* (LOC) from not adapting immediately becomes:

$$LOC = \int_{t^*}^{t^*+\Delta t} \left[f_{12}(v(t)) - f_{or}(v(t)) \right] \mathrm{d}t \tag{6.11}$$

Here, $f_{12}(v(t))$ and $f_{or}(v(t))$ represent the fuel consumption (as a function of speed) for the bulb optimized for 12 knots and the original bulb, respectively. The lost opportunity cost grows with increased Δt, and as lower Δt means more agility, the value of agility can be interpreted as a reduced lost opportunity cost. Over time, the lost opportunity cost accumulates, as displayed in figure 6.4. The aggregated lost opportunity cost can be formulated mathematically:

$$LOC_{agg} = \sum_{i=1}^{N} \left(\int_{t_i^*}^{t_i^*+\Delta t} |f_{12}(v(t)) - f_{or}(v(t))| \mathrm{d}t \right) \tag{6.12}$$
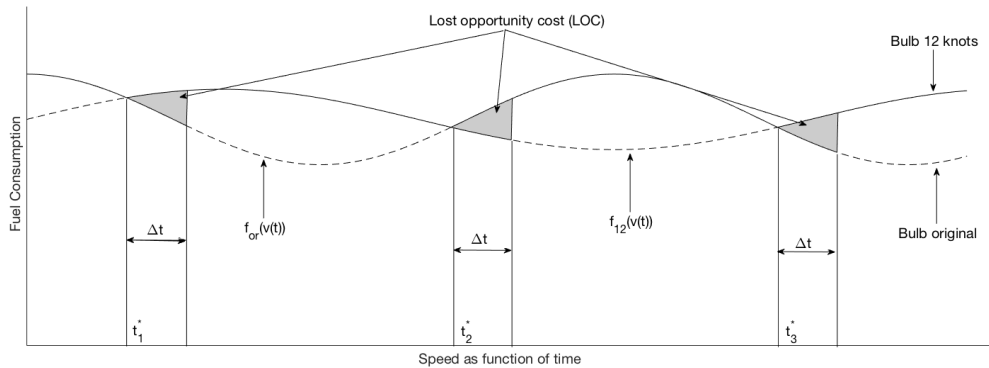
Figure 6.4: Lost opportunity cost: An inverse proxy for the value of agility

Combining the insights from figure 6.4 and equation 6.12, we see that the value of agility is driven by how often the speed crosses the trigger speed, and by how fast the system can adapt to these variations.

6.2.2 Monte Carlo Method for Estimation of Fuel Consumption

As the model samples Ornstein-Uhlenbeck parameters from probability density functions for each transit, and each transit follows a stochastic process according to those parameters, the Monte Carlo simulated fuel savings for a given period is essentially only one *realization* of the potential savings. Consequently, and in line with the estimation branch of the Monte Carlo method (Kroese et al., 2014), the simulations should be repeated many times, and the distributions of the sampled realizations serve as the output for evaluation.

Chapter 7

Case Study

This chapter will present the details and procedure for a case study, which estimates the expected fuel savings from having different levels of bulbous bow agility. The selection of case study is rigorously delimited by the available hydrodynamic data, which in terms is delimited by the available hull models for computational fluid dynamics analyses. Although analyses of AIS data indicate that speed variations occur on both short and medium term for a wide range of containerships, an actual simulation of fuel consumption and potential savings from flexibility can only be carried out for a case where resistance data is available. Thus, a representative set of historical AIS data must be used to describe speed variations, in order to capture the value of bulb agility. A representative set of AIS data comprises speed records for ships with similar dimensions to the hull model used for hydrodynamic analyses, which is addressed in the following section.

7.1   The KRISO Container Ship

The CFD analyses computed in parallel with this study utilize the KRISO Container Ship (KCS), a hull geometry developed and made publicly available by the Korean Research Institute for Ship and Ocean Engineering (KRISO). As the only open-source hull with the shape of a modern containership, the KCS was essentially the only option for CFD analysis. There have been conducted several studies on bulbous bow optimization on the KCS. Filip et al. (2014) optimized the bulbous bow for a typical slow steaming profile, obtaining an average resistance reduction of 7%. Wagner et al. (2014) utilized the KCS for scenario based optimization of the bulbous bow based on noon-to-noon reports from a representative 3,600 TEU containership, obtaining an weighted effective power reduction of 2.7%. Chrismianto and Kim (2014) conducted a parametric bulbous bow design on the KCS, and discovered that larger Froude numbers yields a longer and higher bulbous bow. In addition to pure bulbous bow analyses, the KCS is utilized in a wide range of hull studies. Among them is Tezdogan et al. (2015), who investigated slow steaming's effect on ship behaviour. They showed that slow steaming has beneficial effects on reducing

Table 7.1: Main particulars (full scale), KCS

Main Particulars	Value
Length Between Perpendiculars	230 m
Beam	32.3 m
Design Draught	10.8 m
Design Speed	24 knots

ship motion, in addition to the more obvious reduction in power and fuel consumption. The main particulars of the KRISO Container Ship is presented in table 7.1 Although the KCS does not exist in full scale, it's theoretical payload capacity is 3,600 TEU. Furthermore, the beam indicated in table 7.1 shows that the KCS can be considered a Panamax containership by definition. However, with a length of 230 meters, the ship is definitely in the lower end of the segment with respect to size, which must be accounted for in modelling of speed variations.

7.2 Resistance Data

The resistance data obtained from CFD analyses was on the format presented in table 6.1, and the actual data used in simulations is reformulated and shown in table 7.2. For the analysis of bulb flexibility with variable length, seven different bulb configurations were investigated. Every bulb configuration has the same cross-section, and different lengths. Essentially, the resistance data for ID 1-7 in table 7.2 represents resistance for the KCS with the option of changing the length of the bulb. The first row represents the resistance data for the original KCS, and consequently the base case resistance for comparison to the flexible case. Looking at the reductions it becomes evident that the maximal obtainable fuel savings is 3.7% for this set of bulb configurations. In that case, the ship sails at 15 knots constant speed, with bulb ID 2. However, this is scenario contradicts with the premise of this study, namely that speed variations do occur.

An interesting observation from table 7.2 is the correlation between optimal bulb length and sailing speed. The data indicates that shorter bulbs are better suited for sailing at slower speeds, while higher sailing speeds call for longer bulb design. This is in line with bulb theory; the waves generated by the hull at slow speeds will have less potential than at high speeds. As the internal volume of the bulb determines the potential of the wave generated by the bulb, and the length of the bulb is proportional to its internal volume, a shorter bulb will generate a wave of less potential. Moreover, higher sailing speeds will generate hull waves of longer period, which also is the case for longer bulbs. Following the logic of destructive interference, it is reasonable that

Table 7.2: Resistance [kN], seven bulb lengths, Δy = -0.8 m, Δz = 0.9 m

ID	Δx [m]	12 knots	15 knots	18 knots	21 knots	24 knots
Original	0	**378.1****	**586.7****	**839.4****	1114.1	1776.8
1	-2	**367.8***	570.5	818.4	**1116.8****	**1788.2****
2	-1.35	370.3	**564.9***	817.9	1114.3	1784.3
3	-0.7	370.6	565.3	818.3	1113.2	1781.8
4	0	370.9	570.1	**813.0***	1114.0	1781.1
5	0.7	370.9	570.6	813.5	1112.6	1779.8
6	1.3	371.0	570.7	821.6	**1102.1***	1778.0
7	2	371.5	571.3	823.3	1114.0	**1754.5***
Reduction**	-	-2.8%	-3.7%	-3.1%	-1.1%	-1.3 %

* Lowest resistance in speed regime
** Highest resistance in speed regime
*** Percentage difference between original and best case
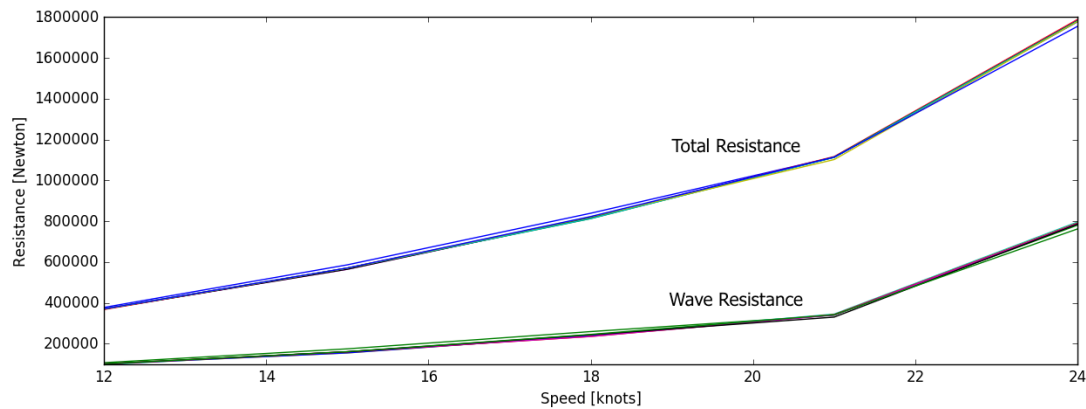
Figure 7.1: Resistance vs speed, seven bulb lengths

shorter bulbs generates better counter acting waves at slow speeds.

While the bulb configurations are optimized with intervals of three knots, the Ornstein-Uhlenbeck process allows the simulated speed to take on speed values in the continuous space. Resistance are roughly proportional to the speed to the power of two, which in theory should make it possible to fit a second order regression line to the data. However, the exponent is not constant across the speed regimes, which complicates the polynomial fit. Thus, the resistance data is interpolated to intervals of 0.1 knots. This simplification may reduce the accuracy of resistance data in the regions where CFD analyses is not conducted, especially in the higher speed regimes. Figure 7.1 shows the wave and total resistance plotted against speed for the different bulb configurations. Due to the relatively low difference in resistance, it is hard to distinguish the lines representing each configuration.

7.2.1 Sea Margin

In order to account for actual sea states, a *sea margin* is added to the calm water resistance obtained from CFD analyses. The sea margin includes added power due to waves, wind and fouling, and is often set to a fixed value in the range between 15% an 35% (Arribas, 2007; Nabergoj and Prpić-Oršić, 2007; MAN, 2011). While Eide (2015) concludes that the sea margin is speed dependent, it will for simplicity be assumed to be constant at 20% in this study. This is argued by the assumption of treating speed as an exogenous variable, and that the key output in this study is the percentage of fuel saved from having a flexible bulb.

7.2.2 Hull and Propeller Efficiencies

In order to convert resistance data into the needed total power, several hull and propeller efficiencies must be estimated. No case-specific calculations on the efficiencies have been conducted, and all numbers are based on estimates from MAN (2011). For the following analyses and estimates, a reference ship is used to retrieve engine and operating data. The reference ship is selected based on a combination of similarity to the KCS and amount of exchanged AIS messages, in order to ensure a solid data basis for comparison to the segment data. For legislative reasons[1], the reference ship must remain anonymous.

The reference ship is equipped with one fixed pitch (FP) propeller, which yields a hull efficiency η_H in the range between 1.1 and 1.4. Knowing that higher block coefficient results in higher hull efficiency, the hull efficiency is set to 1.2 due to the slender nature of mid-sized containerships. The open water propeller efficiency η_O ranges between 0.35 and 0.7. Utilizing the available propeller characteristics of the KRISO Container Ship (five blades, D = 7.9 meters) in combination with data from MAN (2011), the open water propeller efficiency is set to 0.55. For ships with single propellers, the relative rotative efficiency η_R is normally around 1.0 to 1.07. Conservatively, the value is set to 1.0, and the propeller efficiency working behind the ship η_B is obtained by multiplying η_O and η_R.

The final efficiency needed to obtain the total power, the shaft efficiency η_S, is usually around 0.99. Multiplying η_H, η_B and η_S, we obtain a total efficiency η_T of 0.65. Now, the needed total power can be calculated according to equation 6.5 in subsection 6.1.2. The hull and propeller efficiencies used in the case study is summarized in table 7.3.

---

[1]Refers to the agreement with the Norwegian Coastal Administration

Table 7.3: Hull and propeller efficiencies, summarized

Efficiency	Notation	Interrelation	Value
Hull	η_H	-	1.2
Open Water Propeller	η_O	-	0.55
Relative Rotative	η_R	-	1.035
Behind the Hull Propeller	η_B	$\eta_O\,\eta_R$	0.55
Shaft	η_S	-	0.99
Total	η_T	$\eta_H\,\eta_B\,\eta_S$	0.65
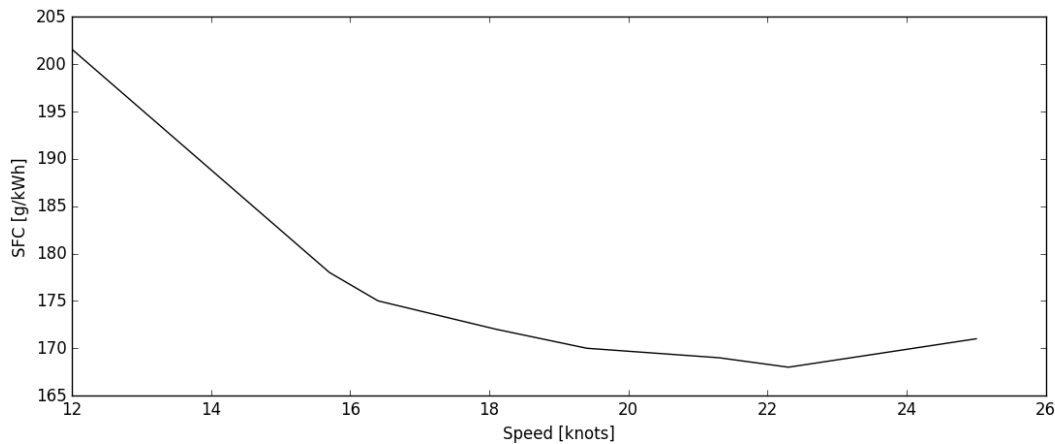
Figure 7.2: Specific fuel consumption vs sailing speed

7.2.3 Specific Fuel Consumption

The reference vessel is equipped with a two-stroke single acting diesel engine, with seven cylinders and a maximum continuous rating (MCR) of 38,000 kilowatts at 100 revolutions per minute. At 90% MCR, the service speed is 24 knots. As there is no available data on the exact engine, specific fuel consumption curves for low speed diesel engines from Stapersma et al. (2002) are calibrated to data points from an engine with similar characteristics (MAN, 2015). Assuming a sailing speed of 25 knots at MCR and a cubic relationship between speed and power, the relationship between sailing speed and specific fuel consumption (SFC) presented in figure 7.2 is obtained. Having calculated total power and SFC as functions of sailing speed, obtaining total fuel consumption as a function of sailing speed is trivial. Figure 7.3 shows the fuel consumption per day as a function of speed for the bulb configurations presented in table 7.2.
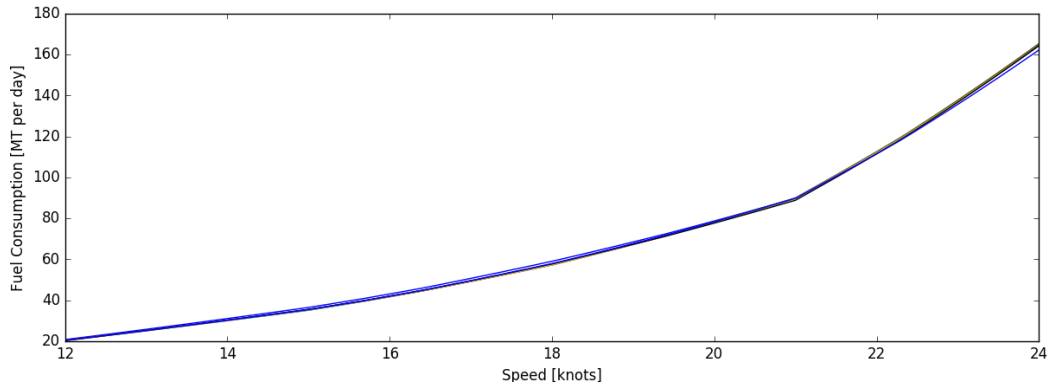
Figure 7.3: Fuel consumption per day
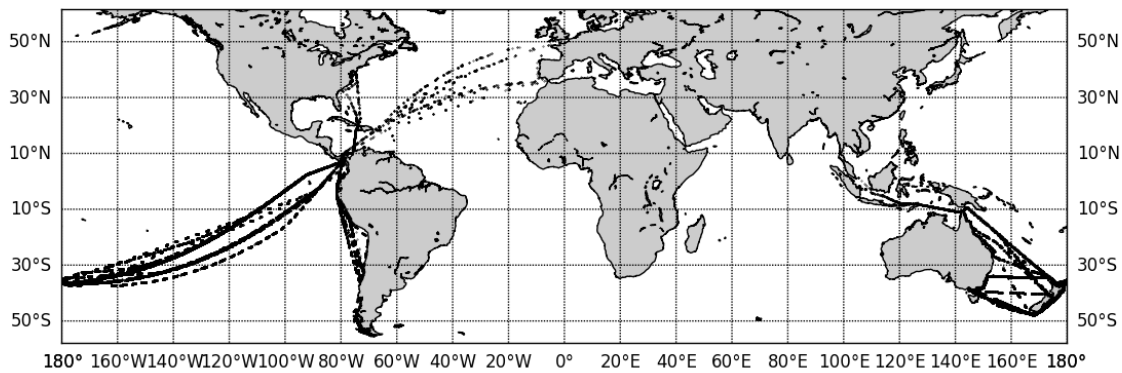
Figure 7.4: Area of operations, reference vessel

7.3 Calibrating Stochastic Parameters

As addressed in subsection 5.2.1, distributions of Ornstein-Uhlenbeck parameters are advantageously obtained by data resampling and parameter estimation of entire segments, since the data basis for individual ships is often insufficient. Because the KCS qualifies as a Panamax vessel, it is reasonable to use parameter probability density functions from this segment. However, the segment data spans more than 700 vessels, with lengths ranging from 250 to 295 meters. The data set is not descriptive in the sense that there could be, and essentially is, both design and operational differences and variations between vessels in the sample group. Using the PDFs from the segment without calibrating for vessel to vessel differences will fail to capture the true value of bulb flexibility, and the fuel savings will be exaggerated. Hence, the parameter PDFs are calibrated to the operating data for the reference ship. Figure 7.4 shows the areas of operation of the reference ship in the period between 2010 and 2015.

Table 7.4: Ornstein-Uhlenbeck parameter comparison, reference ship vs segment

Parameter	Maximum		Minimum		Mean	
	Reference	Segment	Reference	Segment	Reference	Segment
μ	20.6	23.6	13.8	12.42	16.9	16.9
σ	3.2	3.7	0.61	0.15	1.43	0.97
θ	8.52	13.01	0.53	-0.06	2.18	2.18
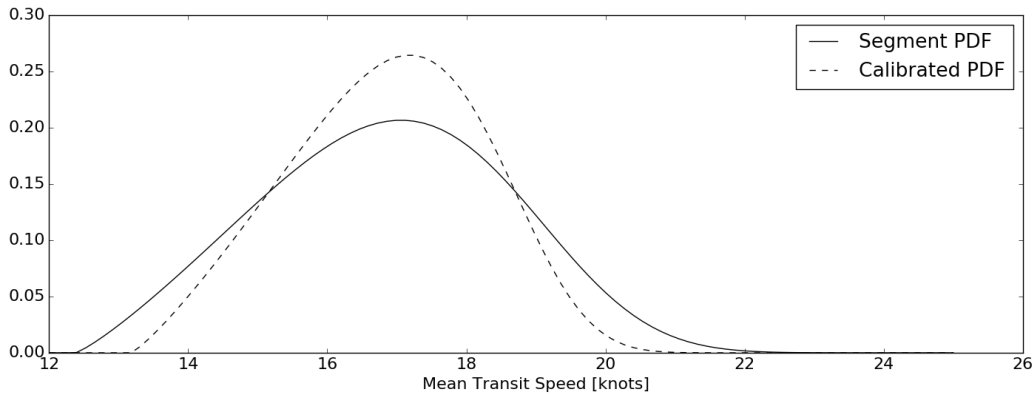
Figure 7.5: Case-calibrated mean speed distribution

Table 7.4 shows a comparison of the Ornstein-Uhlenbeck parameters between the reference vessel and the Panamax fleet. Some significant differences are revealed, whereby the most important are related to the mean transit speeds. The minimum mean transit speed recorded for the reference vessel is 13.8 knots compared to the segment minimum of 12.42 knots, indicating that there exists vessels in the sample group steaming at significant slower speeds than the reference vessel. Thus, the generalized gamma probability density function is calibrated by tweaking the parameters *a*, *c*, *loc* and *scale*, and displayed in figure 7.5.

Calibrating the intra-transit standard deviations is done in a similar manner, by tweaking the *α*, *loc* and *scale* parameters of the inverse gamma distribution. For the mean reversion rates, the *K*, *loc* and *scale* parameters are calibrated according to the exponentially modified Gaussian distribution. As discussed in section 5.2, low mean reversion rates suggest a weak drift towards the mean, and values below a certain threshold threshold may lead to speed processes that takes values above maximum sailing speed, or drifts towards zero. Sampling 1,000,000 mean reversion rates from the distribution returned a minimum value of 0.4, which according to experiments is sufficiently high to avoid unrealistic speed behaviour.
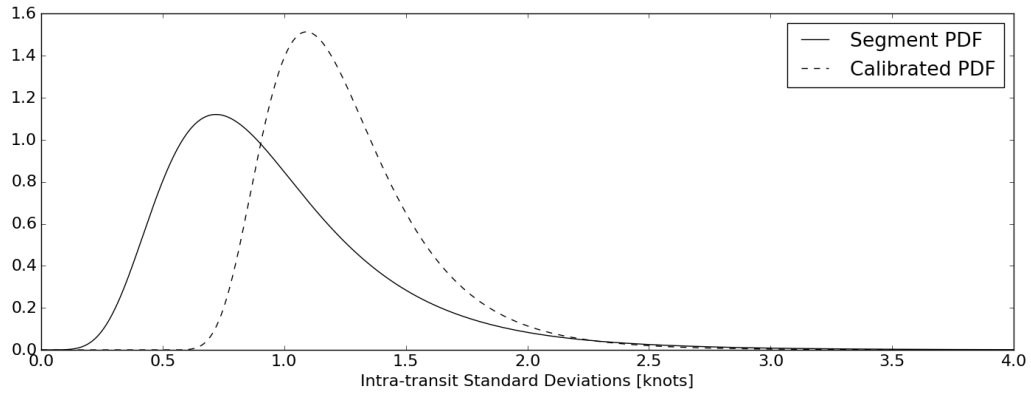
Figure 7.6: Case-calibrated volatility distribution
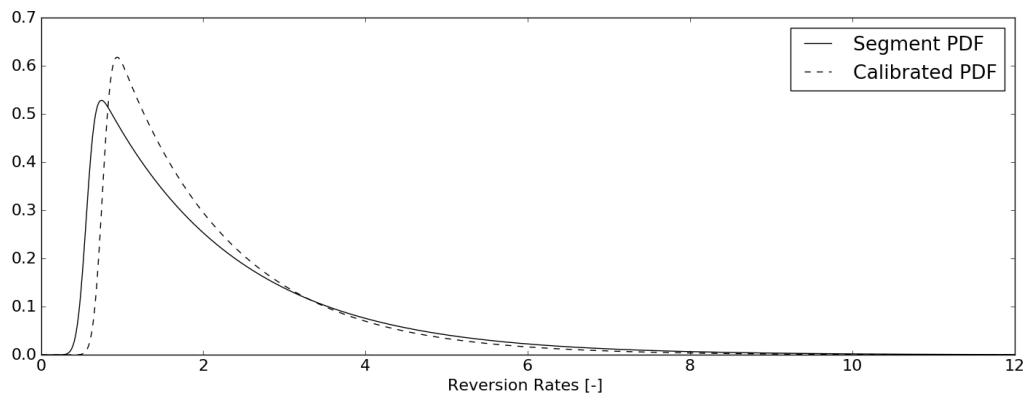
Figure 7.7: Case-calibrated mean reversion rate distribution

Table 7.5: Fuel consumption per nautical mile, DNV GL client data

	2000-3000 TEU [MT/Nm]	4000-5000 TEU [MT/Nm]
Market Average	0.11	0.16
Best In Class Liner	0.085	0.145

7.4   Verification of Fuel Consumption

Given the vast amount of assumptions and simplifications during the power and fuel calculations, the simulated fuel consumption should be compared to empirical consumption data for verification. Andersen (2017) at DNV GL's ECO Insight provided empirical fuel consumption data for different containership segments. The data is based on more than 500 ships, and key numbers are summarized in table 7.5. The original document is found in appendix C.1.

Simulating one years sailing 500 times yielded the results visualized in figure 7.8. The simulations were carried out with the original KCS bulb, which is designed for a service speed of 24 knots. The fuel consumption output is given as an annual average per nautical mile. Recalling that the KCS has a theoretical payload capacity of 3,600 TEU, an average fuel consumption of 0.125 metric tons per nautical mile seems reasonable compared to the empirical data. The relatively wide spread can be ascribed to the the assumption of randomly selecting stochastic speed parameters, which entails that some years will have higher average sailing speed than others. This results in higher fuel consumption per unit distance because of the non-linearity between speed and consumption. As this assumption essentially neglects realistic trade patterns, for example headhaul and backhaul differences, it will yield less accurate results on a year-to-year basis. However, as the desired output is distributions of expected fuel savings, running the Monte Carlo simulations numerous times will yield representative expectations. This assumption will be addressed in further detail in the discussion.

7.5   Model Rules for Bulb Agility

In order to analyze the value of being able to rapidly reconfigure the bulbous bow, the aggregated fuel consumption for one years sailing is simulated with different allowed reconfiguration frequencies. As discussed in section 5.2.1, the finest data resolution analyzed in this study is two hours, consequently also the highest frequency of bulb change possible to value. The lowest frequency subject for valuation is the case where the ship can change bulb configuration in
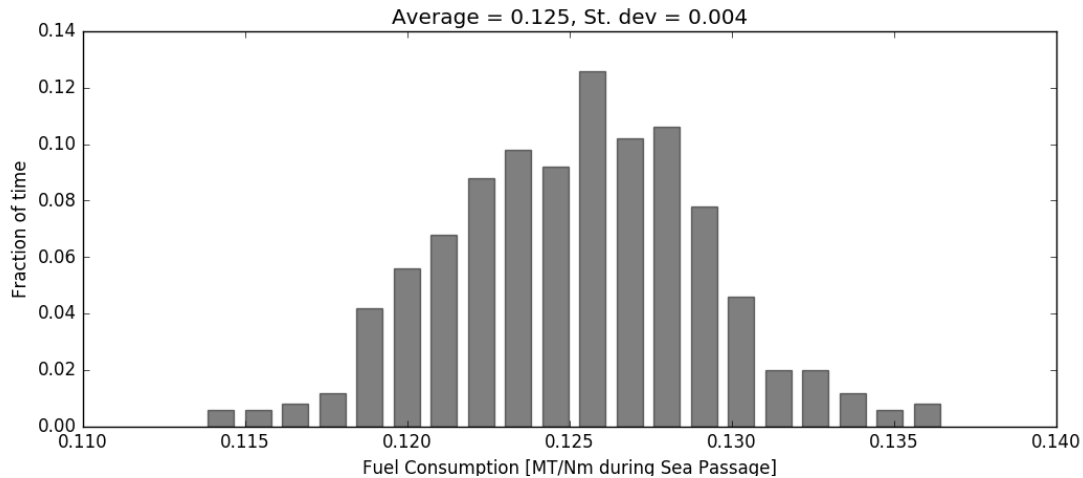
Figure 7.8: Simulated fuel consumption per nautical mile during sea passage

port. Between the extremes, we will analyze the value of being able to reconfigure the bulbous bow every sixth and twelfth hour, in addition to every day, every second day, every third day and every week. As the mean transit duration is set to two weeks, the latter case allows the ship to change configuration once during sailing in addition to in port.

A core issue for the valuation of bulb agility is the model rule for selection of bulb configuration. For the case with the highest level of agility, the model simply selects the bulb configuration that minimizes the fuel consumption at each time step. However, when the agility is restricted, selecting bulb according the speed in a specific increment can lead to severe suboptimality for the next increments. Consider a scenario where the sailing speed drops significantly for a short period, before it recovers. The speed drop may trigger a configuration change to a bulb better suited for lower speeds. However, when the speed recovers to a higher level, the bulb cannot be reconfigured. Thus, the aggregated value contribution from the bulb flexibility might *negative*, which contradicts with the core principles of flexibility in engineering design De Neufville and Scholtes (2011).

The solution to this issue was to assign some predictive capabilities to the model. Take the case where the bulb configuration can be changed every time the vessel is in port. Since the simulated sailing speeds are generated prior to the fuel calculations, the bulb configuration can be selected to fit the average sailing speed for the transit ahead. As the model actually *knows* the future sailing speed and can select bulb based on deterministic knowledge, this assumption may seem optimistic. However, as addressed in chapter 4, the average sailing speed for the upcoming transit is determined before the vessel leaves port. Similarly, if we simulate the case where bulb reconfiguration is allowed every sixth hour, the bulb configuration will be selected based on the
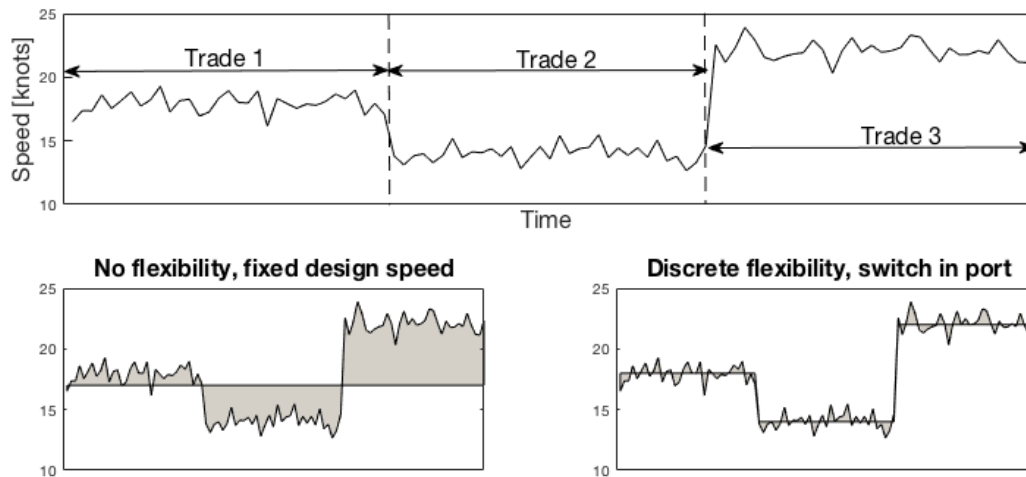
Figure 7.9: Principles of bulb agility

average speed the upcoming six hours. A bulb change in this scenario may represent a scenario where the sea conditions are expected to be rougher for a shorter period, or the vessel must speed up to arrive port at schedule.

Another factor that speaks in favour of the predictive model is the fact that longer predictions will yield more uncertain performance of the bulb. The mean speed of the upcoming three days will have a higher standard deviation than the mean speed of the upcoming six hours, which results in more variations around the mean speed and consequently a lost opportunity cost of not being able to change rapidly. Figure 7.9 explains the logic behind this assumption. In the two lower plots, the horizontal lines represent the *design speeds* for different bulb configurations. The lower left plot displays the case where the bulb is selected to fit the mean speed across the entire period, while the lower right plot shows the case where the bulb configuration can be changed according to the mean speed of the hours ahead. Increasing the agility will lead to more and better suited design speed lines, effectively reducing the grey shaded area which represents unfavorable speeds.

7.6 Transit Characteristics

The transits are assumed to have an average duration of 14 days, and the vessel is assumed to have a sea-passage utilization of 0.75. The latter assumption is based on analyses AIS data, and implies that the vessel spends 75% of the time steaming at speeds above 12 knots.

Chapter 8

Case Study Results

As addressed in subsection 7.2, the absolute maximum obtainable fuel savings for the case with constant area and varying length is 3.7%. Figure 8.1 shows the distribution of fuel savings with two-hour agility, compared to the original bulb, and it can be observed that the average annual saved fuel is 2.859%.

The distribution was obtained from 5,000 Monte Carlo simulations, and table 8.2 shows the distribution of selected bulbs in the simulations. Bulb ID 3, with Δx equal to -0.7 m, is omitted from the table because the configuration is not optimal in any speed regime. It becomes evident that the simulated vessel sails with bulb ID 2 or bulb ID 4 88.8% of the time. Recalling the probability density function for mean transit speeds displayed in figure 7.5, the average value was equal to 16.85 knots. Sampling 1,000,000 values from the distribution reveals that 93.2% of all mean transit speeds are in the range where ID 2 or ID 4 are optimal. The short term variations σ explains why the two configurations are selected 88.8% of the times, and not 93.2%.

The fuel savings declines with increased reconfiguration period, down to 2.76% for the case where reconfiguration is only allowed in port, and the result for different levels of agility is presented in table 8.1. Distributions for all levels of agility is found in appendix B.1. Figure 8.2 shows the value of agility as a function of reconfiguration period. It should be noted that the savings reach maximum at two hours, as speed variability within this period is neglected.
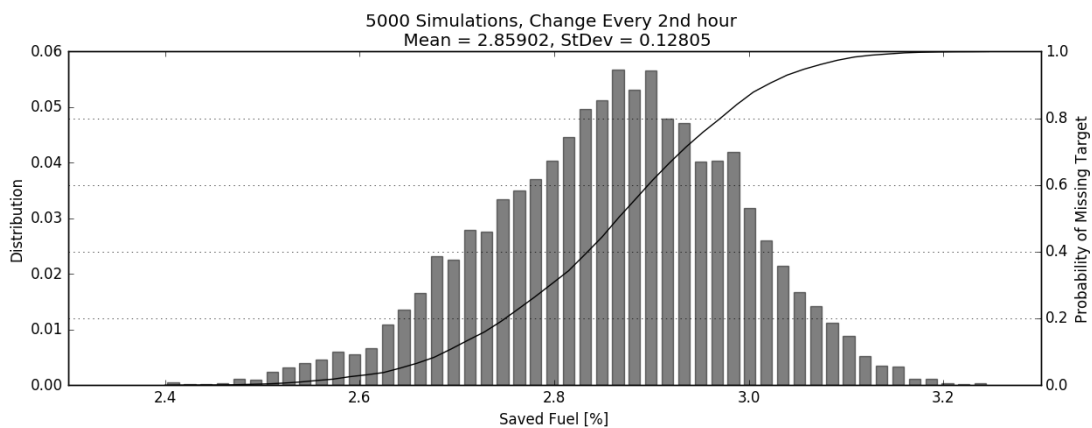
Figure 8.1: Saved fuel distribution, two hour reconfiguration period

Table 8.1: Fuel savings from different levels of agility

	Annual Fuel Reduction		Annual Value*	
Frequency of Change	**Average**	**Standard dev.**	**At 300$/MT**	**At 500$/MT**
2 Hours	2.859%	0.128%	$110,695	$184,491
6 Hours	2.847%	0.129%	$110,230	$183,717
12 Hours	2.838%	0.129%	$109,881	$183,136
1 Day	2.827%	0.131%	$109,446	$182,426
2 Days	2.811%	0.132%	$108,836	$181,394
3 Days	2.797%	0.133%	$108,294	$180,490
1 Week	2.770%	0.136%	$107,248	$178,748
Port - 2 Weeks	2.764%	0.140%	$107,017	$178,361

* 12,906 MT fuel consumed annually. Fuel bill = $3,871,800 at 300 $/MT

Table 8.2: Distribution of selected bulb configurations

	ID 1	**ID 2**	**ID 4**	**ID 5**	**ID 6**	**ID 7**
Δx **[m]**	-2	-1.35	0	0.7	1.3	2
Optimal at [knots]	12-12.9	13-16.6	16.7-18.8	18.9-19.3	19.4-22	22.1-24
Selected[%]	0.8	43.8	45	5.1	5.3	0
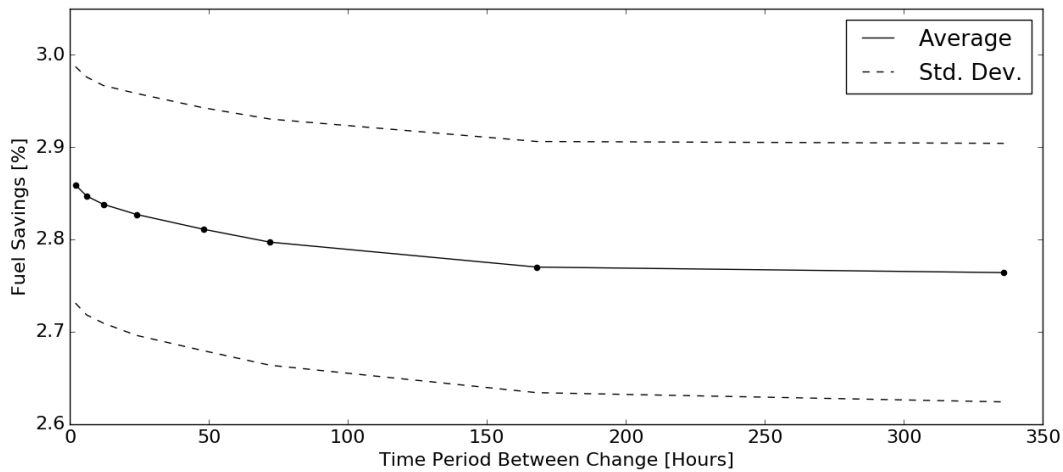
Figure 8.2: Fuel savings as a function of reconfiguration period

Chapter 9

Discussion

9.1 Evaluation of Results

While the constant area with varying length case appears as the most realistic bulb flexibility with respect to structural and technical complexity, there is no doubt that the gained fuel savings are too low to impress potential stakeholders. Fuel savings from bulbous bows retrofits are reported in the range between 5% and 10% (DNVGL, 2015b), leaving few incentives for installing a flexible system should we trust the results obtained in this study. Although the maximum potential savings for the case was 3.7%, it should be emphasized that the average fuel savings of 2.859% is case specific, determined by the operating profile of the reference vessel selected. The analysis was re-simulated with a left-skewed probability density function for the mean transit speed (1 knot lower average), resulting in average fuel savings of 3.13% for the two-hour agility case. However, reduced speed entails reduced fuel consumption, and a percentage increase in saved fuel compared to the base case does not mean higher savings in absolute terms.

9.1.1 Cost-Benefit Discussion

As displayed in table 8.1, the annual monetary value of having bulbous bow flexibility is in the range between $110,695 and $107,017 with today's bunker price. DNVGL (2015b) estimates the investment cost of a retrofit to approximately $600,000 for a 13,100 TEU containership. Dale et al. (2016) concretize the cost breakdown of a bulb retrofit for vessels in the range between 500 TEU and 1000 TEU, and estimate 1 MNOK (approximately $118,000) in fixed costs related to optimization, engineering and approval. Further, they estimate the material costs to the range between 0.25 and 0.7 MNOK ($30,000-$84,000), dependent on the size of the vessel. From these insights we can derive that the cost of a bulb retrofit for a vessel of the size of the KCS will be in the range between $200,000 and $600,000, probably close to the middle.

However, it is rather obvious that the flexible system will increase the costs substantially. In addition to the base costs of labour and steel, costs related to the dynamic parts of the system will

drive the magnitude of the required investment. Additionally, the design and engineering of the system will be more extensive, entailing an extra incurred project cost. Besides the investment cost, the flexible bulb system would probably incur a higher maintenance and operating cost, with respect to both planned and unplanned maintenance, and consumption of lubrication oils and other consumables.

Cost analysis of a flexible bulbous bow system is outside the scope of this thesis, and estimations would consequently be highly speculative. However, for illustrative purposes, the payback time for an investment of $600,000 is calculated. Assuming a discount rate of 10%, the net present value (NPV) with a bunker price of 300$/MT and 500$/MT reaches zero (pay-back) at approximately eight and four years, respectively. The complete NPV analysis is found in appendix B.2. Again, compared to profitability analyses of robust bulb retrofits, where estimated pay-back time is between one and two years dependent on bunker price (DNVGL, 2015b), the outlook of flexible bulb systems is not so optimistic. However, there are two scenarios that could reduce the pay-back time of a flexible bulb system. The first is related to scaling; consider again the 13,100 TEU vessel. While the cost of installing and operating a flexible bulb certainly would be higher than for the full scale KCS, the fuel consumption of such a vessel can be three times larger (Notteboom and Cariou, 2009). Consequently, increasing the investment cost with less than 200% will reduce the pay-back time. The second scenario is when the flexible bulb is included in the new-build specifications, and the costs related to cutting off the original bulb is absent.

On the plus side compared to robust bulb designs, flexible bulbous bows have the advantage of being adaptable to change. While robust bulbs typically are designed to a slow steaming operating profile, they will not perform as intended if the average sailing speeds should revert towards pre-slow steaming levels. Quoting Kjeld Roar Jensen at Clipper Fleet Management[1]: "*Estimating the actual gain when modifying the bulbous bow is quite complex as it depends on the future and usually unknown operational profile, i.e. future loading and speed conditions.*" Here, he refers to estimates of fuel savings from fitting a robust bulbous bow. This would be a minor concern with bulbous bow flexibility.

---

[1]Quote from article: `https://forcetechnology.com/en/maritime-industry/cases/retrofitting-a-new-bulbous-bow`

9.1.2   Evaluation of Resistance Input

The resistance data from CFD analyses was effectively an upper bound of the fuel savings from having bulb flexibility. In addition to determining the maximum fuel savings, the CFD results strictly influenced the distribution of selected bulb designs. As table 8.2 showed, the range between 13 knots and 18.8 knots was covered by only two different bulb configurations. As this speed range constitutes the majority of steaming speeds for the reference vessel, it follows that flexibility beyond these configurations adds little value.

Although the CFD analyses were of high quality and made this study possible, the differences in resistance across bulb configurations were to small to obtain any significant fuel reductions from being able to switch between them. The causalities behind the small differences may be several, one of them being the decision to only alter the length parameter of the bulb. This decision was made because it was, and still is, assumed that it is the most realistic flexibility to incorporate structurally. However, Filip et al. (2014) obtained resistance changes on the KCS in the range between -25% and +40% from altering the width and height of a bulbous bow in different speeds regimes. Working with resistance differences of a magnitude in that order would definitely have resulted in more interesting results with respect to the value of agility.

9.2   Methodology

Numerous assumptions have been made during the process of estimating the value of bulbous bow agility. This section will address the most important assumptions, and discuss their impact on the study.

9.2.1   Speed as Exogenous Random Variable

Treating speed as an exogenous variable, i.e. a variable that affects the model, but not vice versa, is one of the key decisions in this study. The alternative is to treat speed as an endogenous variable, that is, a variable that is determined or influenced by other variables in the model. Bulb configuration is an example of an endogenous variable in the model, as it is effectively determined by the speed variable.

The assumption of treating speed as an exogenous variable essentially neglects the fact that the speed is determined by the commanding officer, and implies that ships are *forced* to follow pre-

defined speed variations. However, the commanding officer will never alter the speed just for the sake of it. There are always underlying reasons, or *agents*, inducing the speed variations, that being met-ocean conditions, schedule, or the ship owners business strategy. In that sense, if the master acts perfectly, all speed variations are just reactions to the behavior of the agents. In behavioural finance, the people trading assets in a stock market are referred to as agents. Their behaviour, i.e. their willingness to buy or sell an asset, will cause the the price to move up or down. Since agents have different preferences and information, the price movements are unpredictable over time, and stochastic of nature. Rather than modelling the behaviour of each individual agent, which obviously is impossible, the stock movements are modelled as a stochastic process based on historical prices. While it for ship speeds actually is possible to model the agents' behaviour (weather, schedule, rates, etc.), we argue that stochastic modelling of ship speeds works under the same assumption as in finance.

However, the option of changing the geometry of the bulbous bow interferes with the assumption of exogenous speed variations. While the incurred costs from increasing the speed may have prevented the ship from speeding up without bulb flexibility, the altered hydrodynamic characteristics with another bulb configuration might lead to a different decision (reaction) by the commanding officer. The hydrodynamic performance of a ship in different speed regimes is an important determinant of variations, and the fact that bulbous bows traditionally are designed to one specific design point makes speed variations undesirable in general. With the option of changing geometry according to the sailing speed, the range of acceptable hydrodynamic performance extends. Thus, instead of just determining the optimal bulb for the sailing speed, we have an optimization problem with two decision variables. Given the circumstances, what are the optimal bulb configuration *and* sailing speed? This is an optimization problem of high complexity, and is not investigated in this thesis. Nonetheless, the hypothesis is that this factor will result in increased speed variations, because the ship can adapt to a wider range of sailing speeds. If the hypothesis is correct, which seems reasonable, it will entail that the estimated fuel savings from bulb agility is a lower bound, as variations drive the value of agility.

9.2.2 AIS Data as Estimator for Speed Variations

Section 4.4 addressed the assumption of analyzing variations in sailing speed from AIS data, and consequently using speed over ground. Recalling that the speed through water (STW) showed less volatility than the speed over ground (SOG), the analysis should be re-conducted with lower short-term volatility. The analyses has been conducted with two-hour resolution, and table 4.4

indicated that the relative volatility of the STW compared to SOG was 84% at this time frame. Adjusting the short-term volatility probability density function downwards has two effects; firstly, and maybe not so obviously, is that the fuel savings from being able to reconfigure the bulb in port increases. This is because the ship will operate closer to the selected bulb's design point through the entire transit when the short-term variations are smaller. Secondly, and more intuitively, is that the value of two hour agility decreases compared to the port agility. When the short-term volatility goes towards zero, the value of both two hour agility and port agility converges towards 2.83% reduced fuel consumption. At zero volatility, the sailing speed is constant over transits, and the option of reconfigure the bulb during transits adds no value.

Additionally, the correlation analysis of STW and SOG showed that the latter captures the actual variations of STW on one and two weeks time frame with high accuracy, suggesting that the mean transit speed distributions should not be corrected. While the data basis was too small to draw quantitative conclusions, the analysis indicated less short-term variations, which in terms results in increased value of port agility, and less relative added value from more rapid reconfigurations. This insight speaks in favour of port agility, which also appears as the most realistic bulb flexibility from a structural complexity point of view.

9.2.3 The Impact of Draught and Trim

Limited by available data (both operational and resistance), this study has not considered draught as a part of varying operating conditions. Draught does definitely vary from transit to transit due to the asymmetrical world trade, and draught variations does definitely affect the resistance and consequently fuel consumption. However, draught variations have less of an impact on fuel consumption than sailing speed. While fuel consumption is roughly proportional to speed to the power of three, the relationship to draught has an exponent of approximately *two thirds* (MAN, 2011). Meng et al. (2016) investigated the relationships between fuel consumption and its determinants speed and draught, and calculated correlation coefficients in the range between 0.82 and 0.92 for speed, and in the range between 0 and 0.36 for draught. Their analysis encompassed containerships of 5,000 and 13,000 TEU, and exemplified the relative impact of speed versus draught. However, although speed is the main determinant of fuel consumption, the impact of the bulbous bow at different draughts can not be neglected. All investigated studies on bulb optimization in the context of varying operating conditions (Filip et al., 2014; Wagner et al., 2014; Lu et al., 2016) has accounted for draught, all of them concluding that draught considerations are important. Preferably, the study should have been conducted with draught data, and

it goes without saying that draught must be considered should someone want to explore the concept further.

While the correlation between trim and bulb performance is not so commonly investigated in the literature, Ljungberg (2017) emphasized that the industry has a great focus on trim optimization for resistance minimization purposes. Trim has definitely an impact on resistance, and it is reasonable to assume that also the bulb performance is affected by this variable.

9.2.4   Not Accounting for Realistic Trade Characteristics

As addressed in section 7.4, the simulation model does not account for realistic trade characteristics. More specifically, the model samples random mean transit speeds according to the probability density function, and is essentially neglecting the fact that vessels sails faster in loaded condition. This entails that the model may sample mean transit speeds that represent typical headhaul transits for an entire simulated period. This is unrealistic in the sense that ships does not only sail fully loaded, and the mean transit speeds will alter from one transit to the next. However, in line with the principles of Monte Carlo methods, running the simulations many times will ensure a representative distribution of outcomes.

Chapter 10

Conclusion

10.1 Concluding Remarks

This thesis has analyzed the value of being able to rapidly reconfigure the bulbous bow according to the sailing speed. The study has essentially been divided into two main parts; one part devoted to the analysis and modelling of sailing speed variability, and one part devoted to the modelling of a flexible bulbous bow intended to thrive under the aforementioned variations. Based on AIS data, historical speed records were fitted to the Ornstein-Uhlenbeck mean-reverting process, which was proposed as a stochastic representation of sailing speed. Combined with resistance data for different bulb geometries, a Monte Carlo method for estimating the fuel savings from being able to switch between the resulting fuel curves was developed, and applied on a case study calibrated to the KRISO Container Ship.

Fuel savings were estimated for reconfiguration periods (agility levels) between two hours and two weeks, resulting in percentage reductions in the range between 2.86% and 2.76%, respectively. The resistance data obtained from CFD effectively bounded the maximum obtainable fuel savings to 3.7%. The small difference between the agility levels is explained by the fact that two bulbs covered the optimality range between 13 and 18.8 knots, resulting in few configurations to switch between during most transits. Hence, it is concluded that the bulb configuration space was too wide and too coarse for a representative containership operating profile. Seven bulb configurations, optimized to design points from 12 to 24 knots (equal spacing), were available, whereby two of them were used 88.8% of the time. Further, it is concluded that the obtained fuel savings are too small to compete with the robust bulb alternative, from which fuel savings are reported in the range between 5% and 10%.

While the quantitative results indicate that the incentives for bulb flexibility are limited compared to robust bulb designs, the thesis has presented a novel approach for valuation of agility in marine systems design based on large amounts of data. The methodology presented succeeded to evaluate the time aspect of flexibility, although the case-specific input yielded low value of agility. It is concluded that the methodology met the objective of estimating the value

of rapidly reconfigurable bulbous bows, and implicitly exemplified the value of agility in marine systems design. However, it is emphasized that the numerous assumptions, potential uncertain input parameters and marginalization of certain fuel consumption-determinants make the analysis incomplete, underscoring that the results should be treated accordingly.

10.2   Recommendations for Further Work

Although the results in this study were less remarkable, bulb flexibility should in theory outperform bulb robustness. Hence, the recommendations for further work is mainly related to finding ways of identifying valuable bulb flexibility. Section 9.1.2 addressed the decision of only investigating bulb flexibility in the length direction, possibly delimiting the potential savings significantly. An alternative approach is to leave the solution space open, and analyze the sensitivity of geometrical changes in several, or preferably all, directions. The work of Filip et al. (2014) suggested for example that height and width flexibility had substantial impact on the resistance with varying sailing speed.

Draught variations should further be incorporated in the flexibility analysis. The impact of draught may be underestimated in this study, and as these variations add another dimension of uncertainty, including draught may increase the value of flexibility and agility. In theory, draught variations should be easier to evaluate and account for, as it remains relatively constant during transits. Hypothetically, this could speak in favour of the agility level where reconfiguration is an option in port only. Analysis of draught does not rely substantially on the frequency aspect of variations, and could be incorporated by generating probability density functions and sample static draught values for each transit. One would obviously need resistance curves for different draught intervals.

The value of agility with long-term trends should also be analyzed. This was not investigated in this study, as the performance of flexibility under long-term trends should be compared to robust bulb designs. Such resistance data was not available. As discussed in section 9.1.1, the key advantage of flexible bulbs is the ability to adapt. Although robust bulbs are designed to perform in a wide range of operating conditions, the performance will decrease as the projected operational profile extends. They are consequently designed to a limited intended operating profile, and subsequently a declining performance should the intended profile shift significantly. For example if sailing speeds reverts towards the levels observed before 2008, the value of being adaptable can increase significantly. However, when bulb flexibility is incorporated to account

for long-term trends, the agility becomes less important. In light of the retrofit trend, an alternative to dynamical flexibility may be to investigate the value of rapid retrofits. That is, bow areas engineered and structurally dimensioned to being able to rapidly retrofit the bulb, while the ship is in water.

It is finally recommended that sailing speed variability is investigated with records of speed through water. Ideally, the analyses of context uncertainty should be conducted in cooperation with a ship owning company that possess large amounts of fleet performance data. In addition to more reliable speed data, a cooperation with a liner may entail access to detailed operating data, providing deeper insight into the correlation between speed, draught, met-ocean conditions and fuel consumption.

Bibliography

Adland, R. and Jia, H. (2016a). Dynamic speed choice in bulk shipping. *Maritime Economics & Logistics*, pages 1–14.

Adland, R. and Jia, H. (2016b). Vessel speed analytics using satellite-based ship position data. In *Industrial Engineering and Engineering Management (IEEM), 2016 IEEE International Conference on*, pages 1299–1303. IEEE.

Andersen, P. (2017). Business Development Leader - ECO solutions at DNV GL. E-Mail Correspondence 18.05.2017.

Arribas, F. P. (2007). Some methods to obtain the added resistance of a ship advancing in waves. *Ocean Engineering*, 34(7):946–955.

Aßmann, L. M. (2012). Vessel speeds in response to freight rate and bunker price movements: An analysis of the vlcc tanker market. Master's thesis.

Aßmann, L. M., Andersson, J., and Eskeland, G. S. (2015). Missing in action? Speed optimization and slow steaming in maritime shipping.

Bang, J., Bjørseth, I., and Hiort, F. (2017). Design of mechanism for flexible bulb.

Brouer, B. D., Karsten, C. V., and Pisinger, D. (2017). Optimization in liner shipping. *4OR*, 15(1):1–35.

Chirica, I. and Giuglea, V. (2015). Adaptive bulbous bow for inland water way ships - ADAM4EVE Project.

Chrismianto, D. and Kim, D.-J. (2014). Parametric bulbous bow design using the cubic Bezier curve and curve-plane intersection method for the minimization of ship resistance in cfd. *Journal of Marine Science and Technology*, 19(4):479–492.

Coraddu, A., Figari, M., and Savio, S. (2014). Numerical investigation on ship energy efficiency by Monte Carlo simulation. *Proceedings of the institution of mechanical engineers, part M: journal of engineering for the maritime environment*, 228(3):220–234.

Dale, E., Gundersen, H., and S. Eide, M. (2016). Teknologier og tiltak for energieffektivisering av skip. *Kartlegging av Teknologistatus, DNV GL/Enova SF*.

De Neufville, R. and Scholtes, S. (2011). *Flexibility in engineering design.* MIT Press.

DNVGL (2015a). Energy Management Study 2015. `https://www.dnvgl.com/maritime/energy-management-study-2015.html`. Accessed: 2017-04-05.

DNVGL (2015b). Retrofitting: Where the savings are. *Maritime Impact*, 2015(01):29.

Eide, E. (2015). Calculation of service and sea margins. Master's thesis, NTNU.

Equasis (2016). Equasis statistics - the world fleet 2015. page 6.

Erichsen, S. (1989). Management of marine design.

Ferreiro, L. D. and Hocker, F. (2007). *Ships and science: the birth of naval architecture in the scientific revolution, 1600-1800.* Mit Press Cambridge, MA, and London.

Filip, G., Kim, D.-H., Sahu, S., de Kat, J., and Maki, K. (2014). Bulbous bow retrofit of a containership using an open source computational fluid dynamics (CFD) toolbox. *SNAME Transactions*, 122:244–262.

Fricke, E. and Schulz, A. P. (2005). Design for changeability (DfC): Principles to enable changes in systems throughout their entire lifecycle. *Systems Engineering*, 8(4).

Gkonis, K. G. and Psaraftis, H. N. (2012). Modeling tankers' optimal speed and emissions.

Hycom. HYbrid Coordinate Ocean Model. Accessed 20.03.2017.

IMO (2011). MARPOL Annex VI, Chapter 4.

Johnson, N. L., Kotz, S., and Balakrishnan, N. (1970). Distributions in statistics: continuous univariate distributions, vol. 2. *NY: Wiley*.

Jonkeren, O., van Ommeren, J., and Rietveld, P. (2012). Freight prices, fuel prices, and speed. *Journal of Transport Economics and Policy (JTEP)*, 46(2):175–188.

Kracht, A. M. (1978). Design of bulbous bows. *SNAME Transactions*, 86:197–217.

Kroese, D. P., Brereton, T., Taimre, T., and Botev, Z. I. (2014). Why the Monte Carlo method is so important today. *Wiley Interdisciplinary Reviews: Computational Statistics*, 6(6):386–392.

Lane, B. C. (2006). AIS parser sdk v1.10. Accessed 26.09.2016.

Lindstad, H., Asbjørnslett, B. E., and Jullumstrø, E. (2013). Assessment of profit, cost and emissions by varying speed as a function of sea conditions and freight market. *Transportation Research Part D: Transport and Environment*, 19:5–12.

Ljungberg, K. (2017). Principal Consultant, Shipping Advisory DNV GL. Phone Call 23.02.2017.

Lu, Y., Chang, X., and Hu, A.-k. (2016). A hydrodynamic optimization design methodology for a ship bulbous bow under multiple operating conditions. *Engineering Applications of Computational Fluid Mechanics*, 10(1):330–345.

Maloni, M., Paul, J. A., and Gligor, D. M. (2013). Slow steaming impacts on ocean carriers and shippers. *Maritime Economics & Logistics*, 15(2):151–171.

MAN, D. (2011). Basic principles of ship propulsion. *MAN Diesel & Turbo, Copenhagen*.

MAN, D. (2015). Marine Engine. *IMO Tier II and Tier III Programme 2015, MAN Diesel & Turbo, Copenhagen*.

Mao, W., Rychlik, I., Wallin, J., and Storhaug, G. (2016). Statistical models for the speed prediction of a container ship. *Ocean Engineering*, 126:152–162.

McNichols, J. P. and Rizzo, J. L. (2012). Stochastic GBM methods for modeling market prices. In *Casualty Actuarial Society E-Forum, Summer 2012*.

Meng, Q., Du, Y., and Wang, Y. (2016). Shipping log data based container ship fuel efficiency modeling. *Transportation Research Part B: Methodological*, 83:207–229.

Nabergoj, R. and Prpić-Oršić, J. (2007). A comparison of different methods for added resistance prediction. In *22nd International Workshop on Water Waves and Floating Bodies, Plitvice/Croatia*, volume 18.

Notteboom, T. and Cariou, P. (2009). Fuel surcharge practices of container shipping lines: Is it about cost recovery or revenue making. In *Proceedings of the 2009 International Association of Maritime Economists (IAME) Conference*, pages 24–26. IAME.

Prpić-Oršić, J. and Faltinsen, O. M. (2012). Estimation of ship speed loss and associated $CO_2 emissions in a seaway. Ocean Engineering, 44 : 1 − −10.$

Rehn, C. F. (2015). Identification and valuation of flexibility in marine systems design. Master's thesis, NTNU.

Ronen, D. (2011). The effect of oil price on containership speed and fleet size. *Journal of the Operational Research Society*, 62(1):211–216.

Skauen, A. N., Helleren, Ø., Olsen, Ø., and Olsen, R. (2013). Operator and user perspective of fractionated AIS satellite systems. In *27 th Annual AIAA/USU Conference on Small Satellites*.

Smestad, B. B. (2015). A study of satellite AIS data and the global ship traffic through the singapore strait.

Smith, T., O'Keeffe, E., Aldous, L., and Agnolucci, P. (2013). Assessment of shipping's efficiency using satellite AIS data.

Sødal, S., Koekebakker, S., and Adland, R. (2009). Value based trading of real assets in shipping under stochastic freight rates. *Applied Economics*, 41(22):2793–2807.

Stapersma, D., Woud, H. K., Institute of Marine Engineering, S., and Kingdom);, T. U. (2002). *Design of propulsion and electric power generation systems*. London (United Kingdom): IMarEST.

Steen, S. (2007). Marin teknikk 3-hydrodynamikk. Motstand og propulsjon. Propell og foilteori.

Sundar, S. (2016). Calibrating & Simulating Natural Gas Spot Prices. `https://se.mathworks.com/matlabcentral/fileexchange/28056-energy-trading---risk-management-with-matlab-webinar-case-study?focused=6788577&tab=example`. Accessed: 2017-02-10.

Tezdogan, T., Demirel, Y. K., Kellett, P., Khorasanchi, M., Incecik, A., and Turan, O. (2015). Full-scale unsteady RANS CFD simulations of ship behaviour and performance in head seas due to slow steaming. *Ocean Engineering*, 97:186–206.

Tufto, J. (2017). Professor, Department of Mathematical Sciences NTNU. Personal Conversation 03.02.2017.

Tupper, E. C. (2013). *Introduction to naval architecture*. Butterworth-Heinemann.

Wagner, J., Binkowski, E., and Bronsart, R. (2014). Scenario based optimization of a container vessel with respect to its projected operating conditions. *International Journal of Naval Architecture and Ocean Engineering*, 6(2):496–506.

WorldShippingCouncil (2014). Top trade routes. `http://www.worldshipping.org/about-the-industry/global-trade/trade-routes`. Accessed: 2017-02-16.

Appendix A

Acronyms

AIS Automatic Identification System

CFD Computational Fluid Dynamics

ETA Estimated Time of Arrival

FP Forward Perpendicular

GB Gigabytes

GPS Global Positioning System

IMO International Maritime Organization

ITTC International Towing Tank Conference

KCS KRISO Container Ship

LOC Lost Opportunity Cost

MCM Monte Carlo Method

MMSI Maritime Mobile Service Identity

OU Ornstein-Uhlenbeck

PDF Probability Density Function

RoRo Roll On Roll Off

S-AIS Satellite Automatic Identification System

SDE Stochastic Differential Equation

SFC Specific Fuel Consumption

SOG Speed Over Ground

STW Speed Through Water

TEU Twenty-foot Equivalent

UTC Universal Time Coordinated

VHF Very High Frequency

Appendix B

Additional Information

B.1 Detailed Results
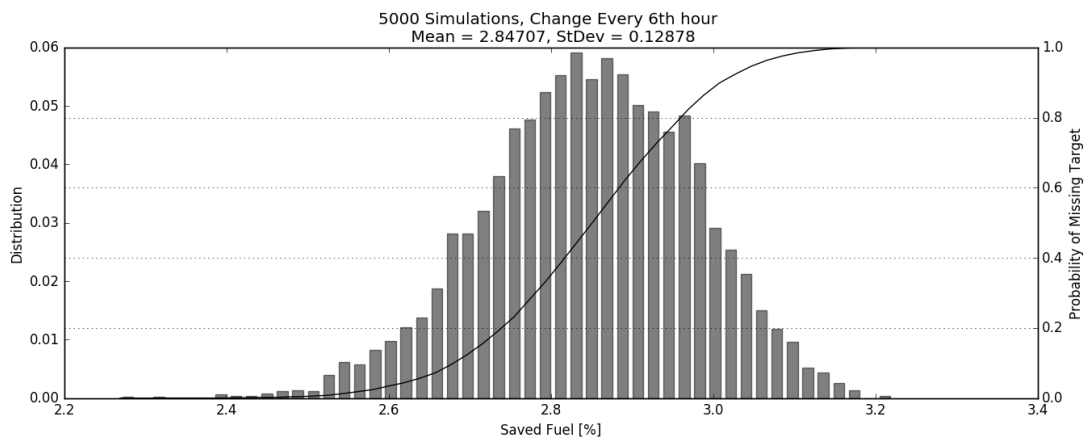
Figure B.1: Saved fuel distribution, six hours reconfiguration period
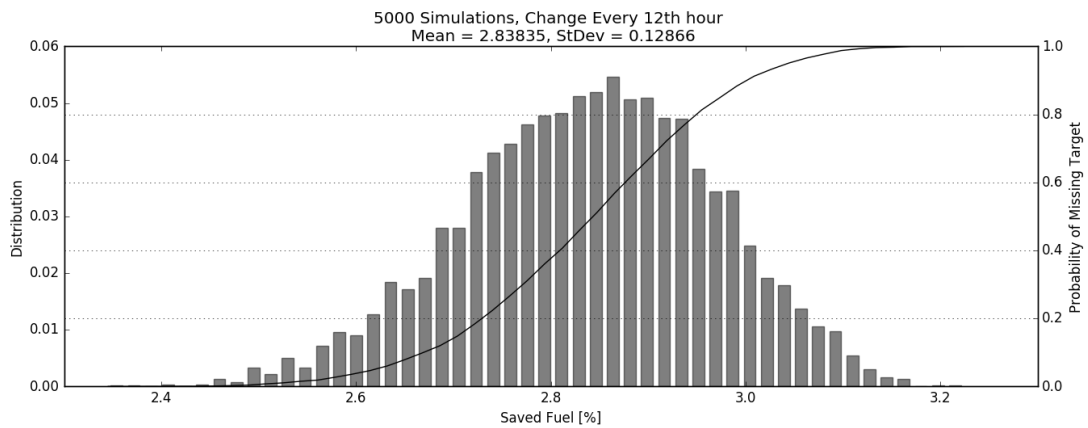
Figure B.2: Saved fuel distribution, twelve hours reconfiguration period
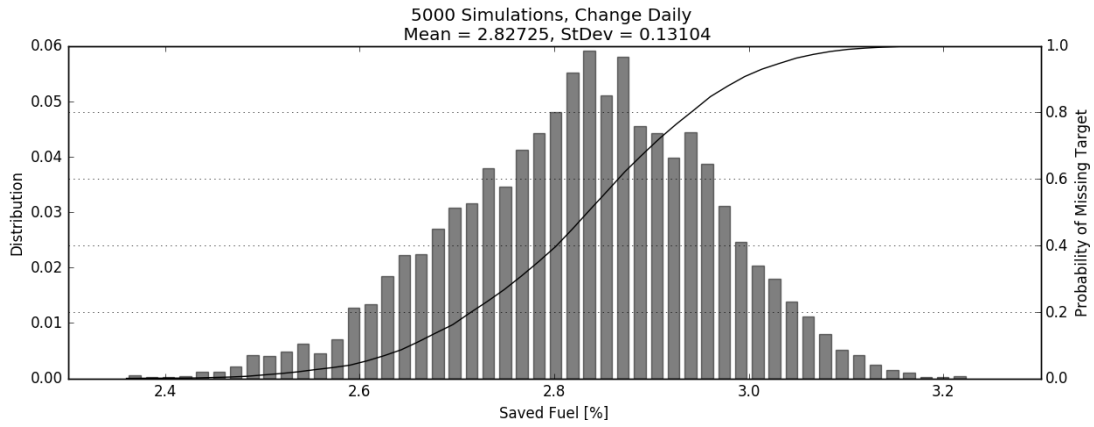
Figure B.3: Saved fuel distribution, one day reconfiguration period
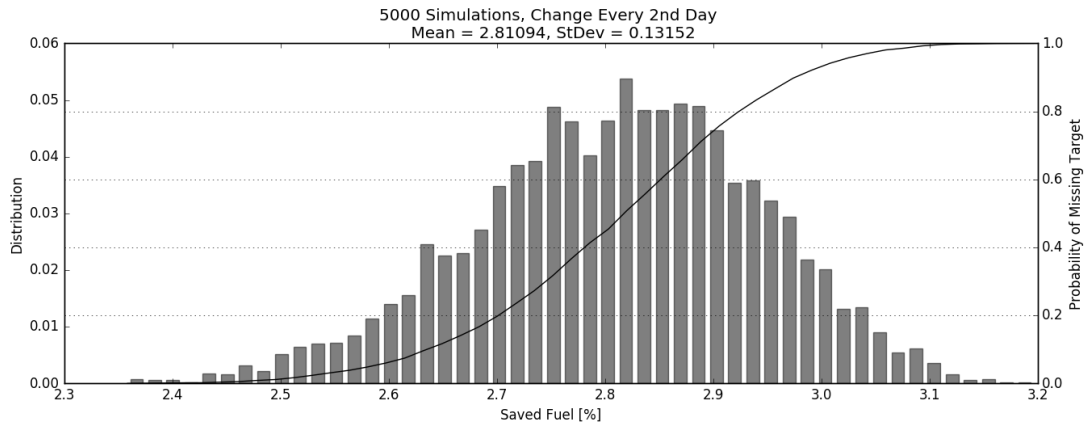
Figure B.4: Saved fuel distribution, two days reconfiguration period
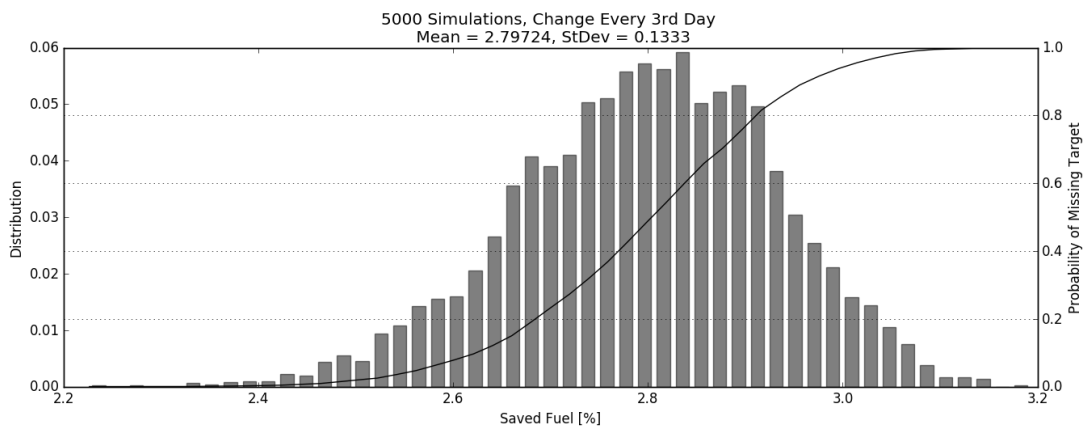
Figure B.5: Saved fuel distribution, three days reconfiguration period
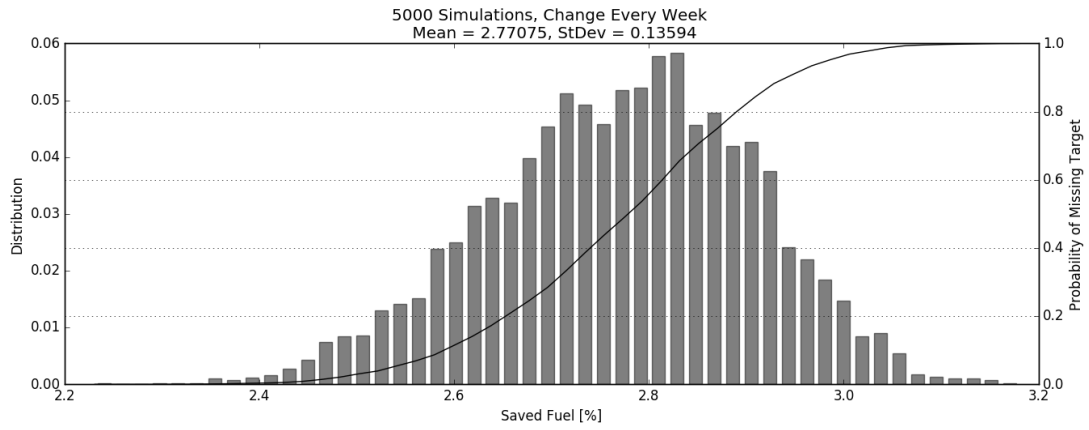
Figure B.6: Saved fuel distribution, one week reconfiguration period
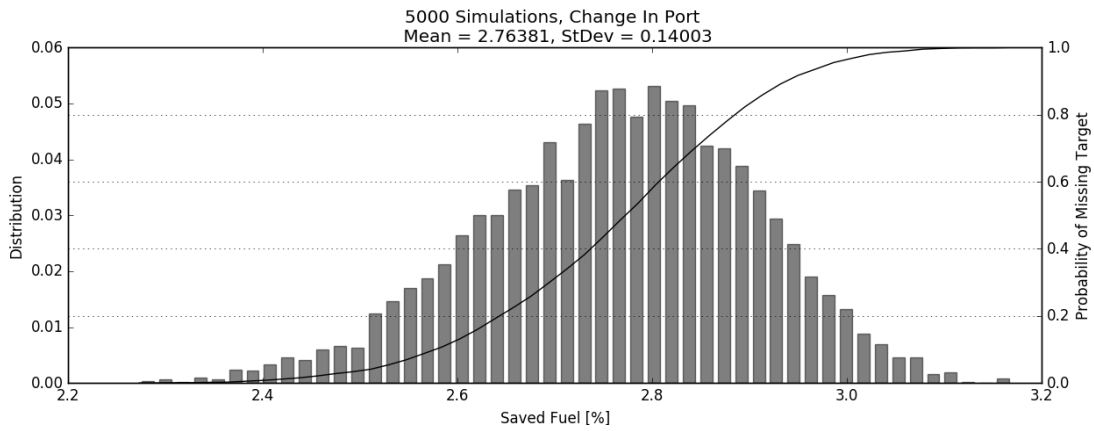
Figure B.7: Saved fuel distribution, two weeks reconfiguration period

B.2 Net Present Value Analysis

The net present value (NPV) is calculated by the following formula:

$$NPV = -I + \sum_{i=1}^{N} \frac{CF}{(1+r)^i} \tag{B.1}$$

Here, *I* represents the investment cost, and is assumed to be \$600,000. *CF* is the cash flow, or the monetary annual savings from bulb agility, and is \$110,695 and \$184,491 at a bunker price of \$300/MT and \$500/MT, respectively. *r* is the discount rate, assumed to be 10%. *N* denotes the number of periods (years) analyzed, and is in figure B.8 visualized from zero to 12 years.
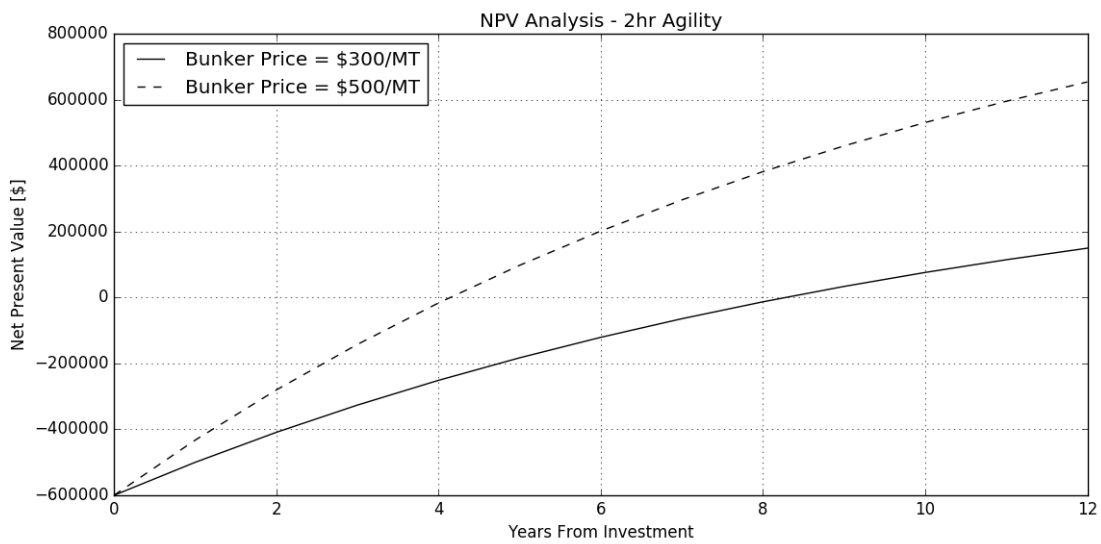
Figure B.8: Net present value, two hours reconfiguration period

Appendix C

DNV GL Empirical Operating Data

C.1 Fuel Consumption Per Nautical Mile

There is a lot to be gained still in performance improvements (example smaller container vessels)

Fuel oil consumption/Nm during sea passage

Market Average
Best in Class Liner

- Double digit difference in Fuel Oil Consumption (= CO2 emissions) between best in class to market average container vessel performance

<1000 TEU +20%

1000 - 2000 TEU +17%

2000 - 3000 TEU +30%

4000 - 5000 TEU +10%

FOC/Nm

0.00   0.06   0.12   0.18
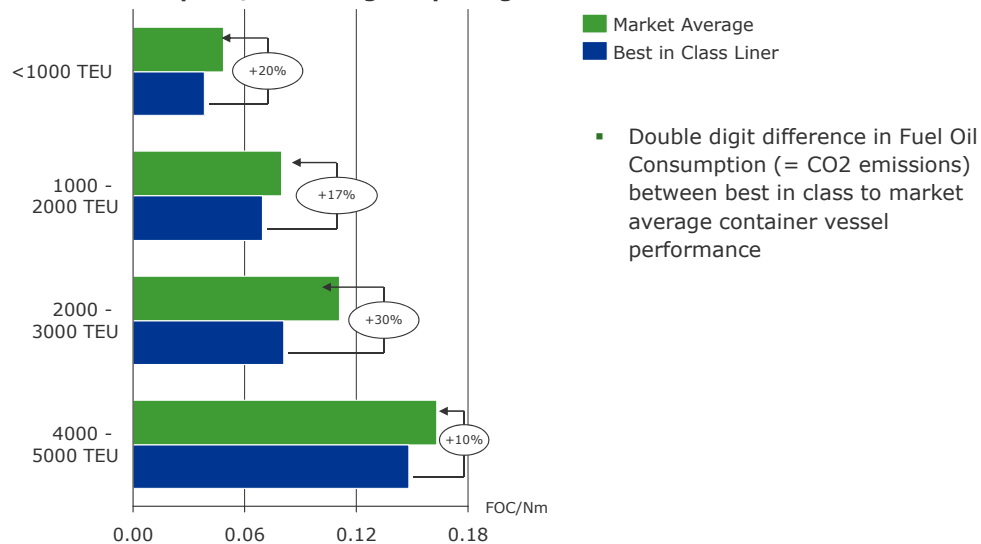
Benchmark against 546 selected vessels operated by MAERSK, CMA CGM, HANJIN, Hapag-Lloyd, OOCL, COSCO, NYK, MOL, HMM, Yang Ming, Evergreen Jan-Dec. 2013.

1   DNV GL © 2015   19 May 2017

ECO Insight   Februar 2016

DNV·GL

Figure C.1: Fuel consumption per nautical Mile: smaller containerships

C.2 Operating Profiles Containerships: 2008-2013
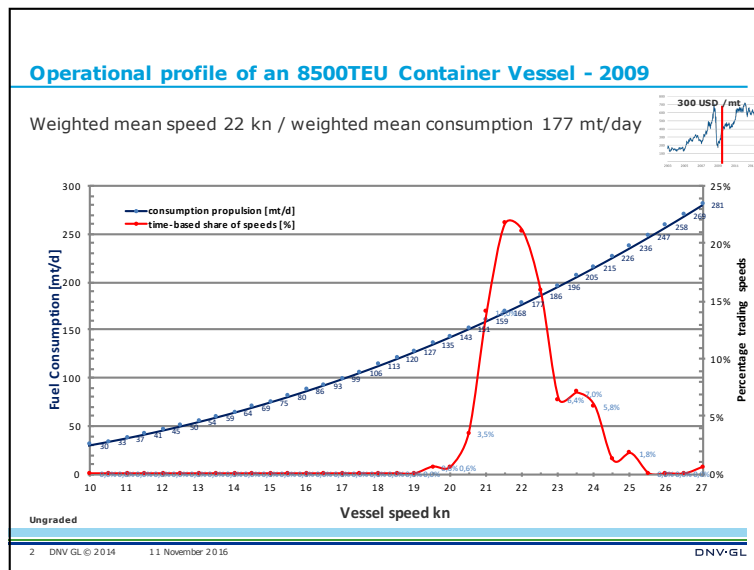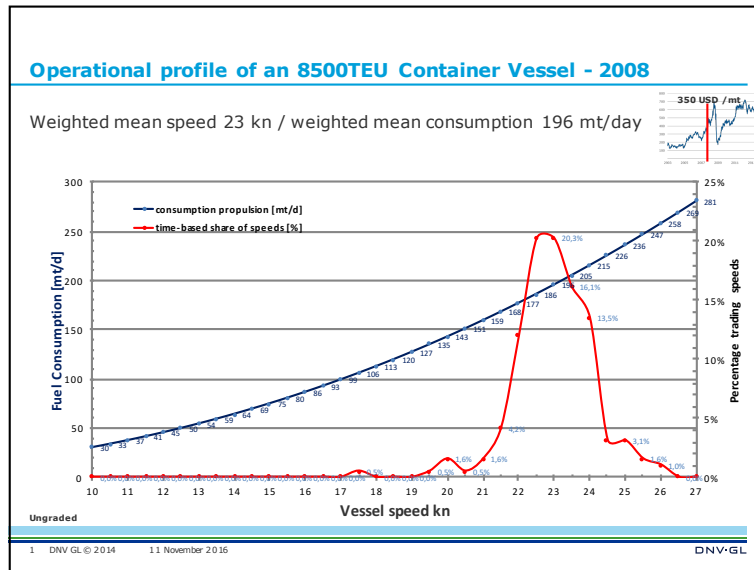
Figure C.2: Operating profile, 8500 TEU containership: 2008 and 2009
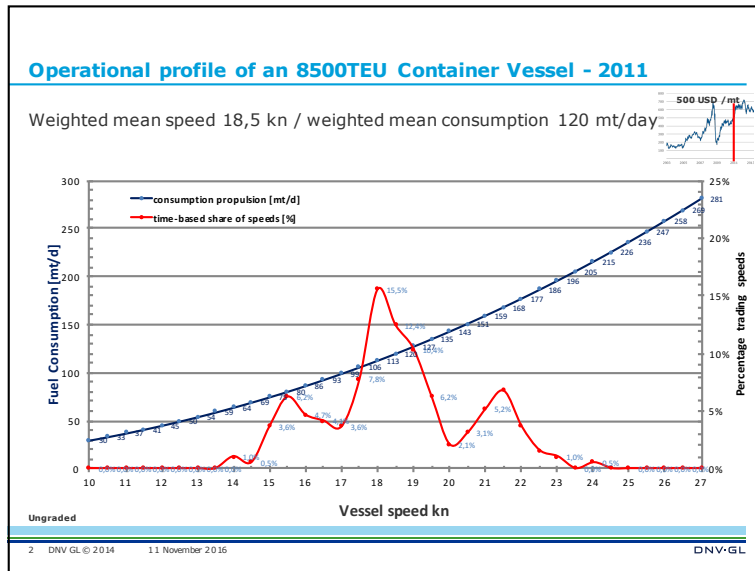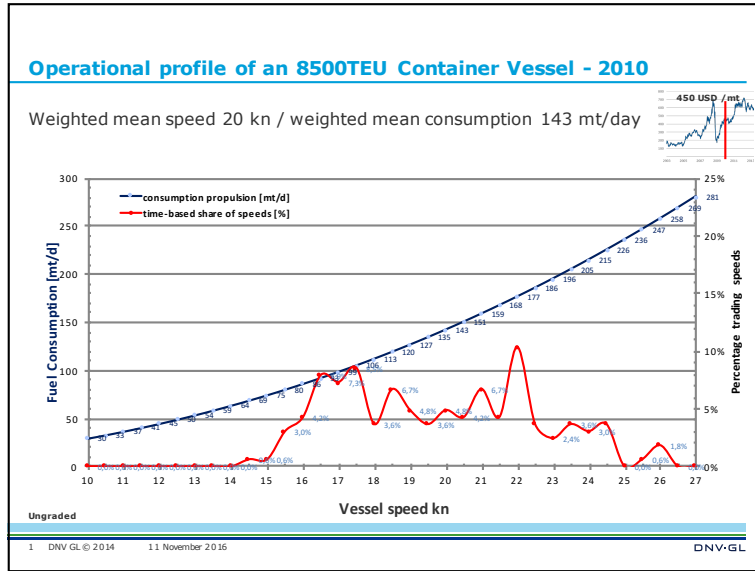
Figure C.3: Operating profile, 8500 TEU containership: 2010 and 2011
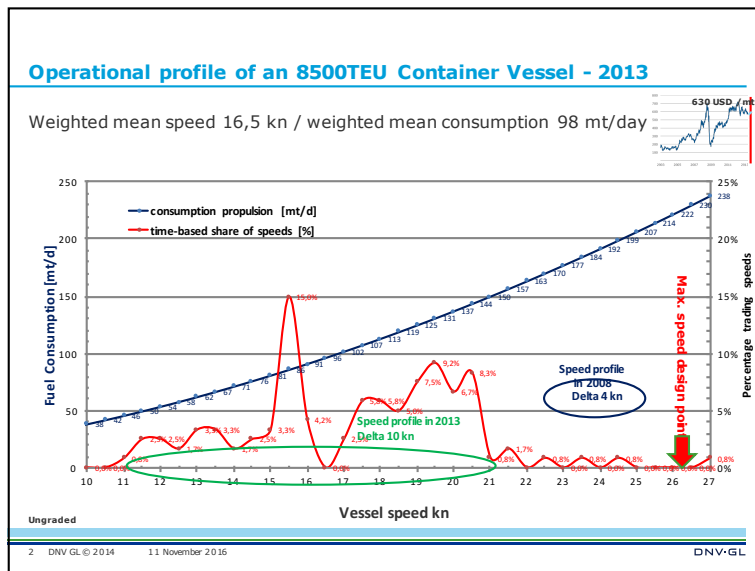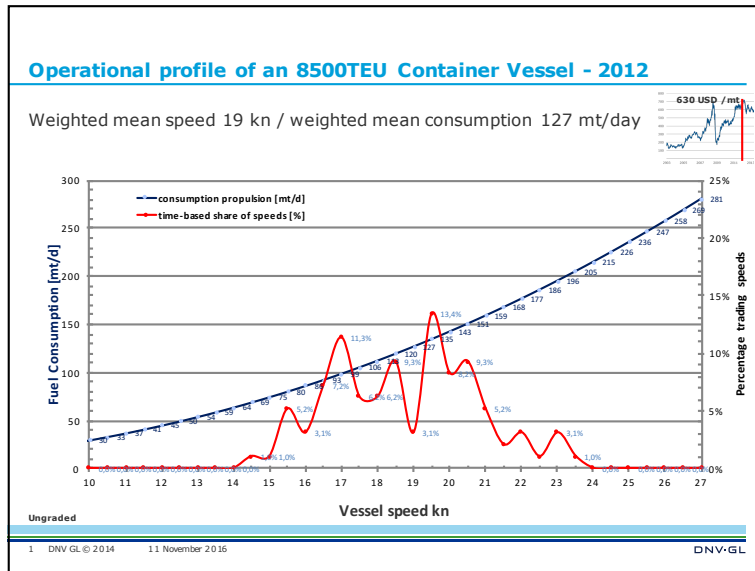
Figure C.4: Operating profile, 8500 TEU containership: 2012 and 2013

Appendix D

Python Code

This appendix presents the most important Python code programmed and used in the thesis.

D.1   Master Script (MasterAnalysis.py)

All files and functions are ran from the Master Script. Many of the different files have interrelated functions, and the master script provides a user interface where the desired functions could be ran by specifying 1 or 0. From this script one can also specify rules for the Ornstein-Uhlenbeck parameter estimation, in addition to specifying Monte Carlo simulation characteristics. The script imports four key files that are presented in the sections following this.

```python
#!/usr/bin/env python3
# -*- coding: utf-8 -*-
"""
Created on Fri Feb 17 10:52:25 2017

@author: jonleonhardsen
"""

import PlotVessels as PV
import OU
import SpeedStatsBigShips as BS
import SpeedStatsPanamax as P
import Generate_Sailingspeeds as GS
import Fuel_Aggregated as FA

Segment = '/Users/jonleonhardsen/Documents/Documents/Skole/AIS/ContainerFleet.db'
Vessel = '/Users/jonleonhardsen/Documents/Documents/Skole/AIS/xyz.db'

#All methods are run from this script, 1 = run
SegmentAnalysis = 1 #1 = analyze segment, 0 = analyze vessel
GlobalMap = 0
LocalMap = 0
DraughtInterpolate = 0
TradeDirectionsSuez = 0
TradeDirectionPacific = 0
FreightRateImpact = 0
MonthlyAverage = 0
GeoDistribution = 0
```

```python
29  SpeedDev = 0
30  SpeedHistogram = 0
31  SpeedForAnalysis = 0
32  GeoAnalysis = 0
33  CumulatedSpeed = 0
34  DraughtAnalysis = 0
35  OrnsteinUhlenbeckGenerator = 0
36
37  BigShips = 0
38  Panamax = 0
39  MuSim = 0
40  FuelCalc = 0
41  FuelAgg = 0
42
43  Pacific = [-120,63,12,28]
44  Atlanter = [0,53,-80,33]
45  MexAu = [180,7.75,-180,-26.10]
46  Global = [180,90,-180,-90]
47  asEur = [120, 50, -15, 0]
48
49  Loc = 4
50
51  if Loc == 1:
52      Pos = Pacific
53  elif Loc == 2:
54      Pos = Atlanter
55  elif Loc == 3:
56      Pos = MexAu
57  elif Loc == 4:
58      Pos = Global
59  elif Loc == 5:
60      Pos = asEur
61
62  #PV calls PlotVessels.py, which essentially does all data extracting, initial analyses,
63  #and visualizations of AIS data.
64  if SegmentAnalysis == 1:
65      PV.ExtractData(Segment,Pos[0],Pos[1],Pos[2],Pos[3])
66  else:
67      PV.ExtractData(Vessel,Pos[0],Pos[1],Pos[2],Pos[3])
68  if GlobalMap == 1:
69      PV.GlobalMap()
70  if LocalMap == 1:
71      PV.LocalMap()
72  if DraughtInterpolate == 1:
73      PV.DraughtInterpolate()
74  if TradeDirectionsSuez == 1:
75      PV.TradeDirectionSuez()
76  if TradeDirectionPacific == 1:
77      PV.TradeDirectionPacific()
78  if MonthlyAverage == 1:
79      PV.MonthlyAverage()
80  if FreightRateImpact == 1:
81      PV.FreightRateImpact()
82  if GeoDistribution == 1:
```

```python
83         PV.GeoDistribution()
84  if SpeedDev == 1:
85         PV.SpeedDev()
86  if SpeedHistogram == 1:
87         PV.SpeedHistogram()
88  if SpeedForAnalysis == 1:
89         PV.SpeedForAnalysis()
90  if GeoAnalysis == 1:
91         minspeed = 12
92         PV.GeoAnalysis(Pos[0],Pos[1],Pos[2],Pos[3],minspeed)
93  if CumulatedSpeed == 1:
94         PV.CumulatedSpeed()
95  if DraughtAnalysis == 1:
96         PV.DraughtAnalysis()
97
98  #If 1, estimate Ornstein-Uhlenbeck Parameters
99  if OrnsteinUhlenbeckGenerator == 1:
100        MaxInterval = 12       #hours
101        MinPeriod = 7          #days
102        PlotSpeed = 1
103        PlotMap = 0            #1 = yes, 0 = no
104        OU.OrnsteinUhlenbeckGenerator(PV.AtTime,PV.AtSpeed,PV.AtLat,PV.AtLon,PlotMap,
           PlotSpeed,MaxInterval,MinPeriod)
105 if BigShips == 1:
106        BS.FetchSpeedStatsBigShips()
107 elif Panamax == 1:
108        P.FetchSpeedStatsPanamax()
109 #If 1, start monte carlo simulations
110 if FuelCalc == 1:
111        FA.FuelCalc()
112 if MuSim == 1:
113        ShipUtilization = 0.75
114        Years = 1
115        AverageTradeDuration = 14 #days
116        iterations = 5000
117        GS.SimulateSailing(ShipUtilization,Years,AverageTradeDuration,iterations)
```

D.2   Data Extraction (PlotVessels.py)

The code presented in this section is an excerpt of the file named PlotVessels.py, which is imported in the aforementioned Master Script. PlotVessels.py has several functions, including extraction of AIS data from SQL databases, initial filtering (erroneous data points), initial analyses (headhaul/backhaul), and plotting of vessel movements and sailing speed time series. The following code is the data extraction function, which takes the file directory to the desired database as input, in addition to coordinates defining the region we want to analyze. The entire file is appended in the zip-file.

```python
#!/usr/bin/env python3
# -*- coding: utf-8 -*-
"""
Created on Fri Nov 18 17:34:45 2016

@author: jonleonhardsen
"""

import sqlite3
def ExtractData(filepath,a,b,c,d):
    #filepath is direction to database, dependent on segment or vessel analysis
    #a, b, c, d is max and min latitude and longitude coordinates
    global speeds
    global timestep
    global lats
    global lons

    speeds = list()
    timestep = list()
    lats = list()
    lons = list()

    conn = sqlite3.connect(filepath)
    cur = conn.cursor()
    SegmentAnalysis = 1
    with conn:
        cur = conn.cursor()
        if SegmentAnalysis == 1:
            cur.execute("select unixtime,sog,latitude,longitude,userid from Panamax1 order by userid, unixtime asc")
            #If we analyze segment, retrieve desired data from database
        else:
            cur.execute("SELECT unixtime,sog,latitude,longitude,userid FROM MessageType1 ORDER BY UNIXTIME ASC")
            #If we analyze vessel, retrieve desired data from database

        VesselData = cur.fetchall()
        maxLon = a
        maxLat = b
        minLon = c
```

```python
39            minLat = d
40            lowtime = 0                #Unixtime, lower limit time period
41            hightime = 100000000000 #Unixtime, upper limit time period
42
43            ####################################################
44            # THE FOLLOWING PARTS FILTERS ON SPEED AND POSITION #
45            ####################################################
46            for i in range(0,len(VesselData)):
47                Datastrip = VesselData[i]
48                Speed = Datastrip[1]
49                untime = Datastrip[0]
50                lat = Datastrip[2]
51                lon = Datastrip[3]
52                if Speed < 30 and Speed > 0 and lat <= maxLat and lat >= minLat \
53                    and lon >= minLon and lon <= maxLon and untime > lowtime and untime <
        hightime:
54                    speeds.append(Speed)
55                    timestep.append(untime)
56                    lats.append(lat)
57                    lons.append(lon)
58        cur.close()
59
60 if __name__ == "__main__":
61      ExtractData(filepath,a,b,c,d)
```

D.3 Ornstein-Uhlenbeck Parameter Estimation (OU.py)

The following code runs the resampling algorithm and the regression for estimation of Ornstein-Uhlenbeck parameters. It is imported as OU.py in the Master Script. It takes time and speed vectors as input, in addition to coordinates, some dummy parameters, and resampling criteria.

```python
#!/usr/bin/env python3
# -*- coding: utf-8 -*-
"""
Created on Wed Feb 22 12:57:53 2017

@author: jonleonhardsen
"""
#THIS CODE IS REFERRED TO AS THE RESAMPLING ALGORITHM AND PARAMETER ESTIMATION REGRESSION
       IN THE THESIS
import matplotlib
import matplotlib.pyplot as plt
matplotlib.style.use('classic')
from mpl_toolkits.basemap import Basemap
import numpy as np
from datetime import datetime
import math
import statistics as st

def OrnsteinUhlenbeckGenerator(Time,Speed,Lat,Lon,MAP,SPEED,MaxInterval,MinPeriod):
    #Time = Time vector in seconds
    #Speed = Speed vector in knots, raw from AIS data, filtered for speed records below
    steaming level
    #(Lat,Lon) = Coordinates
    #MAP, SEED = Plot dummies
    #MaxInterval = Maximum allowed interpolation interval
    #MinPeriod = Pre-defined time interval for resampling
    global TimeSerX
    global TimeSerY
    global TimeLat
    global TimeLon
    global RevRate1
    global MeanLev1
    global VOL1
    global X
    global IntSteps
    global IntTime
    global IntSpeed
    global Y

    AtTime = Time
    AtSpeed = Speed
    AtLat = Lat
    AtLon = Lon
    TimeSerX = list()                    #Preallocated transit time vector in unixtime
```

```python
43    TimeSerY = list()                        #Preallocated transit speed vector
44    TimeLat = list()                         #Preallocated transit latitude vector
45    TimeLon = list()                         #Preallocated transit longitude vector
46    StartTime = list()                       #Preallocated list of transit start times
47    EndTime = list()                         #Preallocated list of transit end times
48    diffsort = list(np.diff(AtTime))         #Interval between speed records
49    RevRate1 = list()                        #Preallocated list of mean reversion rates
50    MeanLev1 = list()                        #Preallocated list of mean speed levels
51    VOL1 = list()                            #Preallocated list of speed volatility
52    N = 1000                                 #Minimum number of records in a transit time
   series
53    for x in range(0,len(AtTime)-1): #Loop through unmanipulated AIS data
54        if diffsort[x] <= MaxInterval*3600:
55            #If yes, append speed records to transit time series
56            TimeSerX.append(AtTime[x])
57            TimeSerY.append(AtSpeed[x])
58            TimeLat.append(AtLat[x])
59            TimeLon.append(AtLon[x])
60
61        elif diffsort[x] > MaxInterval*3600 and len(TimeSerX) > N:
62            #If yes, cut off time series and proceed to next criteria
63            if TimeSerX[-1] - TimeSerX[0] > MinPeriod*12*3600 and len(TimeSerX) > N:
64                #If yes, transit time series is qualified for data resampling
65                StartTime.append(TimeSerX[0])
66                EndTime.append(TimeSerX[-1])
67                TimeFormat = 7200 # 1 = seconds, 60 = minutes, 3600 = hours
68                TimeSpace = EndTime[-1] - StartTime[-1]
69                TimeInt = int((TimeSpace)/TimeFormat)
70                SumSpeed = [0]*TimeInt
71                TimeInc = [0]*TimeInt
72                counttime = [0]*TimeInt
73
74                #The following loops creates average speed samples
75                for i in range(0,len(TimeSerX)):
76                    for j in range(0,TimeInt):
77                        if TimeSerX[i] < TimeSerX[0] + (j+1)*TimeFormat and TimeSerX[i]
   >= TimeSerX[0] + j*TimeFormat:
78                            SumSpeed[j] = SumSpeed[j]+TimeSerY[i]
79                            TimeInc[j] = TimeSerX[0]+ j*TimeFormat
80                            counttime[j] = counttime[j]+1
81                AvSpeed = [0]*TimeInt
82                for i in range(0,len(AvSpeed)):
83                    if counttime[i] > 0:
84                        AvSpeed[i] = SumSpeed[i]/counttime[i]
85                    elif counttime[i] == 0:
86                        AvSpeed[i] = 0
87                #The following loops converts unixtime to datetime
88                TimeInc = [x for x in TimeInc if x > 0]
89                IncSteps = list()
90                for i in range(0,len(TimeInc)):
91                    Unixconv = datetime.fromtimestamp(TimeInc[i])
92                    IncSteps.append(Unixconv)
93                    TimeSerXX = list()
94                    AvSpeed = [x for x in AvSpeed if x > 0]
```

```python
95                    for i in range(0,len(TimeSerX)):
96                        Unixconv = datetime.fromtimestamp(TimeSerX[i])
97                        TimeSerXX.append(Unixconv)
98
99                    #The following loops allocates interpolated speed records where it is
          necessary
100                   IntTime = [0]*TimeInt
101                   for x in range(0,TimeInt):
102                       IntTime[x]=min(TimeSerX) + x*TimeFormat
103                   IntSpeed = [0]*TimeInt
104
105                   for i in range(0,len(TimeInc)):
106                       for j in range(0,len(IntTime)):
107                           if TimeInc[i] == IntTime[j]:
108                               IntSpeed[j] = AvSpeed[i]
109
110                   for i in range(0,len(IntSpeed)):
111                       count = 0
112                       increments = 0
113                       if IntSpeed[i] == 0:
114                           count = 1
115                           lower = IntSpeed[i-1]
116                           for j in range(i+1,len(IntSpeed)):
117                               if IntSpeed[j] == 0:
118                                   count += 1
119                               elif IntSpeed[j] > 0:
120                                   upper = IntSpeed[j]
121                                   break
122                           increments = (upper-lower)/(count+1)
123                           for x in range(i,i+count):
124                               IntSpeed[x] = increments*(1+x-i)+lower
125                       elif IntSpeed[i] > 0:
126                           count = 0
127
128                   IntSteps = list()
129                   for i in range(0,len(IntTime)):
130                       Unixconv = datetime.fromtimestamp(IntTime[i])
131                       IntSteps.append(Unixconv)
132
133                   #The following part is the Ornstein-Uhlenbeck parameter estimation#
134                   #IntSpeed is the resampled data, including averaged and interpolated
          speed samples
135                   dx1 = np.diff(IntSpeed)
136                   dt = 2/24
137                   dxdt1 = dx1/dt
138                   del IntSpeed[-1]
139                   coeff1 = np.polyfit(IntSpeed,dxdt1,1)
140                   res1 = dxdt1 - np.polyval(coeff1,IntSpeed)
141                   revRate1  = -coeff1[0]
142                   meanLevel1 = st.mean(IntSpeed)
143                   vol1       = st.stdev(res1)*math.sqrt(dt)
144                   X = [0]*len(IntTime)
145                   Y = [0]*len(IntTime)
146                   Y[0]=IntSpeed[0]
```

```python
147                    if revRate1 > 0.05:
148                        for i in range(1,len(X)):
149                            Y[i] = Y[i-1] + revRate1*(meanLevel1-Y[i-1])*dt + vol1*math.sqrt(
       dt)*np.random.normal(0,1)
150                            #Y is the simulated speed process
151                        if SPEED == 1:
152                            fig = plt.figure()
153                            ax = fig.add_subplot(111)
154                            ax.plot(TimeSerXX,TimeSerY,'k',label='AIS Data')
155                            ax.plot(IntSteps,IntSpeed,c='k',label='Resampled AIS Data')
156                            plt.plot(IntSteps,Y,'k--',label='Simulated Process')
157                            plt.legend(loc='upper right')
158                            plt.xlabel('Time')
159                            plt.ylabel('Speed [knots]')
160                            plt.show()
161
162                        if MAP == 1:
163                            SpeedMap(TimeLat,TimeLon)
164
165                        RevRate1.append(revRate1)        #STORE ESTIMATED REVERSION RATE
166                        MeanLev1.append(meanLevel1)      #STORE ESTIMATED MEAN LEVEL
167                        VOL1.append(vol1)                #STORE ESTIMATED VOLATILITY
168                        TimeSerX = list()
169                        TimeSerXX = list()
170                        TimeSerY = list()
171                        TimeLat = list()
172                        TimeLon = list()
173                    else:
174                        TimeSerX = list()
175                        TimeSerY = list()
176                        TimeSerXX = list()
177                        TimeLat = list()
178                        TimeLon = list()
179                else:
180                    TimeSerX = list()
181                    TimeSerY = list()
182                    TimeSerXX = list()
183                    TimeLat = list()
184                    TimeLon = list()
185            else:
186                TimeSerX = list()
187                TimeSerY = list()
188                TimeSerXX = list()
189                TimeLat = list()
190                TimeLon = list()
191    global SpeedData
192    w, h = 3, len(VOL1);
193    SpeedData1 = [[0 for x in range(w)] for y in range(h)]
194    for i in range(0,h):
195        SpeedData1[i][0] = MeanLev1[i]
196        SpeedData1[i][1] = RevRate1[i]
197        SpeedData1[i][2] = VOL1[i]
198
199 def SpeedMap(LAT,LON): #Plots the areas where transit time series are extracted from
```

```python
200        minlon  =  max(-180,min(LON)-10)
201        minlat  =  max(-90,min(LAT)-10)
202        maxlon  =  min(180,max  (LON)+10)
203        maxlat  =  min(90,max(LAT)+10)
204        lat0  =  (maxlat+minlat)/2
205        lon0  =  (maxlon+minlon)/2
206        lat1  =  (maxlat+minlat)/2-20
207        fig=plt.figure()
208        ax=fig.add_axes([0.1,0.1,0.8,0.8])
209        m = Basemap(llcrnrlon=minlon,llcrnrlat=minlat,urcrnrlon=maxlon,urcrnrlat=maxlat,\
210                    rsphere=(6378137.00,6356752.3142),\
211                    resolution='l',projection='merc',\
212                    lat_0=lat0,lon_0=lon0,lat_ts = lat1)
213        ax.annotate('Start', xy=(LAT[0], LON[0]), xytext=(TimeLon[0], TimeLat[0]+2),
214                                arrowprops=dict(facecolor='black', shrink=0.05),)
215        m.drawcoastlines()
216        m.fillcontinents()
217        x, y = m(LON,LAT)
218        m.scatter(x,y,0.1,marker='o',c='k')
219        m.drawparallels(np.arange(-90,90,20),labels=[1,1,0,1])
220        m.drawmeridians(np.arange(-180,180,30),labels=[1,1,0,1])
221
222 if __name__ == "__main__":
223        OrnsteinUhlenbeckGenerator()
224        SpeedMap()
```

D.4 Monte Carlo Simulation Scripts

The following two scripts have functions for simulation of sailing speed and associated fuel consumption. Generate_Sailingspeeds.py generates sailing speed sample paths according to the Ornstein-Uhlenbeck process and parameters, and calls Fuel_Aggregated.py for calculation of the associated fuel consumption. Fuel_Aggregated.py takes resistance data for all bulb geometry as input in addition to the speed sample path, and calculates the fuel consumption according to the allowed reconfiguration period.

D.4.1 Simulation of Sailing Speed (Generate_Sailingspeeds.py)

```python
#!/usr/bin/env python3
# -*- coding: utf-8 -*-
"""
Created on Thu Mar  9 13:26:51 2017

@author: jonleonhardsen
"""
import math
import statistics as st
import numpy as np
import matplotlib.pyplot as plt
import Fuel_Aggregated as FA
import scipy
import BulbData as BD

def SimulateSailing(utilization, years, avtradeduration, iterations):
    #This function generates sample paths that represents sailing speed
    #utilization = Fraction of time at sea
    #years = Number of years we want to simulate
    #avtradeduration = Average transit duration
    #iterations = Number of Monte Carlo simulations
    global meanLevel
    global revRate
    global vol
    global Y
    global AverageTradeTime
    global days
    global AnY
    global savedFuel2Hours
    global savedFuelXHours
    global savedFuelPort
    global bulbDistribution
    global selected_bulbs
    global distanceSailed
    global consumedFuelStatic
    global FOCnm
    global simdays
```

```python
38      meanLevel = list()
39      revRate = list()
40      vol = list()
41      bulbDistribution = list()
42      distanceSailed = list()
43      consumedFuelStatic = list()
44      savedFuel2Hours = [0]*iterations
45      savedFuelXHours = [0]*iterations
46      savedFuelPort = [0]*iterations
47      simdays = list()
48      for a in range(0,iterations): #For each Monte Carlo simulation
49          trades = round(utilization*years*365/avtradeduration)
50          dt = 2/24
51          Y = [0]*12*years*365        #Pre-allocate sailing speed vector
52
53          #The following parameters represents OU parameter PDFs
54          vol_A = 10.75
55          vol_LOC = 0.27
56          vol_SCALE = 9.65
57          mean_LOC = 13.18
58          mean_SCALE = 5.31
59          mean_A = 0.42
60          mean_C =5.22
61          mean_LOC = 12.18
62          rev_K = 15.4
63          rev_LOC = 0.76
64          rev_SCALE = 0.09
65
66          for x in range(0,trades):
67              #This loops samples OU parameters for each single transit
68              meanLevel[x] = scipy.stats.gengamma.rvs(mean_A, mean_C, mean_LOC, mean_SCALE)
69              revRate[x] = scipy.stats.exponnorm.rvs(rev_K, rev_LOC, rev_SCALE)
70              vol[x] = scipy.stats.invgamma.rvs(vol_A, vol_LOC, vol_SCALE)
71          x = 0
72          portTime = round((1-utilization)*12*365/trades)       #calculates the time in port/
    not sailing
73          MAXSPEED = 26
74          for i in range(0,len(Y)):
75              #This loop generates sailing speed sample paths
76              if i >= x*12*avtradeduration+portTime and i < (x+1)*12*avtradeduration + (x
    +1)*portTime:
77                  #If yes, the ship is sailing (transit)
78                  Y[i] = Y[i-1] + revRate[x]*(meanLevel[x]-Y[i-1])*dt + vol[x]*math.sqrt(dt
    )*np.random.normal(0,1)
79                  if Y[i] > MAXSPEED:
80                      Y[i] = MAXSPEED
81              elif i >= (x+1)*12*avtradeduration + (x+1)*portTime and i < (x+1)*12*
    avtradeduration + (x+2)*portTime:
82                  #If yes, the ship is in port/not sailing
83                  Y[i] = 0
84              elif i >= (x+1)*12*avtradeduration + (x+2)*portTime:
85                  #If yes, transit (including port time) is finished
86                  x += 1
87                  if x >= trades:
```

```python
88                      break
89                  else:
90                      Y[i] = meanLevel[x]
91
92      days = [0]*len(Y)
93      for i in range(0,len(Y)):                #Time vector
94          days[i] = i/12
95      AnY = list(filter((0).__ne__, Y))        #Removes zeros (speed in port)
96      simdays = [0]*len(AnY)
97      for i in range(0,len(AnY)):              #Time vector for non-zero list
98          simdays[i] = i/12
99
100     FA.AggFuelConsumption(AnY,simdays)       #Sends sample path to fuel consum scrip/
    function
101     savedFuel2Hours[a] = FA.FuelSavings      #Fetches saved fuel for 2hour agility (
    see Fuel_Aggregated for elaboration)
102     savedFuelXHours[a] = FA.FuelSavings1     #Fetches saved fuel for Xhour agility (
    see Fuel_Aggregated for elaboration)
103     savedFuelPort[a] = FA.FuelSavingsPort    #Fetches saved fuel for port agility (see
     Fuel_Aggregated for elaboration)
104
105
106     for i in range(0,len(savedFuel2Hours)):
107         savedFuel2Hours[i] = 100*savedFuel2Hours[i]
108         savedFuelXHours[i] = 100*savedFuelXHours[i]
109         savedFuelPort[i] = 100*savedFuelPort[i]
110
111     ###################################
112     #ULTIMATE AGILITY POST PROCESSING#
113     ###################################
114     savedFuel2Hours = [x for x in savedFuel2Hours if str(x) != 'nan']
115     x = np.linspace(min(savedFuel2Hours),max(savedFuel2Hours),50)
116     acc = [0]*len(x)
117     for i in range(0,len(acc)):
118         for j in range(0,len(savedFuel2Hours)):
119             if savedFuel2Hours[j] <= x[i]:
120                 acc[i] += 1
121     for i in range(0,len(acc)):
122         acc[i] = acc[i]/len(savedFuel2Hours)
123
124     std = round(st.stdev(savedFuel2Hours),5)
125     mean = round(st.mean(savedFuel2Hours),5)
126     fig, ax1 = plt.subplots()
127     histval1, binsval = np.histogram(savedFuel2Hours, bins=50)
128     histval = histval1/sum(histval1)
129     width = 0.7 * (binsval[1] - binsval[0])
130     center = (binsval[:-1] + binsval[1:]) / 2
131     ax1.bar(center, histval, align='center', width=width,color='k',alpha=0.5)
132     ax1.set_xlabel('Saved Fuel [%]', color='k')
133     ax1.set_ylabel('Distribution', color='k')
134     plt.title('%s Simulations, Change Every 2nd hour \n Mean = %s, StDev = %s'%(
    iterations,mean,std))
135
136     ax2 = ax1.twinx()
```

```python
137     ax2.plot(x, acc, 'k')
138     ax2.set_xlabel('Saved Fuel [%]', color='k')
139     ax2.set_ylabel('Probability of Missing Target', color='k')
140     ax2.grid(True)
141     plt.show()
142
143     ################################
144     #LIMITED FLEX POST PROCESSING#
145     ################################
146     savedFuelXHours = [x for x in savedFuelXHours if str(x) != 'nan']
147     x1 = np.linspace(min(savedFuelXHours),max(savedFuelXHours),50)
148     acc1 = [0]*len(x1)
149     for i in range(0,len(acc1)):
150         for j in range(0,len(savedFuelXHours)):
151             if savedFuelXHours[j] <= x1[i]:
152                 acc1[i] += 1
153
154     for i in range(0,len(acc1)):
155         acc1[i] = acc1[i]/len(savedFuelXHours)
156
157     std = round(st.stdev(savedFuelXHours),5)
158     mean = round(st.mean(savedFuelXHours),5)
159     fig, ax1 = plt.subplots()
160     histval1, binsval = np.histogram(savedFuelXHours, bins=50)
161     histval = histval1/sum(histval1)
162     width = 0.7 * (binsval[1] - binsval[0])
163     center = (binsval[:-1] + binsval[1:]) / 2
164     ax1.bar(center, histval, align='center', width=width,color='k',alpha=0.5)
165     ax1.set_xlabel('Saved Fuel [%]', color='k')
166     ax1.set_ylabel('Distribution', color='k')
167     plt.title('%s Simulations, Change Every 6th Hour \n Mean = %s, StDev = %s'%(
        iterations,mean,std))
168     ax2 = ax1.twinx()
169     ax2.plot(x1, acc1, 'k')
170     ax2.set_xlabel('Saved Fuel [%]', color='k')
171     ax2.set_ylabel('Probability of Missing Target', color='k')
172     ax2.grid(True)
173     plt.show()
174
175     ############################
176     #PORT FLEX POST PROCESSING#
177     ############################
178     savedFuelPort = [x for x in savedFuelPort if str(x) != 'nan']
179     xP = np.linspace(min(savedFuelPort),max(savedFuelPort),50)
180     accP = [0]*len(xP)
181     for i in range(0,len(accP)):
182         for j in range(0,len(savedFuelPort)):
183             if savedFuelPort[j] <= xP[i]:
184                 accP[i] += 1
185
186     for i in range(0,len(accP)):
187         accP[i] = accP[i]/len(savedFuelPort)
188
189     std = round(st.stdev(savedFuelPort),5)
```

```python
190    mean = round(st.mean(savedFuelPort),5)
191    fig, ax1 = plt.subplots()
192    histval1, binsval = np.histogram(savedFuelPort, bins=50)
193    histval = histval1/sum(histval1)
194    width = 0.7 * (binsval[1] - binsval[0])
195    center = (binsval[:-1] + binsval[1:]) / 2
196    ax1.bar(center, histval, align='center', width=width,color='k',alpha=0.5)
197    ax1.set_xlabel('Saved Fuel [%]', color='k')
198    ax1.set_ylabel('Distribution', color='k')
199    plt.title('%s Simulations, Change In Port \n Mean = %s, StDev = %s'%(iterations,mean,
       std))
200    ax2 = ax1.twinx()
201    ax2.plot(xP, accP, 'k')
202    ax2.set_xlabel('Saved Fuel [%]', color='k')
203    ax2.set_ylabel('Probability of Missing Target', color='k')
204    ax2.grid(True)
205    plt.show()
206
207    selected_bulbs = [0]*BD.bulbConfigs
208    for i in range (0,len(selected_bulbs)):
209        selected_bulbs[i] = round(bulbDistribution.count(i+1)/len(bulbDistribution),3)
210
211
212 if __name__ == "__main__":
213    SimulateSailing()
```

D.4.2 Bulb Selection and Fuel Consumption (Fuel_Aggregated.py)

```python
#!/usr/bin/env python3
# -*- coding: utf-8 -*-
"""
Created on Mon Mar 13 16:41:20 2017

@author: jonleonhardsen
"""
import numpy as np
import matplotlib.pyplot as plt
import Generate_Sailingspeeds as GS
import math
import statistics as st
import pandas as pd
import BulbData as BD

def FuelCalc():
    #FuelCalc calculates fuel consumption as a function of sailing speed
    global power
    global fuelCons
    global bulbData
    BD.resistanceData() #Runs script that formats and interpolates resistance data for
    different bulbs
    bulbData = BD.x      #Fetch resistance data for bulb configurations
    nH = 1.2
    n0 = 0.55
    nR = 1.00
    nB = n0*nR
    nS = 0.99
    nT = nH*nB*nS
    sea_margin = 0.2
    bulbConfigs = int((len(bulbData[0,:])+1)/2)
    power = np.zeros((len(bulbData[:,0]),bulbConfigs))
    for i in range(power.shape[0]):            #Power calculations
        for j in range(1,power.shape[1]):
            power[i,j] = (1+sea_margin)*bulbData[i,2*j-1]*(0.51444)*bulbData[i,0]/(nT
    *1000)
            power[i,0] = bulbData[i,0]

    plt.figure()
    for i in range(1,power.shape[1]):
        plt.plot(power[:,0], power[:,i])

    plt.xlabel('Speed [knots]')
    plt.ylabel('$P_B$ [kW]')
    plt.show()

    #Fetches data on specific fuel consumption, as presented in thesis
    xl = pd.ExcelFile("/Users/jonleonhardsen/Documents/Documents/Skole/Python/FuelSIm/
    specificfuel.xlsx")
    xl.sheet_names
    sfcpd = xl.parse("Ark4")
    sfc = sfcpd.as_matrix()
```

```python
50
51       plt.figure()
52       plt.plot(sfc[:,0],sfc[:,1],c='k')
53       plt.ylabel('SFC [g/kWh]')
54       plt.xlabel('Speed [knots]')
55       plt.show()
56       fuelCons = np.zeros((len(power[:,0]),len(power[0,:])))
57
58       for i in range(power.shape[0]):        #Fuel calculations
59           for j in range(1,power.shape[1]):
60               fuelCons[i,j] = 24*power[i,j]*sfc[i,1]/10**6
61               fuelCons[i,0] = power[i,0]
62
63       plt.figure()
64       for i in range(1,power.shape[1]):
65           plt.plot(fuelCons[:,0], fuelCons[:,i])
66
67       plt.xlabel('Speed [knots]')
68       plt.ylabel('Fuel Consumption [MT per day]')
69       plt.show()
70
71   def AggFuelConsumption(speedBehaviour,speedDays):
72       #Takes in sampled speed paths from SimulateDailing()
73       global StatAgg
74       global FlexAgg
75       global FlexAgg1
76       global portFlexAgg
77       global bulbIDopt
78       global bulbTheoretical
79       global bulbActual
80       global bulbModePort
81       global FuelSavings
82       global FuelSavings1
83       global FuelSavingsPort
84       distance = 0
85       StatAgg = 0
86       StatAgg1 = 0
87       FlexAgg = 0
88       FlexAgg1 = 0
89       bulbIDopt = [0]*len(speedBehaviour)
90       ############################################################
91       ## Fuel consumption with bulb change allowed every 2 hours ##
92       ############################################################
93       global triggerSpeed
94       global triggerDay
95       triggerDay = list()
96       triggerSpeed = list()
97       for i in range(0,len(speedBehaviour)):
98           idx = (np.abs(fuelCons[:,0]-speedBehaviour[i])).argmin()
99           StatAgg += (2/24)*fuelCons[idx,1]                    #Adds consumed fuel for original
         bulb
100          fuelData = fuelCons[idx,1:]
101          bulbIDopt[i] = (np.abs(fuelData-0)).argmin()+1   #Selects bulb configuration with
         minimal fuel cons
```

```python
102         FlexAgg += (2/24)*fuelCons[idx,bulbIDopt[i]]     #Adds consumed fuel according to
     bulb config
103         distance += fuelCons[idx,0]*2
104
105     FuelSavings = (StatAgg-FlexAgg)/StatAgg
106     GS.bulbDistribution += bulbIDopt
107     #############################################################
108     ## Fuel consumption with bulb change allowed every X hours ##
109     #############################################################
110     bulbTheoretical = [0]*len(speedBehaviour) #Preallocated list for optimal bulb config
     at each time index
111     bulbActual = [0]*len(speedBehaviour) #Preallocated list for selected bulb config
112     minChangeInt = 3 #Minimum allowed switching frequency, 1 = 2 hours, 2 = 4 hours, etc
113     for i in range(0,len(speedBehaviour)):
114         #This loop determines the mean speed determining the bulb configuration
115         if i < len(speedBehaviour):
116             shortTermMean = st.mean(speedBehaviour[i:i+minChangeInt])
117         elif i == len(speedBehaviour)-1:
118             shortTermMean = speedBehaviour[i]
119
120         realIdx = (np.abs(fuelCons[:,0]-speedBehaviour[i])).argmin()
121         idx = (np.abs(fuelCons[:,0]-shortTermMean)).argmin()
122         fuelData = fuelCons[idx,1:]
123         bulbTheoretical[i] = (np.abs(fuelData-0)).argmin()+1 #Determines optimal bulb
     configuration
124         if i > 0 and bulbActual[i-1] != bulbTheoretical[i]:   #Determines optimal and
     allowed bulb configuration
125             if i > minChangeInt-1 and len(set(bulbActual[i-minChangeInt:i])) == 1:
126                 bulbActual[i] = bulbTheoretical[i]
127             else:
128                 bulbActual[i] = bulbActual[i-1]
129         elif i == 0:
130             bulbActual[i] = bulbTheoretical[i]
131         else:
132             bulbActual[i] = bulbActual[i-1]
133
134         FlexAgg1 += (2/24)*fuelCons[realIdx,bulbActual[i]]
135     FuelSavings1 = (StatAgg-FlexAgg1)/StatAgg1
136     #############################################################
137     ## Fuel consumption with bulb change allowed in port       ##
138     #############################################################
139     tradeDur = 14    #Average transit duration
140     trades = math.ceil(len(speedBehaviour)/((tradeDur-1)*12))
141     avSpeed = [0]*trades
142     steps = (tradeDur-1)*12
143     for i in range(1,len(avSpeed)+1):
144         #This loop calculates average speeds for each transit
145         if i*steps <= len(speedBehaviour):
146             avSpeed[i-1] = st.mean(speedBehaviour[(i-1)*steps+1:i*steps])
147         else:
148             avSpeed[i-1] = st.mean(speedBehaviour[(i-1)*steps+1:-1])
149
150     bulbOptTrade = [0]*len(avSpeed)
151     for i in range(0,len(avSpeed)): #This loop selects best bulb according to transit
```

```
        average
152     idx = (np.abs(fuelCons[:,0]-avSpeed[i])).argmin()
153     fuelData = fuelCons[idx,1:]
154     bulbOptTrade[i] = (np.abs(fuelData-0)).argmin()+1
155 bulbModePort = [0]*len(speedBehaviour)
156 for i in range(1,len(bulbOptTrade)+1):
157     if i == 1:
158         for j in range((i-1)*steps,i*steps+1):
159             bulbModePort[j] = bulbOptTrade[i-1]
160     elif i*steps <= len(speedBehaviour):
161         for j in range((i-1)*steps+1,i*steps+1):
162             bulbModePort[j] = bulbOptTrade[i-1]
163     else:
164         for j in range((i-1)*steps+1,len(speedBehaviour)):
165             bulbModePort[j] = bulbOptTrade[i-1]
166 portFlexAgg = 0
167 for i in range(0,len(bulbModePort)):
168     idx = (np.abs(fuelCons[:,0]-speedBehaviour[i])).argmin()
169     portFlexAgg += (2/24)*fuelCons[idx,bulbModePort[i]]
170 FuelSavingsPort = (StatAgg-portFlexAgg)/StatAgg

172 if __name__ == "__main__":
173     FuelCalc()
174     AggFuelConsumption()
```

D.5   List of Electronic Appendages

The following files are appended in the zip-file associated with the study:

- MasterAnalysis.py

- PlotVessels.py (in its entirety)

- OU.py

- Generate_Sailingspeeds.py

- Fuel_Aggregated.py

- BulbData.py (interpolates resistance data from excel-sheet)

- Bulb_data.xlsx (Resistance data for all bulb configurations)

- specificfuel.xlsx (Specific fuel consumption data)